A comparative study on the effect of acid preparation methodologies on bulk organic materials, and a long-core geochemical palaeoenvironmental reconstruction from South China.

BRODIE, CHRISTOPHER,RICHARD

How to cite:

BRODIE, CHRISTOPHER,RICHARD (2011) *A comparative study on the effect of acid preparation methodologies on bulk organic materials, and a long-core geochemical palaeoenvironmental reconstruction from South China.*, Durham theses, Durham University. Available at Durham E-Theses Online: http://etheses.dur.ac.uk/857/

Abstract

This thesis has two aims: i) an investigation of the effect of acid treatment on C/N, $\delta^{13}C$ and $\delta^{15}N$ of organic materials and; ii) the reconstruction of palaeoenvironmental change from a lake sediment sequence from south China, using geochemical proxies. To address these aims, a systematic comparative study was developed to examine the three most common acid treatment methods (capsule method; rinse method; fumigation method) and a range of acid reagents (HCl; H_2SO_3; H_3PO_4), on a range of terrestrial and aquatic, modern and geological sample materials. Acid treatment is a necessary step in the analysis of organic matter (OM) due to the distinct $\delta^{13}C$ of inorganic carbon (IC) relative to the $\delta^{13}C$ of OM; however, there is no consensus on “best practice”.

I find that C/N, $\delta^{13}C$ and $\delta^{15}N$ values of OM are not just dependent upon environmental processes but also on acid treatment method, which adds significant *non-linear* biasing to the OM signal several orders of magnitude above instrument precision. This biasing is caused by the inefficient removal of IC from sample materials *and* the alteration of OM by the acid treatment process. Consequently, this can significantly alter the environmental interpretation of these proxies, for example, in determining OM provenance, indicating that the assumption that the effect of acid treatment on sample OM is either negligible or systematic, is flawed, with biasing in C/N ~ 1 – 100; $\delta^{13}C$ ~ 0.2 – 7.2 ‰ and; $\delta^{15}N$ ~ 0.2 – 1.7 ‰ in my range of samples.

In addition, a long lake sediment sequence was cored from Lake Tianyang, Leizhou Peninsula, south China (20°31’1.11” N, 110°18’43.02” E) to reconstruct palaeoenvironmental variability using a suite of geochemical proxies ($\delta^{13}C$ of bulk OM; XRF elemental ratios, magnetic susceptibility). The Tianyang $\delta^{13}C$ record and elemental ratios (MIS 9 through MIS 6) show a strong glacial – interglacial imprint, providing evidence for periods of aridity during interglacial/interstadial periods in south China. The elemental ratios lose this imprint during MIS 5, likely due to an increase in catchment erosion (captured in the La, Nb, Ni, Th and Au records). Additionally, I tested the hypothesis that Ti concentrations reflect winter AM variability and showed that, whilst this may be valid, a robust interpretation is not possible due to the dilution of sedimentary Ti concentrations by local sources. A regional comparison of the Tianyang records appears to suggest a change in the strength of the land-sea thermal contrast in south China, implying a shift in mosiutre source region.

A comparative study on the effect of acid preparation methodologies on bulk organic materials, and a long-core geochemical palaeoenvironmental reconstruction from South China.

Durham
University

Christopher Richard Brodie

Ustinov College

Thesis submitted for the degree of Doctor of Philosophy

Department of Geography

May 2011

Acknowledgments

My first thanks are offered to Dr. Dave Evans, Prof. Colm O'Cofaigh and Dr. Zong Yongqiang, who, in April 2007, offered me the opportunity to undertake a PhD at Durham University. Financial support for this research, in the form of tuition fees, living expenses and some field and laboratory expenses were provided through the NERC (studentship NE/F007264/1). Additional support was granted through the NERC isotope facility (IP/1047/0508; IP/1165/0510), the NERC Radiocarbon Facility (1423/1009) and the Dudley Stamp Memorial Fund.

I thank my supervisors, Dr. Jeremy Lloyd, Dr. James Casford and Dr. Zong Yongqiang, whose support, encouragement, expertise, advice, friendship and faith in my ability, has led to the completion of this PhD. Their willingness to discuss my work and give unselfishly of their time is something I am eternally grateful and thankful for – a simple acknowledgement here does not do them justice at all! This is extended to Prof. Melanie Leng (NIGL, UK). I am truly indebted to Mel for "takin' a punt" on a rookie academic, providing fantastic academic support which has subsequently led to a substantial amount of the material presented within this thesis. In addition, I extend thanks to the Department of Geography laboratory staff (Frank, Martin, Amanda, Neil, Kathrine) for providing access to preparation and analytical equipment, and training in relevant analytical techniques (e.g. XRF), and to Jean for the morning coffee and toast!

The support for my friends, both at "home" and in Durham, largely through excessive evenings in the pub, mindless stupidity in the office, or just letting me "let off steam" in the form of some incoherent rant, has helped enormously: thanks Ash, Anne, Rob, Robin, Patrick, Vicky, Ed, Dave McC, Nick, Ladan, Rushil, Dianna, Banks, Fluff and Giro for cheering me up, or getting my plastered, when I was in need of it!

Finally, I thank my family for their support and encouragement over the last few years. In particular I thank my parents, Richard and Anne Brodie, my sister Emma Brodie, and my girlfriend, Rachel Finch (and Joe, of course!). Without their encouragement, support and guidance over the years, especially during my younger years from my parents, my life may not have taken me to this point. My final words here go to my grandmother, Jane Simpson, who passed away on 31st August 2010 after a long battle with Dementia and Alzheimer's: you will always have a special place in, and bearing on, my life.

Dedication

This thesis is dedicated to my family, primarily my parents Richard and Anne Brodie, and to my girlfriend, Rachel Finch. I also dedicate this Ph.D. thesis to “my only lassie”; my grandmother Jane Simpson (1935 – 2010), who passed away before I could complete my research.

Declaration and Statement of Copyright

I declare that the material presented in this Ph.D. thesis is the result of my own research, unless otherwise cited. Further, I confirm that no part of this thesis has been submitted for any other degree at this university, or for consideration at any other degree awarding institution.

Christopher Richard Brodie B.Sc (Hons)
31st May 2011

Table of Contents

Abstract i
Acknowledgments iii
Dedication iv
Declration and Statement of Copyright v
Table of Contents vi
List of Tables ix
List of Figures x

CHAPTER 1: Introduction

1.1 Introduction 1
1.2. Regional Setting 2
  1.2.1 Climate and Palaeoclimate 2
1.3 Proxies 4
1.4 Application of stable isotope geochemistry 5
1.5 Instrument analysis 6
1.6 δ^{13}C Pilot Study 8
1.7 Thesis aims 9
1.8 Thesis outline 11

Chapter 2: Evidence for bias in C and N concentrations and δ^{13}C composition of terrestrial and aquatic organic materials due to pre-analysis acid treatment methods

2.1 Introduction 13
2.2 Sample materials 15
2.3 Sample preparation methods 17
  2.3.1 Cleaning protocol 17
  2.3.2 Acid reagents 17
2.4 Acidification methods 18
  2.4.1 Rinse method 19
  2.4.2 Capsule method 19
  2.4.3 Fumigation method 20
2.5 Analytical methods 21
  2.5.1 C/N and δ^{13}C 21
  2.5.2 Supernatant analysis 22
2.6 Data analysis 23
2.7 Results 23
  2.7.1 Determination of carbon blank 23
  2.7.2 Effect of sample size on %C and %N 23
  2.7.3 Small versus normal sample sizes in our sample materials 24
  2.7.4 Sample material results 26
    2.7.4.1 Materials from known values 26

2.7.4.2 Other sample materials 27
2.8 Discussion 38
2.8.1 Method offsets 38
2.8.2 Effect of capsule 40
2.8.3 Small versus normal sample size 41
2.8.4 Proportionality 41
2.8.5 Dissolution of IC 42
2.8.6 C/N ratio 44
2.9 Summary and Recommendations 46
2.9.1 Recommendations 47

CHAPTER 3: Evidence for bias in measured δ^{15}N values of terrestrial and aquatic organic materials due to pre-analysis acid treatment methods.

3.1 Introduction 51
3.2 Sample materials and acid treatment methods 53
3.2.1 Sample materials 53
3.2.2 Acid treatment methods 53
3.3 Analytical methods 54
3.4 Data analysis 55
3.5 Results 55
3.6 Discussion 62
3.6.1 Methodological differences in δ^{15}N 62
3.6.2 Effect of capsule type 63
3.6.3 Coupled offsets in δ^{13}C and δ^{15}N 64
3.6.4 δ^{13}C and δ^{15}N cross-plots 65
3.6.5 Inorganic nitrogen 65
3.7 Summary and recommendations 70

CHAPTER 4: Evidence for bias in C/N, δ^{13}C and δ^{15}N values of bulk organic matter, and on environmental interpretation, from a lake sedimentary sequence by pre-analysis acid treatment methods.

4.1 Introduction 72
4.2 Unresolved issues 75
4.3 Materials and methods 76
4.3.1 Core material 76
4.3.2 Preparation methods 77
4.3.2.1 Cleaning protocol 77
4.3.2.2 Rinse method 77
4.3.2.3 Capsule method 77
4.3.2.4 Untreated 77
4.3.3 Analytical methods 77
4.3.3.1 C/N and δ^{13}C 77
4.3.3.2 δ^{15}N 78
4.3.4 Data analysis 78

4.4 Results 78
  4.4.1 %C and %N 78
  4.4.2 C/N and δ^{13}C 79
  4.4.3 δ^{15}N 79
4.5 Discussion 84
  4.5.1 Methodological differences 84
  4.5.2 Artificial concentration of %C and %N 87
  4.5.3 Implications for the interpretation of C/N, δ^{13}C and δ^{15}N 88
4.6 Implications for accuracy and precision 90
4.7 Summary and recommendations 93

CHAPTER 5: Down core palaeoenvironmental reconstruction from Lake Tianyang

5.1 Introduction 95
5.2 Lake setting 97
  5.2.1 Past research on Lake Tianyang 98
5.3 Materials and methods 100
  5.3.1 Sedimentology 100
  5.3.2 C/N and δ^{13}C of organic matter 102
  5.3.3 XRF elemental analysis 102
  5.3.4 Core scanning 103
  5.3.5 ^{14}C analysis 103
5.4 Results and discussion 104
  5.4.1 Chronology 104
    5.4.1.1 Radiocarbon Datings 104
    5.4.1.2 Tuned Age Model 106
  5.4.2 C/N and δ^{13}C 109
  5.4.3 XRF elemental ratios 112
  5.4.4 Magnetic Susceptibility (χ) 116
5.5 Glacial – Interglacial change: A Synthesis 117
5.6 Winter monsoon proxy 122
5.7 Regional comparison 125
5.8 Synthesis and conclusions 129

CHAPTER 6: Summary

6.1 Thesis aims 132
6.2 Effect of acid treatment on C/N and δ^{13}C of organic material 132
6.3 Effect of acid treatment on δ^{15}N of organic material 133
6.4 Effect of acid treatment on C/N, δ^{13}Cand δ^{15}Non organic materials in a down core sequence 134
6.5 Multi-proxy palaeoenvironmental reconstruction from Lake Tianyang 135

References 136

List of Tables

Chapter 1

Table 1.1 Comparison of St. Andrews and NIGL δ^{13}C results 9

Chapter 2

Table 2.1 Description of sample materials 16
Table 2.2 Acid strength conversion 18
Table 2.3 ANOVA results for "small" versus "normal" analyses 25
Table 2.4 Limitations of acid treatment methods and solutions 49

Chapter 3

Table 3.1 Mean ± standard deviation for SOILB, BROC and TYC 61
Table 3.2 ANOVA results for δ^{15}N from SOILB, BROC and TYC 62

Chapter 4

Table 4.1 ANOVA results for C/N and δ^{13}C from Lake Tianyang samples 82
Table 4.2 ANOVA results for δ^{15}N from Lake Tianyang samples 84
Table 4.3 Summary of bias on C/N, δ^{13}C and δ^{15}N in down core records 93

Chapter 5

Table 5.1 XRF Standard values 103
Table 5.2 New AMS ^{14}C dates from Lake Tianyang 104
Table 5.3 Previously reported ^{14}C datings from Lake Tianyang 106
Table 5.4 Age model: ^{14}C datings and SPECMAP "tie-points" 108
Table 5.5 Elemental concentrations of Lake Tianyang catchment rock 115

List of Figures

Chapter 1

Figure 1.1 Lake Tianyang location map 1
Figure 1.2 Schematic illustration of Asian monsoon 4
Figure 1.3 Schematic illustration of EA-IRMS 7
Figure 1.4 Theoretical representation of bias on C/N, δ^{13}C and δ^{15}N 10

Chapter 2

Figure 2.1 Changes in %C and %N as a function of sample size 24
Figure 2.2 %C, %N, C/N and δ^{13}C results for SOILB 28
Figure 2.3 %C, %N, C/N and δ^{13}C results for BROC 29
Figure 2.4 %C, %N, C/N and δ^{13}C results for ALGAE 30
Figure 2.5 %C, %N, C/N and δ^{13}C results for NEW 31
Figure 2.6 %C, %N, C/N and δ^{13}C results for TYC 32
Figure 2.7 %C, %N, C/N and δ^{13}C results for GRN 33
Figure 2.8 %C, %N, C/N and δ^{13}C results for MOR 34
Figure 2.9 %C removed from total organic C in rinse method 35
Figure 2.10 AAS results of rinse method supernatant 36
Figure 2.11 Relative proportional offset in %C, %N and C/N 43
Figure 2.12 Bi-plots of C/N versus δ^{13}C for SOILB and BROC 45

Chapter 3

Figure 3.1 C/N, δ^{13}C and δ^{15}N results for SOILB 58
Figure 3.2 C/N, δ^{13}C and δ^{15}N results for BROC 59
Figure 3.3 C/N, δ^{13}C and δ^{15}N results for TYC 60
Figure 3.4 Bi-plots of δ^{13}C versus δ^{15}N for SOILB, BROC and TYC 67
Figure 3.5 SOILB bootstrap estimate of %C versus %N bi-plot 68
Figure 3.6 BROC bootstrap estimate of %C versus %N bi-plot 69
Figure 3.7 TYC bootstrap estimate of %C versus %N bi-plot 69

Chapter 4

Figure 4.1 Partial core lithology for Lake Tianyang 77
Figure 4.2 %C, %N, C/N and δ^{13}C down core comparison records 81
Figure 4.3 δ^{15}N down core comparison records 84

Chapter 5

Figure 5.1 Map of Leizhou Peninsula and Lake Tianyang contour map 97
Figure 5.2 Cross section of Lake Tianyang 98
Figure 5.3 Previous reconstructions on Lake Tianyang 99
Figure 5.4 Lake Tianyang core lithology for upper 40.00 m 101
Figure 5.5 Age-depth plot of new Tianyang chronology 109
Figure 5.6 Correlation of pollen data with SPECMAP stacked δ^{18}O 110
Figure 5.7 Lake Tianyang δ^{13}C, XRF and χ records 113
Figure 5.8 Regional comparison of Tianyang records 128

Chapter 1

Introduction

1.1. Introduction

The climate of South China is strongly seasonal, owing to the dominant influence of the Asian monsoon (AM), the associated summer precipitation of which is vital to the livelihoods of several billions of people. Therefore understanding the variability of the AM, and how it may change in the future, is vital, but requires an understanding of palaeo-AM changes. However, the spatial resolution of long term palaeoclimatic records of the AM is currently very low in south Asia, especially from terrestrial archives (Wang et al, 2005). In an attempt to improve the scientific understanding of palaeoclimatic change in South China, a long sedimentary sequence was sampled from Lake Tianyang, Leizhou Peninsula, south China (Figure 1.1), for organic and inorganic geochemical analyses.

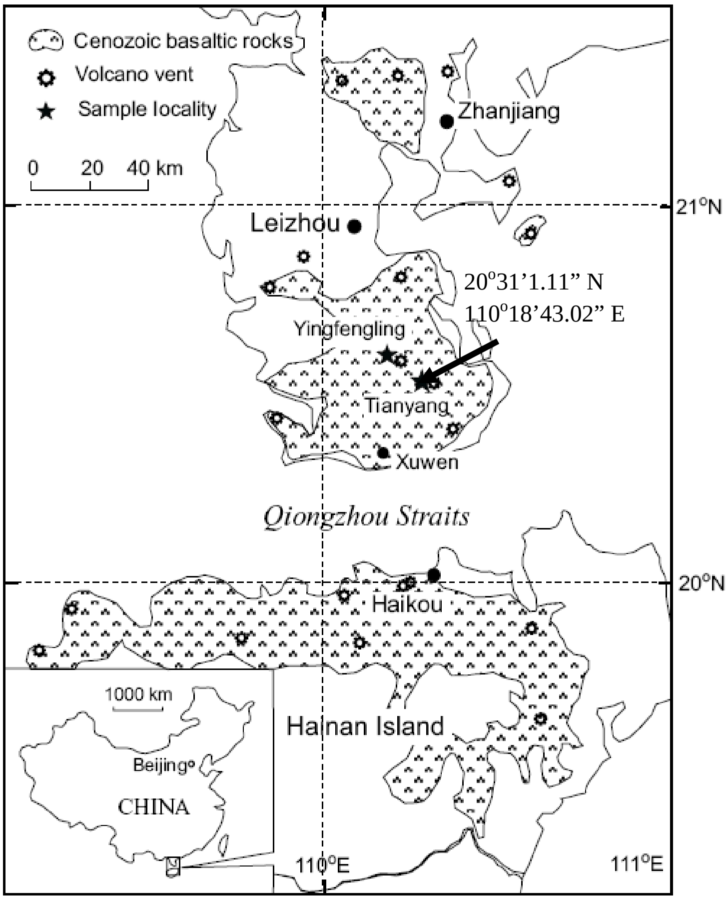

Figure 1.1: Location map of Lake Tianyang, south China (Adapted from Yu et al., 2006: 357).

1.2. Regional Setting

Lake Tianyang is situated to the south of Leizhou Peninsula, ~80 – 100m above mean sea level with a catchment surface area of ~7.3 km^2. There is currently no standing water body due to the drainage outlet to the southeast of the basin and the infilling of the lake by sedimentation (Zheng and Lei, 1999). The peninsula is characterised by a flat volcanic topography, with ~39 volcanic craters (Mingram et al, 2004) that form small catchment maar lakes, the main deviation from this flat topographical setting. Given the typically small catchment area and deep profile of maar lakes (e.g. Hutchinson, 1957), like Lake Tianyang, they respond relatively quickly to changes in climate. The signature of such changes is recorded in the long sedimentary record constrained by the crater rim (i.e. small area). Previous low resolution research on Lake Tianyang indicates that the sedimentary record spans several glacial-interglacial cycles (e.g. Chen et al., 1990; Zheng and Lei, 1999). A detailed investigation of the sedimentary record can, therefore, contribute an important palaeoenvironmental reconstruction to the literature in a key climatic area.

The geology of the Leizhou Peninsula is dominated by basalt, dating from the early Pleistocene, and is part of the Leiqiong formation which covers an area of ~ 7000 km^2 (Ho et al, 2000). Specifically, Lake Tianyang is part of the middle Pleistocene Shimaoling formation and is a maar crater lake typical of the region (e.g. Mingram et al, 2004). Ho et al (2000) presented a key geochemical summary and volcanic history of the Leizhou Peninsula, and indicated the main period of volcanic activity was the early – middle Pleistocene. The basalts in Leizhou Peninsula are rich in olivine and quartz tholeiites, with coexisting titanomagnetite (~50 wt% Fe and ~24 wt % Ti) and ilmenite (~ 40 wt% Fe and ~51 wt% Ti)(Ho et al, 2000) and have typically high concentrations of Aluminum (Al), Iron (Fe), Magnesium (Mg), Titanium (Ti), Niobium (Nb), Nickel (Ni), Lanthanum (La), Barium (Ba) and Gold (Au).

1.2.1. Climate and Palaeoclimate

The character of the regional climate is strongly seasonal, with warm, wet summers (June - August) and cool, dry winters (December - February). This phenomenon, known as the Asian monsoon (AM), has been generally described as a large “land-sea breeze” system (e.g. Webster, 1998), the strength and intensity of which is primarily controlled by regional land-sea thermodynamics and seasonal changes in insolation within the tropics (e.g. Gao et al., 1962; Ramage, 1971; Webster, 1987; 1998; An et al., 2000;

Wang et al., 2005; Nakagawa et al., 2006). Through the boreal summer, the insolation maximum moves northward, strengthening the north-south land-sea thermodynamic contrast across Asia resulting in increased (and rapid) sensible heating across the Tibetan plateau and continental Asia. This develops continental low pressure systems (with coexisting high pressure systems over the adjacent oceans). This results in wind patterns blowing predominantly from a south/south-westerly direction and increasing evaporation across moisture source regions (Indian Ocean, South China Sea (SCS), Western Pacific Warm Pool (WPWP) and Western Pacific). The summer AM initiates over west Asia (India) first (in May) which is not paralleled over east Asia (e.g. China) until late May/early June, when insolation maxima causes increased moisture flux over SCS and WPWP. In China, this broadly results from the pressure gradient force between the Australian high, Western Pacific high and the Asian continental low propagating cross-equatorial flow over Indonesia which interacts with the Intertropical Convergence Zone (ITCZ; or monsoon trough) leading to the onset of monsoon precipitation. As East Asia does not have the orographic barrier in the Himalayas, the rain-bearing front (Mei-Yu front) can reach farther north (~ 30^{o}N) than the south-western front, which is blocked by the Himalayas. This causes Asia to experience warm, wet summer periods, and cold, dry winter periods. By September/October the insolation maxima begin to move southwards, and with it the ITCZ. This results in reduced sensible heating across the Asian continent which, over the boreal winter months, causes continental high pressure cells to form in contrast to the low pressure cells over the adjacent oceans. This causes cold, dry winds to flow from a north-easterly direction cross the Asian continent (see Figure 1.2).

The AM is an important inter-hemispheric land-sea-air system connected to global and regional climate at orbital and sub-orbital timescales (e.g. Ramage, 1971; Kutzbach, 1981; Webster, 1998; An, 2000; Wang et al., 2005; Nakagawa et al., 2008). For example, changes in the intensity of the Siberian high and westerly jet stream have been invoked as a possible mechanism that strengthens the winter monsoon and weakens the summer monsoon during cold periods (e.g. An, 2000; Wang et al, 2001; Yancheva et al, 2007; Nakagawa et al, 2008). Research on cave speleothem records in sub-tropical China (e.g. Wang et al, 2001; Yuan et al 2004; Cheng et al, 2009), Qinghai-Tibetan Plateau ice core records (Thompson et al, 1997), loess/palaeosol sequences from central and northern China (e.g. Porter and An, 1995; Chen et al, 1999; An et al, 2000; Porter, 2000), a lake sequence from Japan (Nakagawa et al, 2008) and from sedimentary sequences from the South China Sea (Wang et al, 1999; Sun et al, 2003) has improved our understanding of orbital scale variability of the Asian monsoon (AM) over the past two glacial – interglacial cycles. In general, they focus on summer AM variability (commonly discussed as changes in precipitation), and broadly agree that the summer AM is dominated by a ~23 ka cycle which is synchronous with northern hemisphere summer insolation at 65^{o}N, implying a direct link to solar forcing. These records lend support to the theory for direct solar modulation of the AM region by the precession cycle (~ 23 – 19 ka) (Kutzbach, 1981; Kutzbach and Street-Perrot, 1985; Kutzbach and Guetter, 1986; Prell and Kutzbach, 1987; Rossignol-Strick et al, 1998; Ruddiman, 2006) and suggest a weakening of the summer AM during glacial/stadial periods and a strengthening during interglacial/interstadial periods.

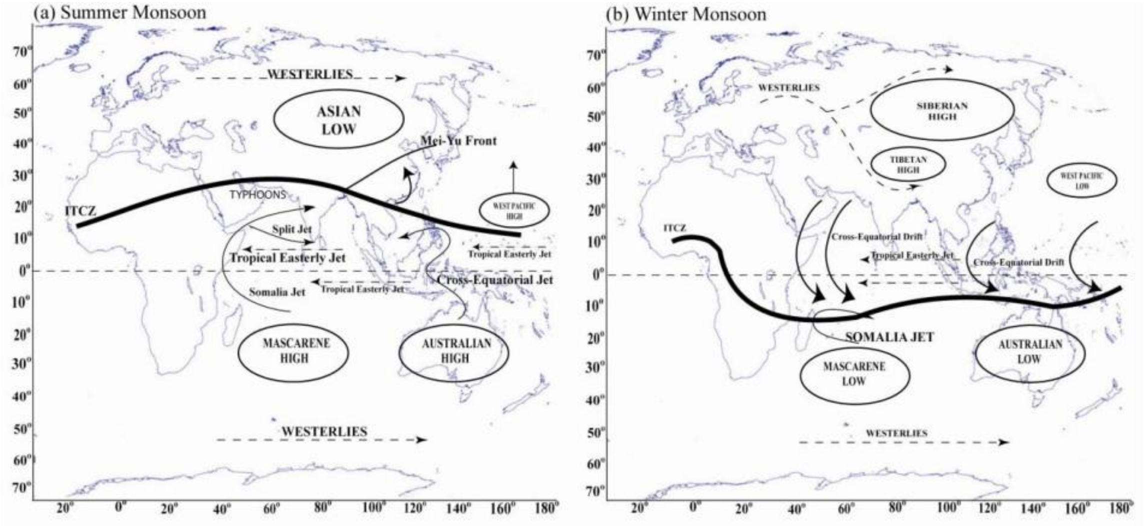

Figure 1.2: Generalised schematic of Asian summer (a) and winter (b) monsoon.

1.3. Proxies

The reconstruction of palaeoenvironmental and palaeoclimatic change from lacustrine sediment sequences is commonly achieved through the measurement and interpretation of organic and inorganic proxies (e.g. Meyers, 1994; Burnett et al, 2010; Scholz et al, 2010). For example, C/N, δ^{13}C and δ^{15}N values from bulk organic matter (OM) have been commonly employed to understand OM provenance and vegetation type (e.g. C_3 v C_4 plants)(e.g. Talbot and Johannessen, 1992; Meyers, 1997; Street-Perrot et al., 1997, 2004; Turney, 1999; Scholz et al, 2010; Yu et al, 2010). Consequently, they have become an important tool for understanding biogeochemical processes at a variety of spatial and temporal scales during the last two decades (e.g. Altabet et al, 1995; Meyers, 1997; Sharpe, 2007; Zong et al, 2006; Galy et al, 2008; Langdon et al, 2010; Yu et al, 2010). Research based on these proxies underpins the understanding of past climate variability and has helped interpret centennial to glacial-interglacial timescale shifts outside of high-latitude regions (e.g. Street-Perrot et al, 1997, 2004; Turney, 1999; Lucke et al, 2003; Baker et al, 2005; Mampuku et al, 2008; Scholz et al, 2010; Wei et al, 2010). Elemental ratios in lake sediments have also been used to increase the understanding of within catchment processes, such as redox changes (e.g. Fe, Mn, Cu), catchment erosion (Sr, Rb, Ti, Nb, La) and lake productivity (U, Th, Ba)(e.g. Davison, 1993; Boyle 2001). Therefore, this study will employ C/N and $\delta^{13}C$ and heavy metal elemental ratios as proxies to reconstruct the palaeoenvironment of Lake Tianyang.

1.4. Application of stable isotope geochemistry

The application of stable isotopes as a means of understanding environmental processes matured from the seminal work of Urey (1947) who presented the theoretical grounds for isotopic fractionation and suggested such fractionations could be related to environmental processes. Fractionation of stable isotopes refers to the natural chemical and/or physical process(es) which lead to the division of isotopes of an element within a substance (e.g. photosynthesis). For example, Carbon has three isotopes; two stable isotopes, ^{12}C (the most abundant) and ^{13}C, and one radioactive isotope (^{14}C). However, it is the fractionation between ^{12}C and ^{13}C that has been largely adopted to investigate environmental processes. For example, during photosynthesis plants preferentially diffuse ^{12}C into their structure by assimilation of atmospheric or dissolved CO_2. However, two major photosynthetic pathways exist: the Hatch-Slack photosynthetic pathway, broadly utilised by C_4 plants; and the Calvin-Benson photosynthetic pathway, commonly utilised by C_3 plants. This fundamental genetic difference represents a measureable fractionation process in the environment resulting in C_3 plants typically with $\delta^{13}C$ values in the range of –22 to –35 ‰, and C_4 plants with $\delta^{13}C$ values in the range of –6 to –15 ‰.

The organic carbon signature is, however, potentially contaminated by the presence of inorganic carbon (IC; e.g. calcite, dolomite, siderite) due to the significantly different $\delta^{13}C$ signature of IC (–15 to + 10 ‰; e.g. Hoefs, 1973; Sharpe, 2007). For a hypothetical sample with 1% IC ($\delta^{13}C \approx -3$ ‰) and 12% OC ($\delta^{13}C \approx -25$ ‰), $\delta^{13}C$ would be enriched by 1.8 ‰. Therefore, prior to the analysis of organic C, it is necessary to remove the contaminating IC from the sample material. This is commonly achieved by acid treatment (e.g. Froelich, 1980; Verardo et al, 1990; Nieuwenhuize et al. 1994; Meyers, 1997; King et al, 1998; Lohse et al, 2000; Leng et al, 2005; Larson et al, 2008; Fernandes and Krull, 2008). A number of fundamentally different pre-analysis acid treatment methods are clear from the literature, using a variety of different acid reagents and strengths: (i) the “rinse” method, which involves acid digestion of the sample for ~ 24 h followed by sequential water rinses; (ii) the “capsule” method, which involves the in-situ acidification of the sample material in a silver capsule and; (iii) the “fumigation” method, which involves the exposure of sample aliquots to acid fumes for ~8 h or more. However, no consensus on “best practice” is evident in the literature.

1.5. Instrument analysis

The measurement of C/N, δ^{13}C and δ^{15}N values of bulk OM is commonly achieved in palaeoenvironmental studies by Elemental Analyser Isotope Ratio Mass Spectrometry (EA-IRMS), a technique today that provides extremely high accuracy and precision (Figure 1.3). The EA-IRMS analytical process undertakes five primary steps (e.g. Sharpe, 2007; Muccio and Jackson, 2009):

i) Combustion: combustion of sample and conversion to gas phase in a combustion furnace of an EA (CO_2 for analysis of carbon; N_2 for nitrogen analysis);

ii) Ionisation: ionisation of the sample gas (in the ion source module of the mass spectrometer). In the ion source, ions are formed from the sample gas, accelerated and focussed into a narrow high energy beam;

iii) Mass Analysis: separation of these ions by deflection into a circular path by discrimination of mass to charge ratio under an electromagnetic field (in the mass analyser module of the mass spectrometer);

iv) Ion detection: measurement of separated ions which allows the abundance of each ion present to be measured (in the detector module of the mass spectrometer) and;

v) Ion separation and measurement: collection of separated ions in ion detectors, which converts the ions into an electrical impulse signal and amplifies it, before the resultant signal is processed into mass spectra.

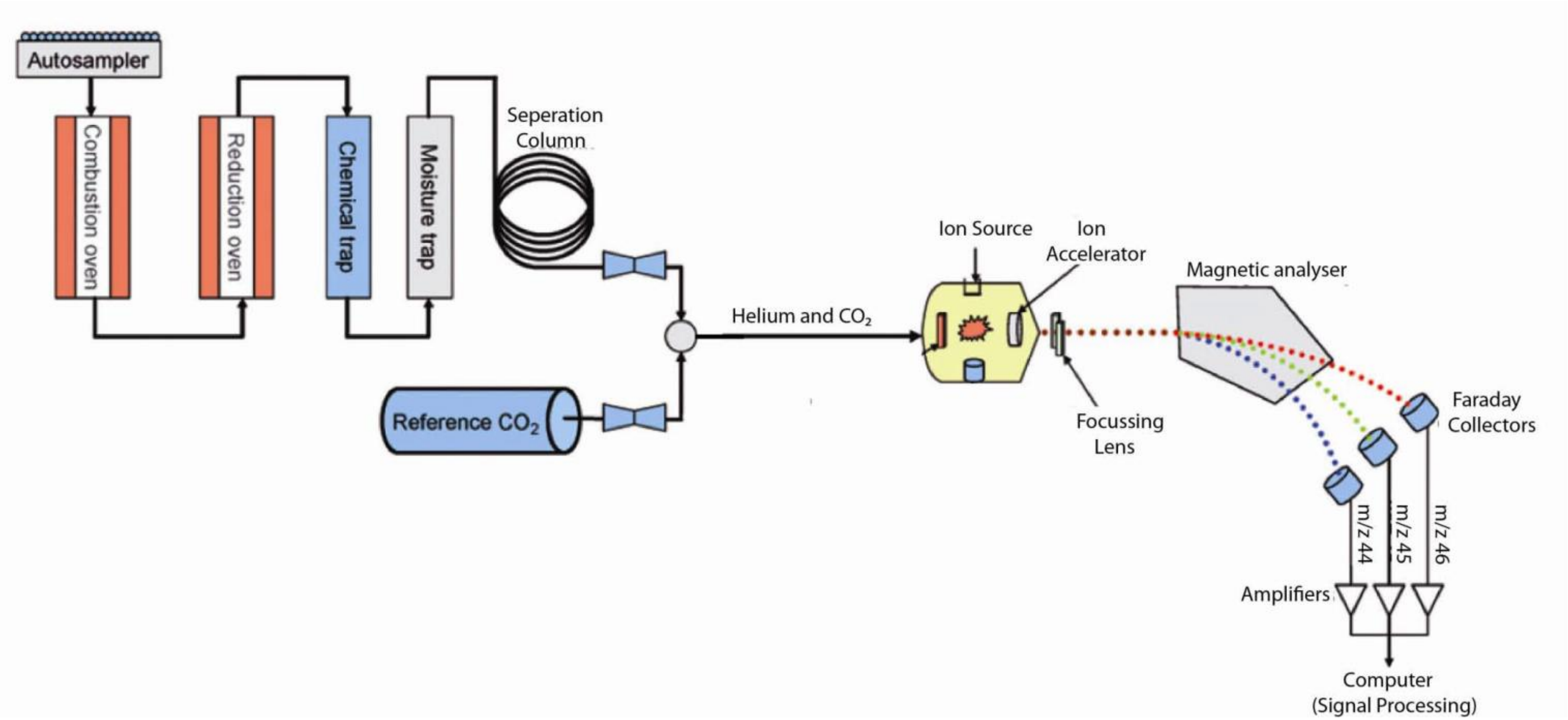

Figure 1.3: Schematic of EA-IRMS analytical setup. Sample materials are loaded into the autosampler, normally in a foil capsule for solid samples (i.e. sediments), and dropped sequentially into a combustion furnace in a flow of helium gas. The sample is combusted to CO_2 (for carbon), and N_2 (for nitrogen) in the reduction oven from nitrous oxides with the concomitant removal of excess O_2. The chemical and moisture trap then removes H_2O before the sample gas is separated by gas chromatography into CO_2 and N_2. The sample gas analyte is then transferred “on-line” to the IRMS for analysis where it is ionised, followed by an ion separation and detection of the separated ions (after electrical amplification of the ions). The resultant electrical impulse that is detected is processed into mass spectra of relative abundance of isotopes in the sample gas.

The stable isotope $\delta^{13}C$ and $\delta^{15}N$ values of analysed sample material are derived relative to isotopic standard reference materials to eliminate any potential systematic error or bias from analytical measurements. Values are then quoted with reference to internationally recognised standards such as Vienna Pee Dee Belemnite (V-PDB) for carbon and atmospheric air for nitrogen (IAEA, 1995). Measured isotope ratios are derived as a ratio of a low abundance isotope to the high abundance isotope (e.g. $^{13}C/^{12}C$ and $^{15}N/^{14}N$) and reported in the delta (δ) notation (Coplen, 1996) as parts per thousand (‰):

$$\delta\ R_{\text{sample-standard}}\ (‰) = [\ (R_{\text{Sample}} / R_{\text{Standard}}) - 1]\ \text{x}\ 1000$$

where R = the measured ratio of the sample and standard respectively. Instrument precision is expressed as the standard deviation (σ) of replicate analysis of standard reference materials.

1.6. $\delta^{13}C$ Pilot Study

An initial pilot dataset for C/N and $\delta^{13}C$ values of bulk OM from the Lake Tianyang sediment was analysed at the School of Geography and Geosciences at St. Andrews University followed by detailed analysis at the NERC Isotope Geoscience Laboratory (NIGL), Keyworth. I cross-validated $\delta^{13}C$ measurements acquired at St Andrews University at NIGL (Table 1.1) prior to undertaking this detailed analysis. This cross-validation showed considerable differences in $\delta^{13}C$ values in the range of ~ 0.1 – 3.5 ‰; these differences are significantly greater than instrument precision (from St. Andrews and NIGL $\leq$ 0.2 ‰) and represent additional imprecision of the measured $\delta^{13}C$ values. The pre-analysis acid treatment method at both laboratories fundamentally differed: St. Andrews University Geoscience Laboratory followed the “capsule” method using 10% HCl as the acidifying reagent, whereas NIGL followed the “rinse” method using 5% HCl as the acidifying reagent. However, an inherent assumption of this acid treatment approach, regardless of the method or acid reagent used, is that there is no bias to OM and, if there is, it is at least systematic and proportional between acid treatment methods. Given the widespread application and measurement of C/N, $\delta^{13}C$ and $\delta^{15}N$ values of bulk OM geochemistry in palaeoenvironmental research (and across other disciplines), the lack of a robust systematic comparison and understanding of the potential for bias on measured C/N, $\delta^{13}C$ and $\delta^{15}N$ values from pre-analysis acid treatment methods undermines a rigorous scientific approach. This thesis, therefore, presents a reassessment of the accuracy and precision on C/N, δ^{13}C and δ^{15}N values on organic materials prior to undertaking a palaeoenvironmental reconstruction of the Lake Tianyang sedimentary record.

Table 1.1: Comparison of measured δ^{13}C values from St. Andrews University and NERC Isotope Geosciences Laboratory

Sample Depth (m)	St. Andrews δ^{13}C (‰)	NIGL δ^{13}C (‰)	Difference (‰)
8.76	-9.93	-7.24	2.69
9.08	-25.05	-24.24	0.81
9.56	-19.62	-17.97	1.65
10.36	-25.64	-25.01	0.63
10.52	-23.57	-24.50	0.93
12.28	-19.04	-20.31	1.28
12.44	-17.09	-20.63	3.54
12.60	-17.79	-15.37	2.42
12.76	-20.04	-18.94	1.10
12.92	-24.60	-24.68	0.08
14.20	-25.595	-25.70	0.10

1.7. Thesis aims

The aims of this thesis are:

1. To investigate the effect of pre-analysis acid treatment methods on C/N and δ^{13}C values of OM in a range of environmental materials. (Chapter 2)
2. To investigate the effect of pre-analysis acid treatment methods on δ^{15}N values of OM in a range of environmental materials. (Chapter 3)
3. To investigate the effect of pre-analysis acid treatment methods on C/N, δ^{13}C and δ^{15}N values of OM in a down-core sedimentary sequence. (Chapter 4)
4. To develop of multi-proxy record of environmental change from Lake Tianyang. (Chapter 5)

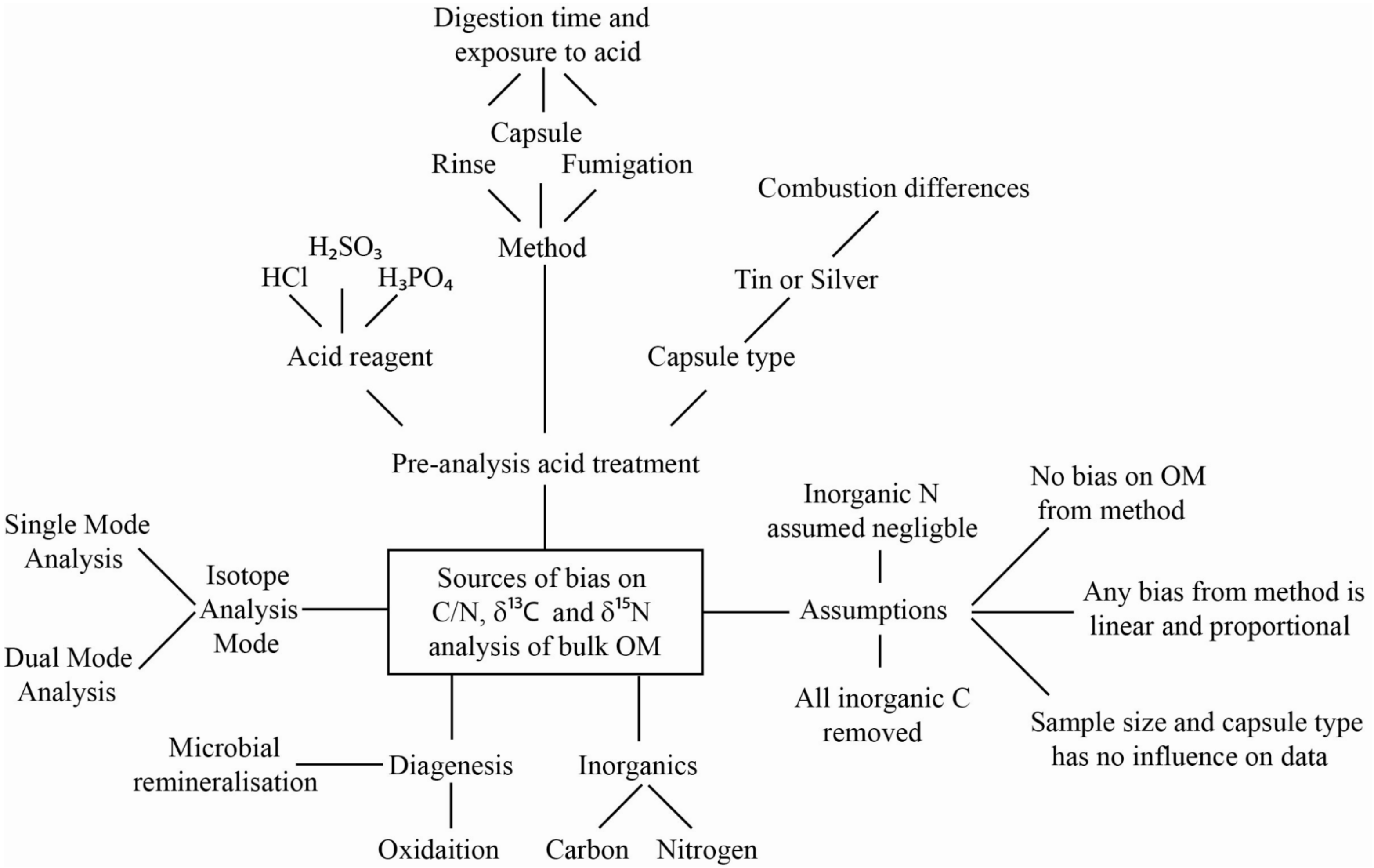

Figure 1.4: Theoretical representation of potential source of bias on C/N, δ^{13}C and δ^{15}N values.

1.8. Thesis outline

Chapter 2 addresses the first research aim and presents the results of a comprehensive systematic comparative study of pre-analysis acid treatment methods on a suite of environmental organic materials. I show that elemental C and N composition varies in a nonlinear and disproportionate manner within and between methods, but does not necessarily result in an isotopic shift. Further, the $\delta^{13}C$ of sample OM can vary significantly within and between acid treatment methods. This biasing is unpredictable.

Chapter 3 takes this systematic method of investigation a step further by investigating $\delta^{15}N$ of OM and presents the results of a smaller comparative study, guided by the results from chapter 2. I illustrate that measured $\delta^{15}N$ values vary significantly within and between acid treatment methods, and in different proportions to $\delta^{13}C$. This biasing too is unpredictable.

Based on the findings of chapters 2 and 3, and in the context of reconstructing the Lake Tianyang palaeoenvironmental history, chapter 4 presents a comparative study of these pre-analysis acid treatment methods on a sedimentary sequence of samples from Lake Tianyang. I show that there are inconsistencies in the application of any single method down-core, and significant differences within and between methods in C/N, $\delta^{13}C$ and $\delta^{15}N$ values. This significantly reduces the accuracy and precision of measured C/N, $\delta^{13}C$ and $\delta^{15}N$ values and can influence environmental interpretation.

Chapter 5 presents results and discussion of a geochemical analysis of the upper 40 m section of sediment from Lake Tianyang, based primarily on $\delta^{13}C$ and XRF elemental data. I report evidence of glacial-interglacial scale variability in our multi-proxy record alongside evidence questioning the validity of sedimentary Ti concentrations as a proxy for winter monsoon wind strength variability.

Finally, chapter 6 concisely summarises the primary findings of the preceding chapters.

CHAPTER 2

Evidence for bias in C and N concentrations and $\delta^{13}C$ composition of terrestrial and aquatic organic materials due to pre-analysis acid treatment methods.

Brodie, C.R., Leng, M.J., Casford, J.S.L., Kendrick, C.P., Lloyd, J.M., Zong, Y.Q., and Bird, M.I. (2011) Evidence for bias in C and N concentrations and $\delta^{13}C$ composition of terrestrial and aquatic organic materials due to pre-analysis acid preparation methods. Chemical Geology. 282, 67 – 83.

2.1 Introduction

The accurate determination of the concentrations of carbon [C] and nitrogen [N] (from which C/N is derived) and carbon isotopic composition ($\delta^{13}C$) of organic matter (OM) have been regarded as key proxies for our interpretation of environmental processes. C/N ratios are widely used to examine OM source mixing and alteration in sediments (e.g. Meyers, 1997; Baisden et al, 2002) and $\delta^{13}C$ to identify carbon sources and photosynthetic pathways in plants (e.g. C_3 and C_4 plant differentiation; Meyers, 2003; Sharpe, 2007). They are used to assess carbon reservoir turnover times and soil C dynamics (e.g. Harris et al, 2001); determine trophic levels in environmental systems (Bunn et al, 1995; Pinnegar and Poulnin, 1999; Kolasinski et al, 2008); for primary productivity reconstructions and estimation of carbon burial rates; and to understand mineralisation processes (e.g. Midwood and Boutton, 1998; Freudenthal et al, 2001; Leng and Marshall, 2004). These interpretations are grounded in the assumption that we can reliably determine C/N and $\delta^{13}C$ concentrations in OM. It is common place to consider carbon in two major forms; organic (OC) and inorganic (IC), and either one can act as a contaminant in the measurement of the other because of their distinct isotopic signatures. The accurate determination of C/N and $\delta^{13}C$ composition of OM must involve the complete removal of the contaminating IC fraction from the total carbon, which is achieved by acid treatment. An inherent assumption of these acid treatment methods is that any offsets in C/N and $\delta^{13}C$ are linear and proportional.

There are a small number of focussed studies which have investigated the effects of acidification methods and acid types on specific terrestrial or aquatic materials, though with contradictory results regarding the offsets to C/N and $\delta^{13}C$ values (e.g. Gibbs, 1977; Froelich, 1980; King et al. 1998; Lohse et al. 2000; Harris et al. 2001; Kennedy et al. 2005; Schmidt and Gleixner, 2005; Fernandes and Krull, 2008). The results of these studies show that the acidification method can influence the elemental and isotopic signatures of C and N and suggests that offsets in C/N and $\delta^{13}C$ due to acid treatment methods can be significant. Losses of C and N from OM from different acid treatments have previously been reported ranging from 5 to 78% and 0 to 50% respectively (e.g. Froelich, 1980; Yamamuro and Kayanne, 1995; Bunn et al, 1995; King et al. 1998; Lohse et al. 2000; Schubert and Nielsen, 2000; Ryba and Burgess et al, 2002; Schmidt and Gleixner, 2005). The extent of losses from sample OM appears to vary within and between methods and environments, and with IC content (Froelich, 1980). Results for shifts in $\delta^{13}C$ value are contradictory, indicating enrichments in $\delta^{13}C$ of 0.2 – 8.0 ‰ (e.g. Schubert and Nielsen, 2000; Kolasinski et al. 2008), or depletions in $\delta^{13}C$ of 0.1 – 1.9 ‰ (Kennedy et al; 2005; Komada et al. 2008) as well as no change (e.g. Midwood and Boutton, 1998; Kennedy et al, 2005). Enrichment in $\delta^{13}C$ value is widely interpreted to be through residual IC in sample material (e.g. Kolasinski et al. 2008). In addition, Hydrochloric (HCl), sulphurous (H_2SO_3), and phosphoric (H_3PO_4) acid, at varying strengths, have all been used as the acidifying reagent.

Thus I infer that changes in %C and %N (and therefore C/N values) are not necessarily linear or proportional and may show significant within and between method variability in results from the same sample material (e.g. King et al, 1998; Lohse et al, 2000; Schubert and Nielsen, 2000; Ryba and Burgess, 2002; Schmidt and Gleixner, 2005; Fernandes and Krull, 2008). Schmidt and Gleixner (2005) calculated relative change in C/N values of bulk OM before and after acidification by Hydrofluoric acid on 20 different soils and shales. They reported that acid treatment altered the chemical composition of bulk OM through hydrolysis, changing C/N values in a range of +1 to +19%, concluding that this was driven primarily by loss of N-rich materials (e.g. proteins, amino acids and polysaccharides): this conclusion is similar to that of Ostle et al (1999). These compounds are typically enriched in ^{13}C, and their loss would inevitably lead to a depletion of $\delta^{13}C$. These inconsistencies suggest there is a need for a systematic study to investigate within and between method variability on C/N and $\delta^{13}C$ values from different environmental materials.

C/N ratios tend to range from 3 to 9 (aquatic; protein rich), 10 to 20 (aquatic/terrestrial sources) and > 20 (terrestrial biomass; protein poor) and are widely interpreted as an indicator for fraction of terrestrially derived OC in marine systems and changes in allochthonous and autochthonous OC in freshwater systems (e.g. Meyers, 1997; Sharpe, 2007). Specifically, C/N ratios are more likely indicators of terrestrially derived organic N in these environments (cf. Perdue and Koprivnjak, 2007). Isotope values ($\delta^{13}C$) of OM can range from ≈ –6 to –35 ‰ (see overviews in Tyson, 1995; Meyers, 1997; Sharpe, 2007), and can differentiate between C_3 ($\delta^{13}C \approx -22$ to –35 ‰) and C_4 plants ($\delta^{13}C \approx -6$ to –15 ‰) in certain environments (e.g. lakes, soils) whilst IC is enriched in ^{13}C relative to OC with values ranging from –15 to +10 ‰ (freshwater to Proterozoic marine IC, Hoefs, 1973; Sharpe, 2007). Larson et al. (2008) noted that even minor amounts of IC (less than 1% by mass) could lead to an overestimation of % C and significantly enrich $\delta^{13}C$ in the sample measured for OC. For a hypothetical sample with 1% IC ($\delta^{13}C \approx -3$ ‰) and 12% OC ($\delta^{13}C \approx -25$ ‰), $\delta^{13}C$ would be enriched by 1.8 ‰ which is significantly greater than instrument precision, the offset increasing with increasing amounts of IC. In addition, algae, for example, preferentially utilise ^{12}C to produce organic matter that averages 20 ‰ lower than IC $\delta^{13}C$ forming from the same dissolved inorganic carbon pool (Leng et al. 2005).

This chapter presents the results of the first systematic comparison of the three most common acid treatment methods on a range of terrestrial and aquatic materials, from modern and geological settings. I examine the effect of acid treatment on the reliability of C/N and $\delta^{13}C$ values from these environments and test the null hypothesis that there is no significant difference in C/N and $\delta^{13}C$ results between acid treatment methods. The three most common methods are: (1) acidification followed by sequential water rinse ("rinse method"; e.g. Midwood and Boutton, 1998; Ostle et al. 1999; Schubert and Nielsen 2000; Galy et al, 2007); (2) acidification in silver capsules ("capsule method"; e.g. Verardo et al. 1990; Nieuwenhuize et al. 1994a; 1994b; Lohse et al. 2000; Ingalls et al, 2004); and (3) acidification by exposure of the sample to an acid vapour ("fumigation method"; e.g. Harris et al. 2001; Komada et al. 2008). In contrast, measurements for N (elemental and isotopic) are commonly undertaken on untreated sample material (e.g. Muller, 1977; Altabet et al, 1995; Schubert and Calvert, 2001; Sampei and Matsumoto, 2008).

2.2 Sample materials

For this study 7 environmental materials were selected that represent both aquatic (marine and freshwater) and terrestrial settings (Table 2.1). Modern and geological samples which vary in their IC, OC and total nitrogen content were used, giving a range of refractory OC and total nitrogen content as well as different $\delta^{13}C$ values. All sample materials were freeze dried and freeze milled in a Spex Centriprep 6850 freezer miller impact grinder (cooled by liquid nitrogen). Freeze-drying reduces the likelihood of the volatile organic losses possible from oven drying (e.g., Talbot, 2001). Freezer milling, relative to ball milling and hand grinding, reduced the likelihood of loss of volatile organic materials and the generation of black carbon, and negates the effect of poor homogenisation of C and N within the sample (e.g. Baisden et al, 2002). All samples were finely ground to achieve grain size $\leq 63\ \mu m$.

Table 2.1: Description of sample materials. Values for %C, %N, C/N value and δ^{13}C are reported where known. [1]International organic soil standard from LECO corporation (part no. 502 – 308). [2]Internal NIGL laboratory standard. [3,4]Measured on untreated sample material. Values are calibrated to V-PDB against standards NBS-18 and NBS-19, and crossed checked with NBS-22.

Sample Identifier	**Location**	**Description**	**%C**	**%N**	**C/N**	**δ^{13}C (‰)**
SOILB[1]	–	International soil standard from LECO corporation (Soil 502-308; LECO, 2010)	3.00±0.05	0.20±0.01	15.0	–24.3±0.1
BROC[2]	52°49’51.69” N, -1°15’10.61” E	*Brassica oleracea* (broccoli). Plant grown in Nottingham University field trials at Sutton Bonnington	41.8±0.05	4.4±0.01	9.5	–27.4±0.1
ALGAE[3]	52°54’22.93” N, -1°13’52.57” E	Filamentous green algae Cladaphora from Attenborough Ponds, Nottingham.	16.2±0.05	1.7±0.01	9.5	–26.9±0.2
NEW	53°04’5.04” N, -1°13’17.05” E	Surface sediment sample from carbonate rich Newstead Abbey lake	-	-	-	-
TYC[4]	20°31’1.11” N, 110°18’43.02” E	Down-core lake sediment sample from maar Lake Tianyang, south China (6.62 m depth).	5.82±0.05	0.14±0.01	41.6	–16.8±0.2
GRN	68°58’0.77” N, 53°11’1.19” E	Marine surface sample from Egedesminde Dyb, Disko Bugt, Greenland (846 m below sea level).	-	-	-	-
MOR	38°01’56.34” N, 14°50’39.67” E	Middle Miocene marine marl sediment (coccolith dominated) from Moria, Itlay.	-	-	-	-

2.3 Sample preparation methods

2.3.1 Cleaning protocol

Prior to sample preparation, stainless steel sampling equipment and glassware (e.g. beakers; volumetric flasks) were acid washed in 1% nitric acid, rinsed in deionised water, then washed in 2% neutracon® solution, followed by a final rinse in deionised water before being heated to 550°C for 3 h. For the capsule and fumigation methods, Ag capsules were pre-combusted (550°C for 3 h) to remove organic contaminants. For the fumigation method, the desiccator was bathed in neutracon® for 24 h and then preleached in the chosen acid for each individual experiment. It is imperative that any grease sealant on the desiccator rim is removed using an acetone followed by deionised water rinse prior to cleaning. Schubert and Nielsen (2000) reported that the grease sealant can significantly shift isotopic values (up to –12 ‰), particularly in samples with low OC, because it is readily volatilised by acid vapour. Laboratory gloves were worn throughout the cleaning and sampling procedures to minimise the risk of contamination.

2.3.2 Acid reagents

The three acid reagents chosen for this study (HCl, H_2SO_3, H_3PO_4) represent those most commonly used for IC dissolution and are all non-oxidising reagents. Acid concentration is reported in % w/w but molarity and normality equivalents are given in Table 2.2. The HCl was Fisher Trace Analysis Grade (H/1190/PB17) which has a stock concentration of 36%. The concentration of HCl reported in the literature varies significantly (in the range of 1 – 36% w/w) (e.g. Froelich, 1980; Bird et al. 1994; Schubert and Nielsen, 2000). For the capsule and rinse methods, 5%, 10% and 20% w/w HCl concentrations diluted into pre-cleaned volumetric flasks were used. The 20% HCl treatment was selected as Larson et al (2008) reported it to be an effective agent for the dissolution of siderite. The fumigation method was undertaken using 20% and 36% w/w HCl as it readily volatilises at these strengths and can therefore develop and maintain a more strongly acidic vapour relative to weaker solutions. HCl is widely reported to react quantitatively with IC fractions but can also affect OM (e.g. King et al, 1998; Lohse et al, 2000).

The H_2SO_3 used was Fisher Laboratory Grade (J/8500/17) with a stock of 6% w/w concentration. McNicholl et al (1994) and Caughey et al (1995) noted that commercially available H_2SO_3 can contain measurable amounts of C because chemical production companies do not generally assay H_2SO_3 for C. Caughey et al (1995) further noted for 6% w/w H_2SO_3, a minimum of 1 ml was required to dissolve 0.36 mg of calcite. Although H_2SO_3 does not readily react with labile organic compounds, it is significantly less corrosive to robust IC minerals such as dolomites and siderites (e.g. Chang et al, 1996). Losses of C using H_2SO_3 have been reported at < 2% (Gibbs, 1977; Caughey et al, 1995). H_3PO_4 used was Fisher Trace Analysis Grade (O/0503/PB17) with a stock of 98% w/w concentration from which a 6% w/w concentration was diluted. Losses of OC (from ~2% to 45%) for all acids used in this study have been reported (e.g. Gibbs, 1977; Froelich, 1980; King et al, 1998; Lohse et al, 2000) with drying cycles proposed to exacerbate these losses through volatilisation (Bisutti et al, 2004).

Table 2.2: Acid strength conversion

Acid	Molarity	Normality
HCl % w/w		
36% stock	11.64	11.64
20%	6.02	6.02
10%	2.87	2.87
5%	1.40	1.40
H_2SO_3 % w/w		
6% stock	0.73	1.46
H_3PO_4 % w/w		
98% stock	18.44	55.32
6%	0.63	1.89

2.4 Acidification Methods

Before the three sample treatment methods were tested, an estimation of %C was made on NEW, TYC, GRN and MOR by acidifying samples with 5% HCl and analysing them by elemental analyser. An investigation into the effect of sample size on %C and %N values was also undertaken on a range of untreated sample weights on SOILB and BROC, chosen due to the abundance of material, their known composition and their negligible IC content. Together, this allowed for a sufficient weight of sample to be weighed out and treated for ‘small’ (~90 µg C for the capsule and fumigation methods) and ‘normal’ (~500 µg C for all 3 methods) C/N and $\delta^{13}C$ analysis. All acidifications for each method were carried out in triplicate to ensure accurate and precise analytical data. A description of the acidification methods is provided below.

2.4.1 Rinse Method

Approximately 250 mg of sample material was placed in a 500 ml beaker and 50 ml of the chosen acid reagent added and left for 24 h. Depending on the IC content, additional acid was added to maintain an acidic solution (checked with litmus paper) and left for a further 24 h if necessary. An aliquot was collected to assess the amount of solubilised OM by UV-Vis analysis and to characterise the IC chemistry by analysis of the Ca, Mg, Mn, and Fe concentrations by Atomic Absorption Spectrophotometry (AAS). After 24 h, the beaker was topped up to 500 ml with deionised water and the sample material allowed to settle for a further 24 h. Once settled, the supernatant was decanted, ensuring minimal disturbance of the remaining material, and the beaker then topped up again to 500 ml with deionised water. Dilution was repeated 3 times in total with an overall minimum of 1200 ml of deionised water used. After the final decanting, the excess water (50 to 100 ml) was allowed to evaporate in a drying oven at ~50^{o}C. Once dry, the sample was loosened from the base of the beaker with a clean plastic spatula and transferred to an agate pestle and mortar, ground, and a known quantity weighed into a tin (Sn) capsule (~500 µg C after IC treatment in all rinse samples). Capsules were then crimped. During the decanting process, where any visible sample loss occurred, these samples were discarded and the treatment repeated.

2.4.2 Capsule Method

This method involved in-situ acidification of sample material within a silver (Ag) capsule (the receptacle into which the sample is introduced to the elemental analyser) and is adapted from the method described by Verardo et al (1990). Acidification was carried out in Ag capsules with additional samples further wrapped in Sn (designated Ag+Sn). The lower melting point of Sn (232^{o}C) relative to Ag (962^{o}C) may help improve the combustion of samples in the reaction tube due to a momentary exothermic flash combustion from Sn capsules.

The samples were weighed into open Ag capsules (to provide ~90 µg “small” and ~500 µg “normal” C after acidification) and recorded. The capsules were then transferred on a metal tray to a cold hotplate in a fume cupboard and 10 µl of distilled water was added to moisten the samples. This reduces the potential of an initial vigorous reaction from IC bearing materials that can lead to sample spitting or rapid capillary action causing effervescing material in the capsules to overflow. After moistening, 10 µl of the chosen acid reagent was added to the cold sample before the hotplate temperature was slowly increased to ~50^{o}C. Additional acid was then added in steps of 10 µl, 20 µl, 30 µl, 50 µl and 100 µl without allowing the sample to dry out between additions. The samples were monitored for signs of effervescence indicating an IC reaction. Monitoring was initially achieved by visual inspection but as the effervescence reduced, the reaction was checked using a binocular microscope at 50x magnification. The stepped addition of acid described here reduced problems associated with the ambiguous effervescence end-point; however, a final 200 µl of acid was added to act as a “fail safe”. Lukasewycz and Burkhard (2005) reported that results for %C in surficial sediment from Lake Michigan varied between 3.3 and 4% as a result of the subjective nature of the effervescence end-point.

After the addition of the final aliquot of acid the capsules were left on the hotplate for ~1 h to dry thoroughly. Depending on the acid used and the IC content of the material, hygroscopic salt deposition was observed during this stage (e.g. Larson et al, 2008), particularly on samples with appreciable IC content (e.g. MOR). Once dry, the capsules were removed from the hotplate and left to cool before being crimped. Occasionally, there was sample loss from the capsule, especially at the reaction stage on samples with IC, due to “spitting” or rapid capillary action over spilling the capsule rim; these samples were discarded and the treatment repeated.

2.4.3 Fumigation method

The fumigation method involved placing the sample in an Ag capsule that was subjected to continuous acidic vapour (e.g. Harris et al, 2001). The samples were weighed into open Ag capsules (to provide ~90 µg “small” and ~500 µg “normal” C after IC treatment) and recorded and then transferred to a sample tray. Approximately 50 µl of deionised water was added to each capsule – this allowed acid fumes to dissolve into the water creating an acidic solution to attack sample IC (cf. Yamamuro and Kayanne, 1995; Harris et al, 2001; Komada et al, 2008). The fumigation method can be less effective on dry materials, particularly those high in IC, where salt crystallisation may encapsulate unreacted IC (e.g. Hedges and Stern, 1984). Approximately 50 ml of the chosen acid was added to a prepared glass container and placed in the base of the desiccator. A mass balance was calculated to ensure enough acid was available to neutralise sample IC, assuming 100% IC in each sample. An acid proof shelf (thoroughly rinsed in deionised water) was placed in the desiccator and the sample tray was rested on top. The desiccator was placed under vacuum and the samples left to fumigate for ~6 h (after Harris et al, 2001). Komada et al (2008) reported an increase in contaminant C by up to ~50% with fumigation times greater than 10 hours. After ~6 h, the sample tray was removed and samples were allowed to dry over a hotplate at ~50^{o}C. Once dry, capsules were crimped.

2.5 Analytical methods

2.5.1 C/N and δ^{13}C

%C, %N and ^{13}C/^{12}C ratios (*δ^{13}C values*) of sample OM were analysed using an online system comprising a Costech ECS4010 elemental analyser (EA), a VG TripleTrap, and a VG Optima mass spectrometer at the NERC Isotope Geosciences Laboratory, with data reduction carried out using DataApex Clarity ver 2.6.1 software package. The samples in the Sn (rinse method) or Ag±Sn (capsule/fumigation method) were placed in the carousel of the elemental analyser. The samples are sequentially dropped, in a continuous flow of helium carrier gas, into a 1020^{o}C furnace (to promote rapid and complete sample and capsule combustion). A pulse of oxygen gas promotes exothermic flash oxidation of the foil capsules, and the product gases are further oxidised by chromium and silver cobaltous oxide (CoO) in the lower part of the EA furnace. After removal of excess oxygen and water by passage through hot copper and magnesium perchlorate (which reduces nitrogen oxides to N_2 and removes water), the remaining CO_2 and N_2 then pass through a GC column to separate them prior to quantification using a thermal conductivity detector. The Clarity software package acquires and evaluates this information, producing %C and %N data for the sample. The helium stream then carries the CO_2 and N_2 through a trap at –90^{o}C (for complete removal of water), before reaching the Triple Trap held at –196^{o}C. Here the CO_2 is frozen, allowing the N_2 and helium to vent to atmosphere. The TripleTrap is then evacuated before warming and expanding the sample CO_2 into the inlet of the Optima. For very small samples (within the capsule and fumigation methods described here), a secondary cryogenic trap in the mass spectrometer was used, which introduces the CO_2 directly into the source. Each run contains 10 replicates of the laboratory primary standard (BROC) and a secondary standard. From knowledge of the laboratory standard's δ^{13}C value versus V-PDB (derived from regular comparison with international calibration and reference materials NBS-18 and NBS-19 and cross checked with NBS-22), the ^{13}C/^{12}C ratios of the unknown samples were converted to δ^{13}C values versus V-PDB as follows: $\delta = [(R_{sample}/R_{standard}) - 1].10^3$ (‰), where R = the measured ratio of the sample and standard respectively.

Three control materials were included in each analytical run: external standard SOILB (2 replicates; see Table 2.1), internal NIGL standard BROC (10 replicates; see Table 2.1) and independent external standard SOILC (2 replicates; LECO corporation organic standard, part no. 502 – 062). SOILC is a low organic standard reference material with known values: 0.83±0.02% for %C, 0.1±0.002% for %N and –17.3±0.2 ‰ for $\delta^{13}C$. All standards returned values that were statistically insignificant from known sample values (p-value > 0.05) indicating that our analytical measurements were accurate and precise.

2.5.2 Supernatant analysis

The supernatant collected from the rinse method was analysed for dissolved components. An aliquot from the first 400 ml was analysed for %OC using a Cary 50-Bio UV-Vis Spectrometer. Samples were scanned at the 254 nm wavelength following standard aqueous analysis methods (Eaton et al., 1995) and used as an indicator of % total dissolved OC. Measurements were calibrated against a Potassium Hydrogen Phthalate standard (stock produced as 2.1254 g in 1000 ml). Samples were measured four times and an average derived and reported in mg/l. The %C removed from the total sample OC was estimated as:

%C removed from the total available OC = (mg OC in supernatant / weight of sample material treated (mg)) * 100

where “mg OC in supernatant” is taken from the calibrated UV-Vis measurement. The supernatant was further analysed for Ca, Mg, Fe, and Mn using a Varian Spectra 220 FS AAS spectrometer and the SpectraAA software package. Concentrations were calculated following an integration procedure and measured in triplicate for 5 s each with a 5 second delay between measurements. Mg samples were spiked with 1000 µg ml^{-1} Lanthanum Chloride to reduce molecular interferences due to the proximity of the Mg wavelength to 200 nm. Measurements for UV-Vis and AAS were corrected for matrix effects of the acid reagents.

2.6 Data analysis

Acid treatments within each sample material were compared with one another, and where applicable assayed or untreated sample values by one-way analysis of variance (ANOVA) at the $\alpha = 0.05$ significance level. All data were checked for normality using a Shapiro-Wilk test prior to analysis, and where non-normally distributed were $\log_{10}$ transformed before analysis. A p-value < 0.05 is used to indicate a statistically significant difference. An assessment of the % relative proportional change of %C, %N and C/N was derived from

% Proportional change = $((X_{\text{acidified}} - X)/X)*100$

where X = known (SOILB), untreated (BROC, ALGAE), or mean values (NEW, TYC, GRN, MOR) of sample materials.

2.7 Results

2.7.1 Determination of carbon blank

Capsule and acid blanks were analysed to test for C and N contamination. Ag capsules were acid treated in triplicate with an additional batch prepared to further wrap in Sn capsules. I also measured untreated Ag, Sn and Ag+Sn capsules. Blanks were measured using the same analytical procedure as the samples. Capsule and acid blanks recorded values below machine detection limit. However, 6% H_3PO_4 significantly elevated blank values (22 µg of C and 17 µg N) suggesting a source of contamination.

2.7.2 Effect of sample size on %C and %N

Untreated samples of SOILB and BROC with a range of weights from 10 to 450 µg C and 1 to 60 µg of N were analysed for %C and %N respectively. The data (Figure 2.1) show relatively consistent %C and %N values down to 120 µg C ($1\sigma = 0.14$) and 10 µg N ($1\sigma = 0.04$) for SOILB and 80 µg C ($1\sigma = 1.0$) and 10 µg N ($1\sigma = 0.7$) for BROC (Kendrick, 2009). Below these sample weights, %C and %N values are overestimated by up to 1.2% for C ($1\sigma = 6.9$) and 0.6% for N ($1\sigma = 0.4$) for SOILB and 15.3% for C ($1\sigma = 6.9$) and 51.2% for N ($1\sigma = 17.1$) for BROC, thus returning inaccurate results. This analytical artefact is the result of the difficulty distinguishing the CO_2 and N_2 measured peak areas generated from the sample relative to the baseline conditions. This problem will vary between instruments and therefore the accuracy of small sample analysis could differ significantly between laboratories and have implications for "dual-mode" analysis (simultaneous measurement of C and N). Our analysis here has shown that the extent of overestimation can vary significantly between sample materials (e.g. between environments).

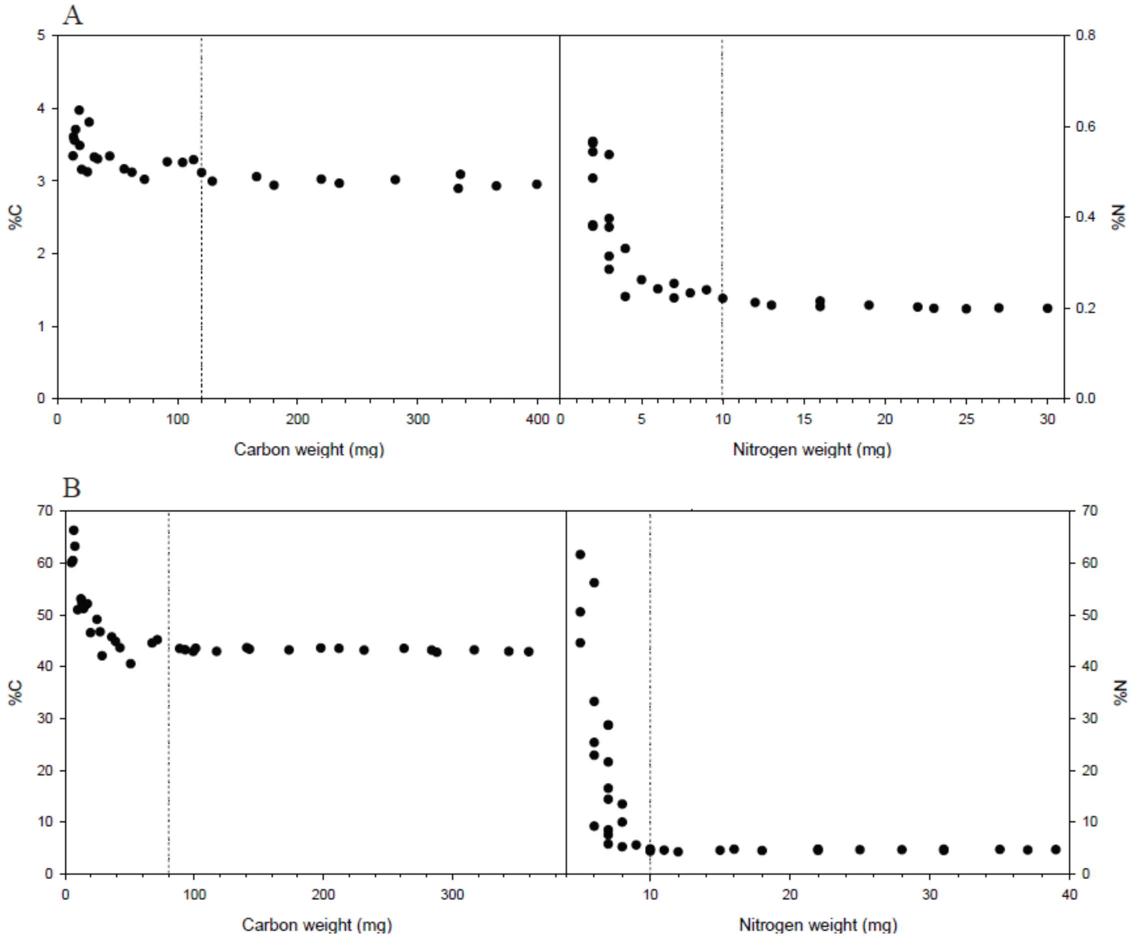

Figure 2.1: Changes in %C and %N in SOILB (A) and BROC (B) as a function of sample size

2.7.3 Small versus normal sample sizes in our sample materials

Where sample sizes approach the threshold limit (see Figure 2.1)("small" sample sizes) any reactive loss of C and N may move these samples across the threshold. Normal sample sizes (~ 500 μg C) are deemed safely removed from the threshold. ANOVA results of 'small' and normal' analyses data from the capsule method are in Table 2.3. For %C, %N, C/N and δ^{13}C, the majority of the data were significantly different ($p < 0.05$; highlighted in grey boxes). Generally, 'small' sample size data consistently overestimated %C and %N with offsets in δ^{13}C upwards of 0.6 ‰ (with no clear trend in either enrichment or depletion). Therefore, the %C, %N, C/N and δ^{13}C values for each sample material, across all methods and acids presented in Figures 2.2 – 2.8, are plotted from 'normal' sample size data. Data are reported as the mean ± standard deviation (σ) and C/N data is reported as a mass ratio.

Table 2.3: Results of ANOVA for "small" versus "normal" sample size analysis in capsule method. Comparisons are significantly different where P-value < 0.05 (highlighted in grey boxes).

		5% HCl				**10% HCl**				**20% HCl**				**6% H_2SO_3**				**6% H_3PO_4**			
		%C	**%N**	**C/N**	**$\delta^{13}C$**	**%C**	**%N**	**C/N**	**$\delta^{13}C$**	**%C**	**%N**	**C/N**	**$\delta^{13}C$**	**%C**	**%N**	**C/N**	**$\delta^{13}C$**	**%C**	**%N**	**C/N**	**$\delta^{13}C$**
BROC	P-value	0.04	0.00	0.00	0.08	0.08	0.01	0.00	0.30	0.03	0.05	0.02	0.04	0.18	0.06	0.04	0.88	0.31	0.25	0.00	0.06
	R-squ	49.85	79.05	88.41	37.90	38.61	62.83	81.12	10.62	51.26	44.30	59.72	50.38	23.37	44.88	50.71	0.00	9.92	15.10	72.60	44.41
ALGAE	P-value	0.01	0.67	0.01	0.06	0.04	0.22	0.00	0.01	0.00	0.01	0.01	0.04	0.02	0.01	0.01	0.76	0.00	0.00	0.09	0.00
	R-squ	69.93	0.00	62.37	43.35	46.02	18.44	93.94	47.85	73.66	64.79	70.47	50.57	60.02	64.92	64.70	0.00	97.22	94.71	35.94	76.65
SOILB	P-value	0.00	0.00	0.01	0.00	0.00	0.00	0.00	0.00	0.21	0.03	0.00	0.00	0.03	0.06	0.04	0.01	0.00	0.01	0.01	0.04
	R-squ	73.32	92.78	67.87	76.96	82.63	96.42	75.83	81.42	19.05	52.65	78.87	84.64	50.66	46.71	47.53	64.72	80.15	67.85	60.69	79.82
NEW	P-value	0.00	0.04	0.00	0.00	0.01	0.00	0.00	0.13	0.00	0.00	0.00	0.01	0.01	0.70	0.04	0.00	0.11	0.23	0.24	0.57
	R-squ	83.96	47.08	84.53	93.90	66.11	94.97	94.91	29.59	82.84	75.18	78.83	63.57	67.82	0.00	49.80	78.19	31.98	17.24	16.78	0.00
TYC	P-value	0.33	0.00	0.62	0.39	0.00	0.00	0.01	0.08	0.53	0.35	0.02	0.00	0.00	0.19	0.01	0.02	0.01	0.20	0.00	0.09
	R-squ	8.73	77.10	0.00	3.50	75.94	76.34	61.75	31.52	0.00	6.80	55.75	81.04	78.18	21.57	61.18	57.21	62.44	20.55	87.58	37.12
GRN	P-value	0.24	0.30	0.00	0.00	0.14	0.00	0.00	0.00	0.02	0.00	0.00	0.00	0.00	0.13	0.00	0.07	0.00	0.00	0.01	0.00
	R-squ	16.83	11.26	83.25	81.45	27.92	85.46	95.03	92.12	58.25	87.63	89.43	71.36	89.34	28.95	81.36	41.37	95.44	86.86	69.00	95.06
MOR	P-value	0.00	0.91	0.09	0.00	0.00	0.00	0.00	0.00	0.00	0.00	0.765	0.00	0.00	0.00	0.00	0.00	0.00	0.00	0.03	0.00
	R-squ	71.39	0.00	36.78	79.97	75.13	84.60	71.36	74.34	81.34	87.29	0.00	89.35	94.75	95.57	93.44	99.44	77.08	72.44	51.58	94.20

2.8 Sample material results

2.8.1 Materials from known values

The external C certified international soil standard, SOILB, and internal standard material, BROC, show significant variability within and between methods. For SOILB, %C and C/N showed the greatest variability within and between methods, particularly in the capsule method (Figure 2.2). The C/N values ranged from 13.2 to 19.3 calculated from %C and %N of acidified samples and from 9.1 to 17.3 calculated from %C of acidified samples and %N from untreated samples (p-value < 0.01). The known C/N value is 15.0. δ^{13}C ranged from –24.1 to –25.3 ‰ (known value –24.3 ‰), with the rinse method data higher relative to known values, and the capsule and fumigation method data. ANOVA between the acid treatment methods confirm that 6% H_3PO_4 capsule was significantly lower than all other treatments and known values for %C (p-value $= 0.03$), %N (p-value $= 0.01$), C/N (p-value $= 0.02$) and δ^{13}C (p-value < 0.01). The 20% HCl capsule for δ^{13}C was also significantly lower (p-value < 0.01) and the 36% HCl fumigation method was significantly higher for C/N (p-value < 0.01). Comparison of acid reagent strength within methods (e.g. 5% HCl versus. 10% HCl versus 20% HCl) showed 20% HCl to produce lower values for C/N and δ^{13}C relative to other acid reagents within and between methods (p-value < 0.01). Samples in Ag only capsules generally produce lower values relative to samples in Ag+Sn capsules for %C, %N, C/N, but higher values for δ^{13}C (Figure 2.2 and Table 2.4 for ANOVA p-value summary for all materials). Loss of OM following the rinse method ranged from 1.1 to 4.0% of the available sample organic carbon with 20% HCl resulting in greatest loss (Figure 2.9). AAS analysis (Figure 2.10) shows Fe as the dominant metal mobilised during acid treatment (~139 mg/l).

BROC showed greatest variability within and between methods for %C and %N (Figure 2.3). The rinse method %C, %N and C/N values were on average higher than the capsule and fumigation results, with the highest mean for %C (42.7%; ~ 4% higher than the capsule and fumigation methods, and ~1% higher than the known value). The 6% H_3PO_4 capsule method gave significantly lower values from all other treated values and untreated values for %C, %N, C/N, but higher δ^{13}C as found for SOILB. C/N values on acidified samples ranged from 7.2 to 13.1 and from 6.1 to 9.6 using measured %C and untreated %N. δ^{13}C ranged from –28.4 to –27.0 ‰, compared with the untreated value of –27.4 ‰ with the rinse method results approximately 1 ‰ more depleted than known, capsule and fumigation results. UV-Vis data indicated a loss of OM from 3.4 to 25.5% (Figure 2.9) of the available OM pool. AAS analysis showed a small flux of Ca and Mg (mean of 13.5 mg/l and 6.5 mg/l respectively)(Figure 2.10).

2.8.2 Other sample materials

Our other sample materials also show significant within and between method variability. For ALGAE, the capsule method showed significantly lower %C and %N values compared with the rinse and fumigation methods (mean difference of c.13% and c.1% respectively; p-value <0.01) and greatest variability for %C, %N and C/N (Figure 2.4). C/N values ranged from 5.9 to 10.8 calculated from %N of acid treated samples, with the capsule method producing values < 10. C/N values calculated from treated %C and untreated %N ranged from 4.3 to 13.6. $\delta^{13}C$ ranged from –27.2 to –27.9 ‰ across all methods, largely influenced by the 6% H_3PO_4 method (0.7 ‰ depletion) and 20% HCl rinse method (0.5 ‰ depletion), with all other measurements within 0.4 ‰. Acid comparison of $\delta^{13}C$ values indicate results using the same strength acid but in a different method were significantly different (e.g. 20% HCl capsule, 20% HCl rinse and 20% HCl fumigation; p-value < 0.01). The effect of capsule type in the 20% HCl fumigation method was particularly pronounced for $\delta^{13}C$ (0.8 ‰ difference). Loss of OM from the available sample OM pool following the rinse method ranged from 1.8 to 3.1% (Figure 2.9). AAS analysis indicated a small amount of leaching of Ca followed by Mn (Figure 2.10).

In NEW, %C, C/N and $\delta^{13}C$ showed the greatest variability within the fumigation method (Figure 2.5). The mean values of %C and %N in the rinse method were notably higher than for the capsule and fumigation methods by ~7% and ~0.8% respectively. C/N values ranged from 7.1 to 13.1, principally influenced by the 6% H_3PO_4 capsule method (driving %N change) and the 20% HCl fumigation method (driving %C change), and were statistically different (p-value = 0.02). Otherwise, C/N values were more consistent than in other materials tested. The range of $\delta^{13}C$ was from –28.5 to –26.8 ‰, largely influenced and weighted by the 20% HCl fumigation method that was ~1.2 ‰ depleted from the mean (p-value < 0.01). For %C and %N, samples in Ag+Sn capsules showed relatively higher values (except for 6% H_3PO_4 which showed slight decreases) and depleted $\delta^{13}C$ values (as much as 0.7 ‰). Loss of OM following the rinse method ranged from 0.6 to 4.0% of the available OM pool (Figure 2.9). AAS results (Figure 2.10) showed a significant amount of Ca after treatment (from 330 to 730 mg/l).

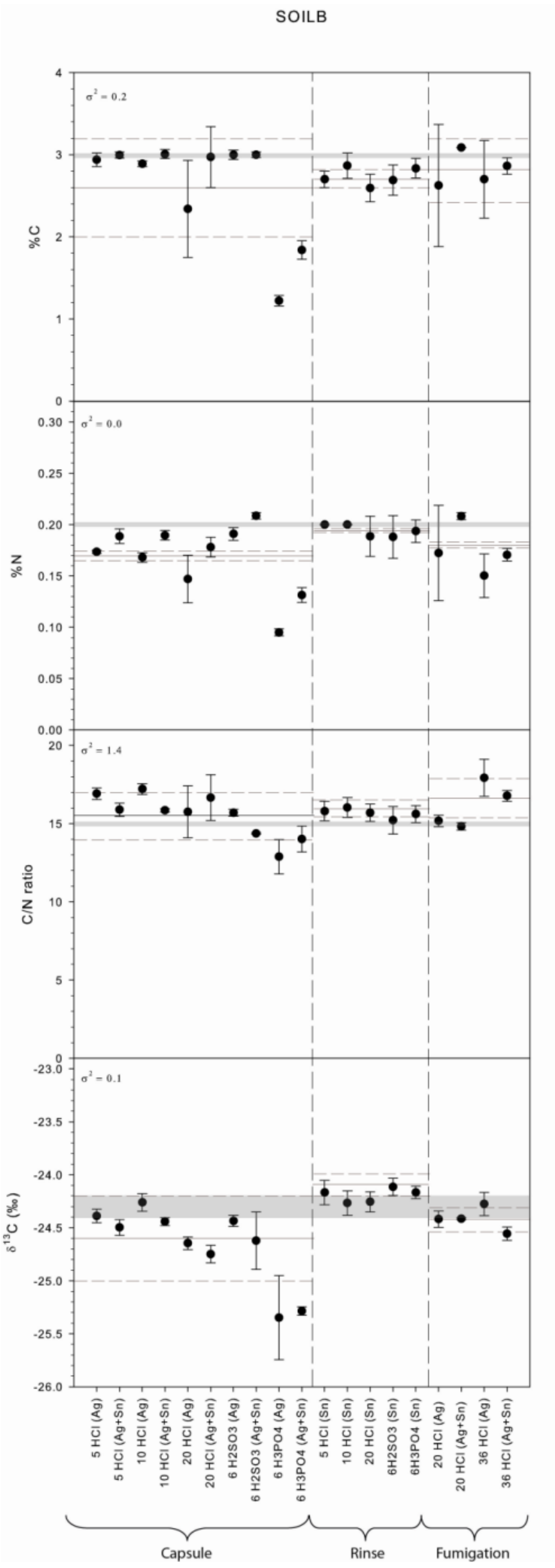

Figure 2.2: SOILB %C, %N, C/N and $\delta^{13}C$ values for each method and acid. Horizontal solid grey lines indicate mean values for each acid treatment method, and perforated grey lines 1σ. Horizontal grey boxes indicate known values. Vertical perforated lines split the capsule, rinse and fumigation methods.

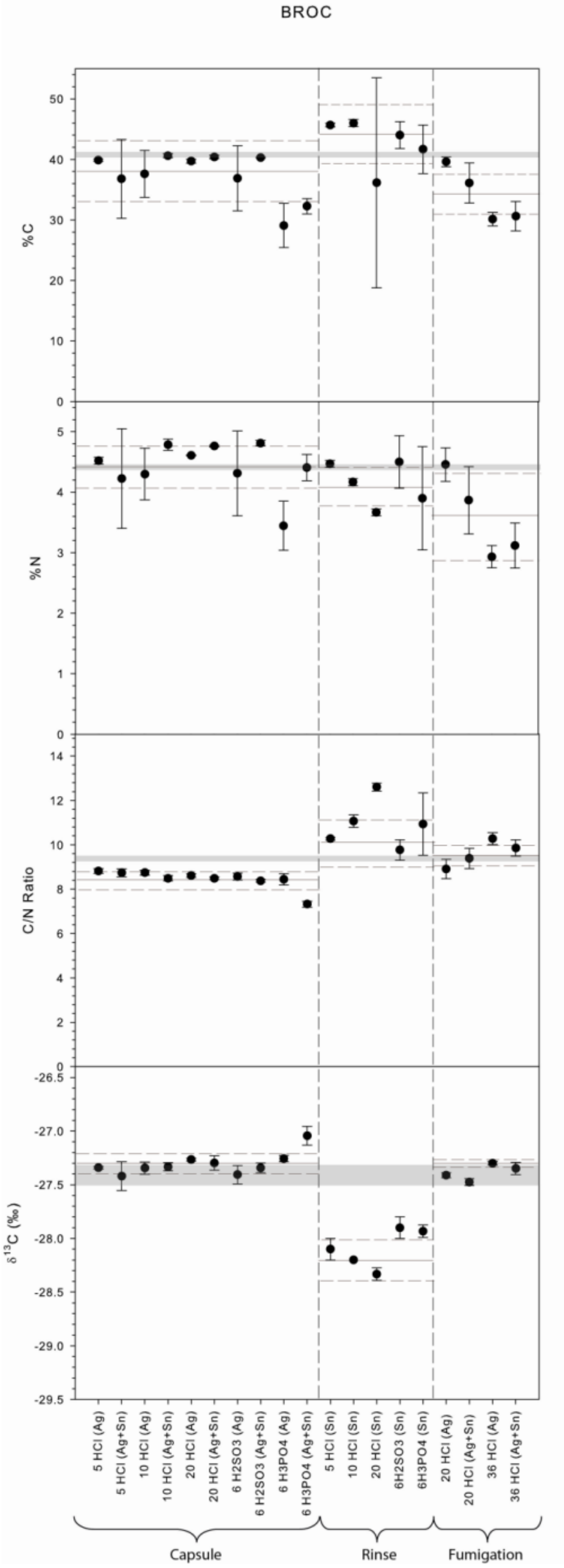

Figure 2.3: BROC %C, %N, C/N and $\delta^{13}C$ values for each method and acid. Horizontal solid grey lines indicate mean values for each acid treatment method, and perforated grey lines 1σ. Horizontal grey boxes indicate known values. Vertical perforated lines split the capsule, rinse and fumigation methods.

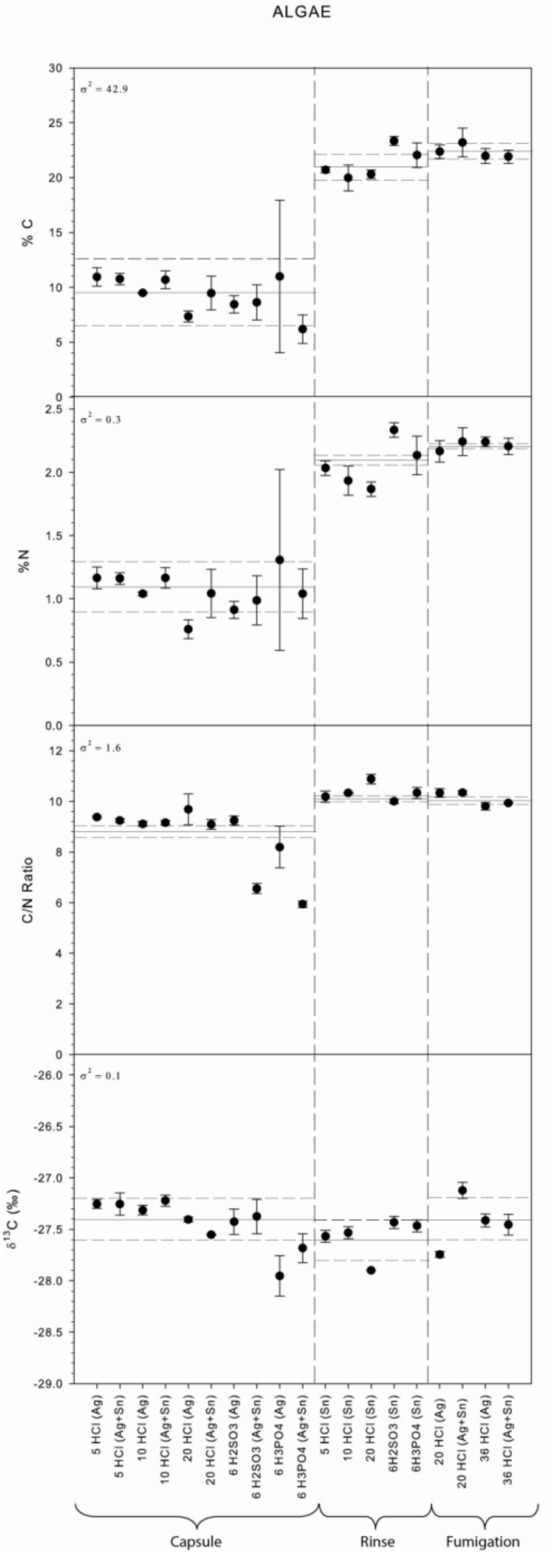

Figure 2.4: ALGAE %C, %N, C/N and $\delta^{13}C$ values for each method and acid. Horizontal solid grey lines indicate mean values for each method, and perforated grey lines 1σ. Vertical perforated lines split the capsule, rinse and fumigation methods.

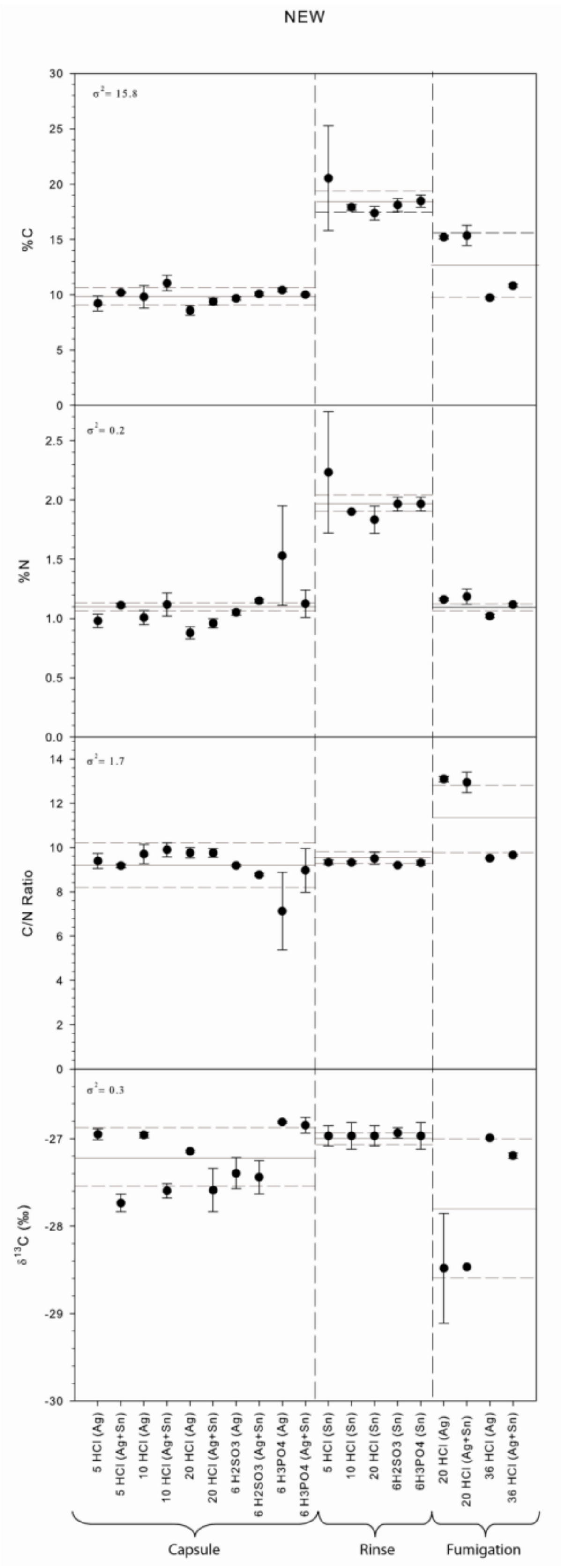

Figure 2.5: NEW %C, %N, C/N and $\delta^{13}C$ values for each method and acid. Horizontal solid grey lines indicate mean values for each acid treatment method, and perforated grey lines 1σ. Vertical perforated lines split the capsule, rinse and fumigation methods.

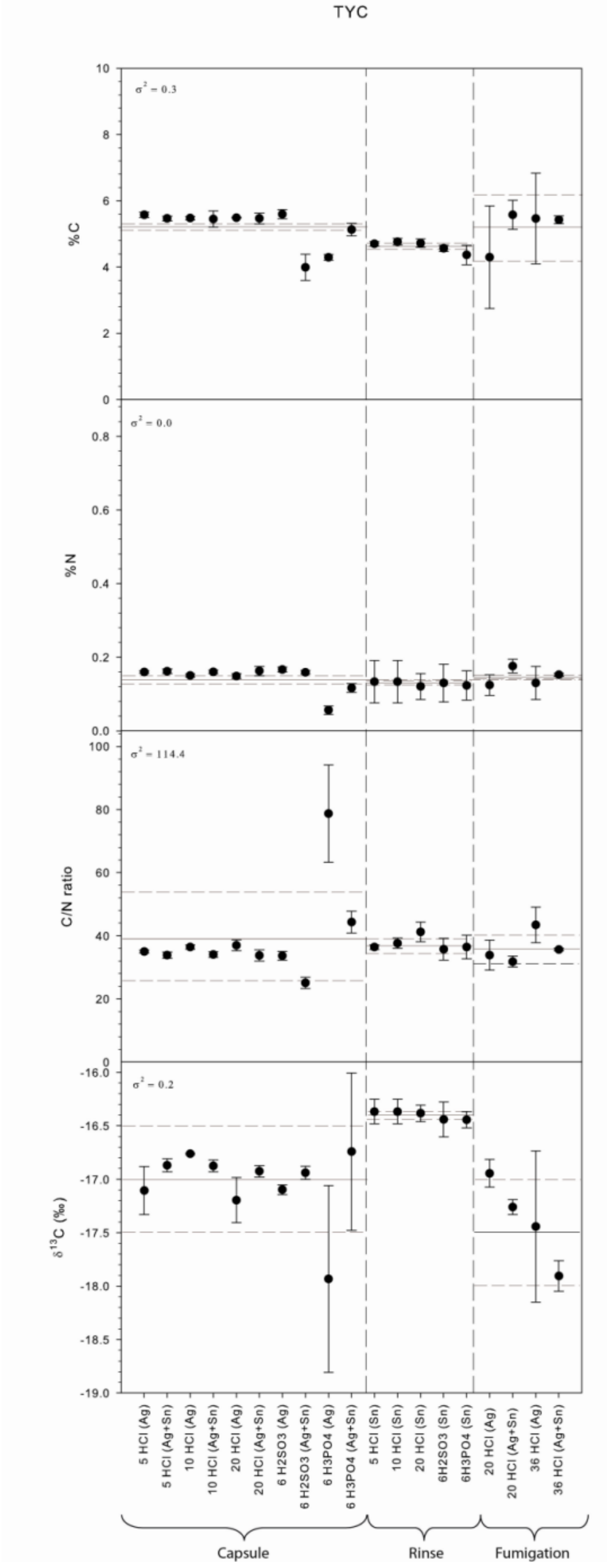

Figure 2.6: TYC %C, %N, C/N and $\delta^{13}C$ values for each method and acid. Horizontal solid grey lines indicate mean values for each acid treatment method, and perforated grey lines 1σ. Vertical perforated lines split the capsule, rinse and fumigation methods.

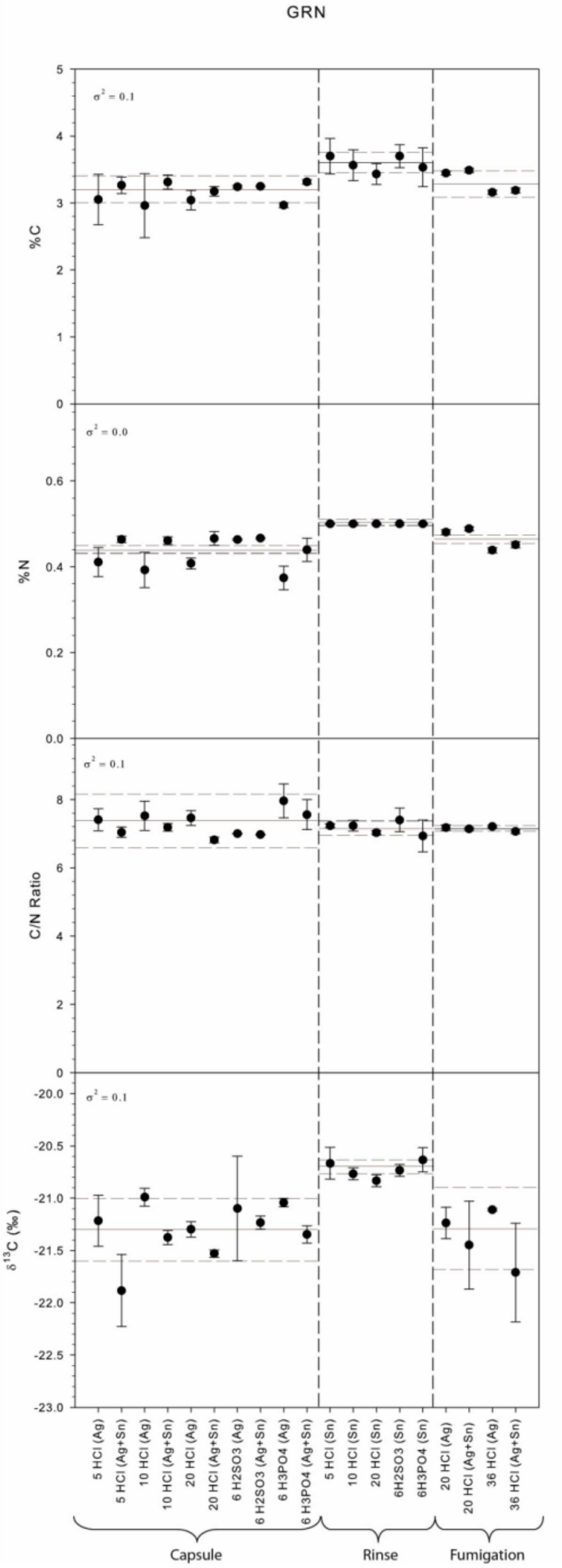

Figure 2.7: GRN %C, %N, C/N and $\delta^{13}C$ values for each method and acid. Horizontal solid grey lines indicate mean values for each acid treatment method, and perforated grey lines 1σ. Vertical perforated lines split the capsule, rinse and fumigation methods.

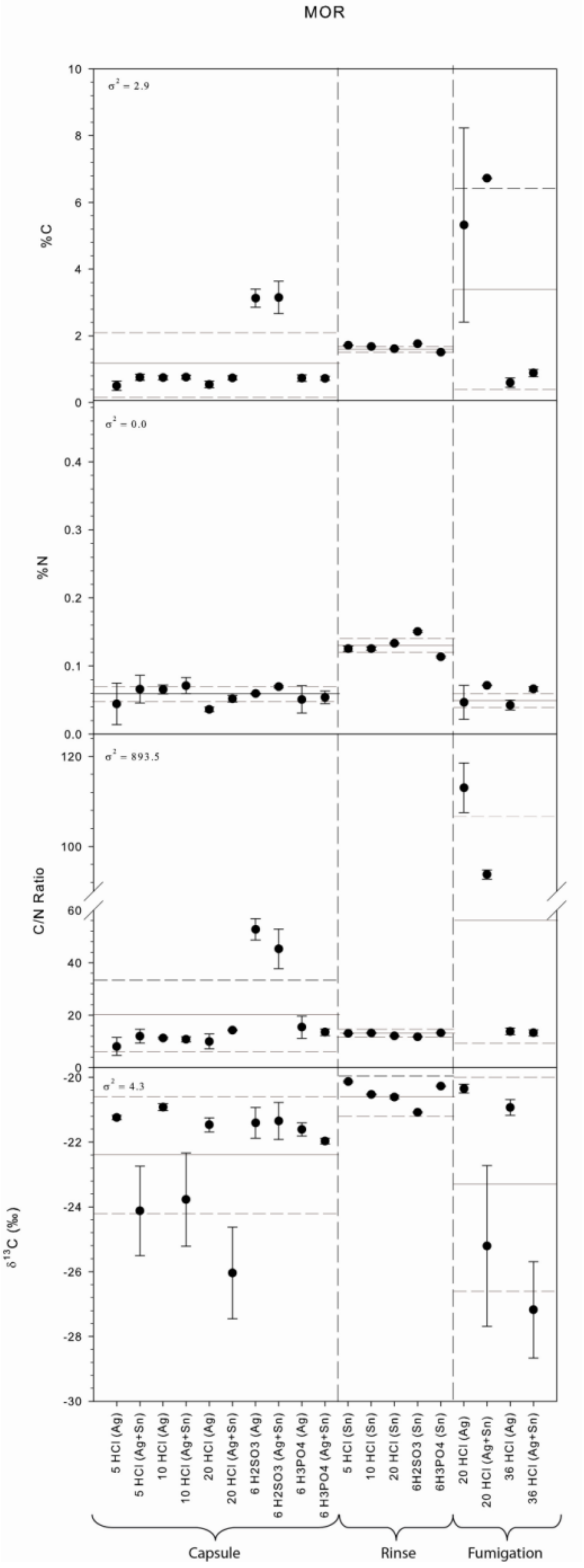

Figure 2.8: MOR %C, %N, C/N and $\delta^{13}C$ values for each method and acid. Horizontal solid grey lines indicate mean values for each acid treatment method, and perforated grey lines 1σ. Vertical perforated lines split the capsule, rinse and fumigation methods.

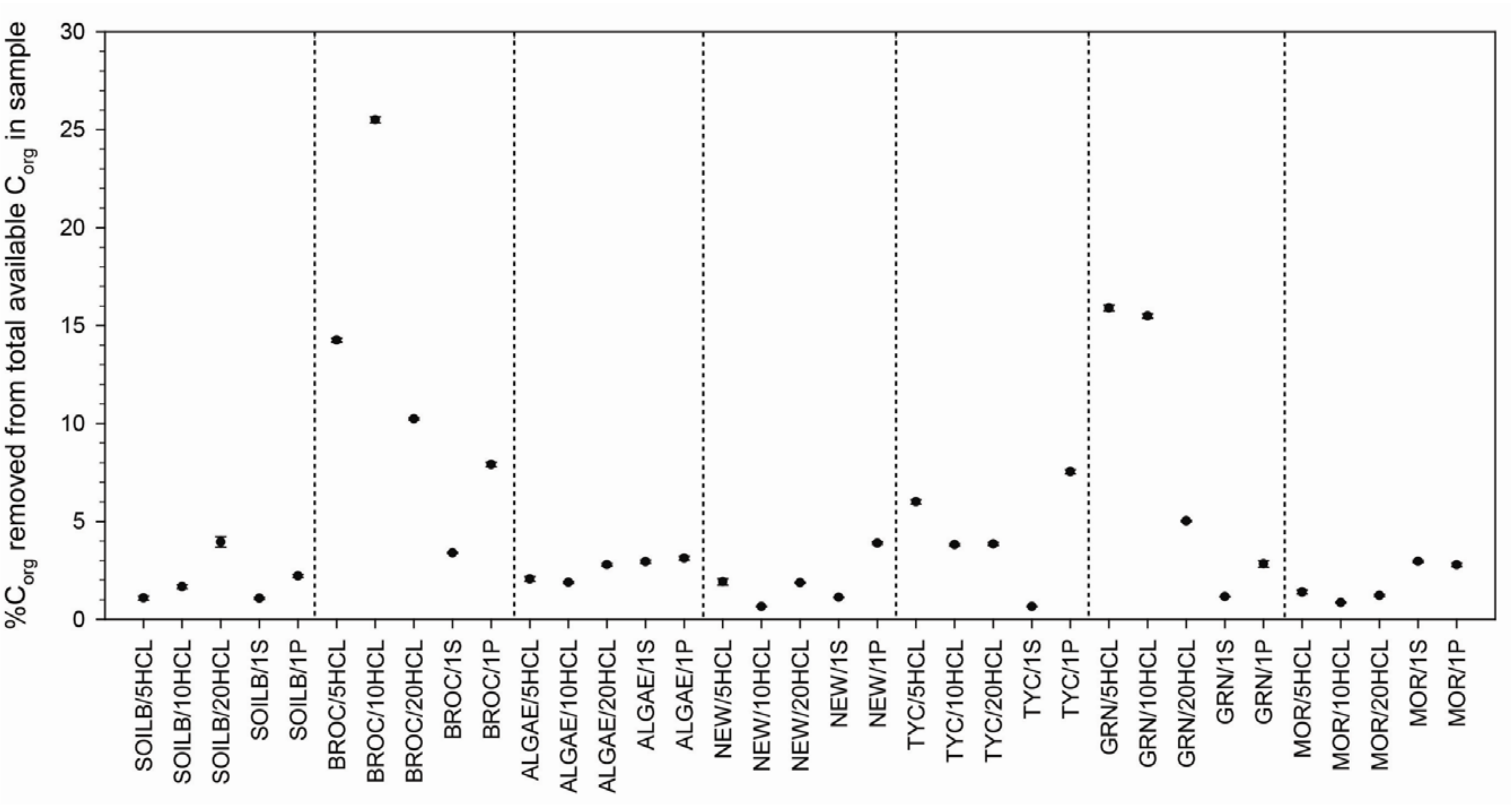

Figure 2.9: %C removed from available C in sample material from rinse method supernatant. Mean values are plotted ±1σ.

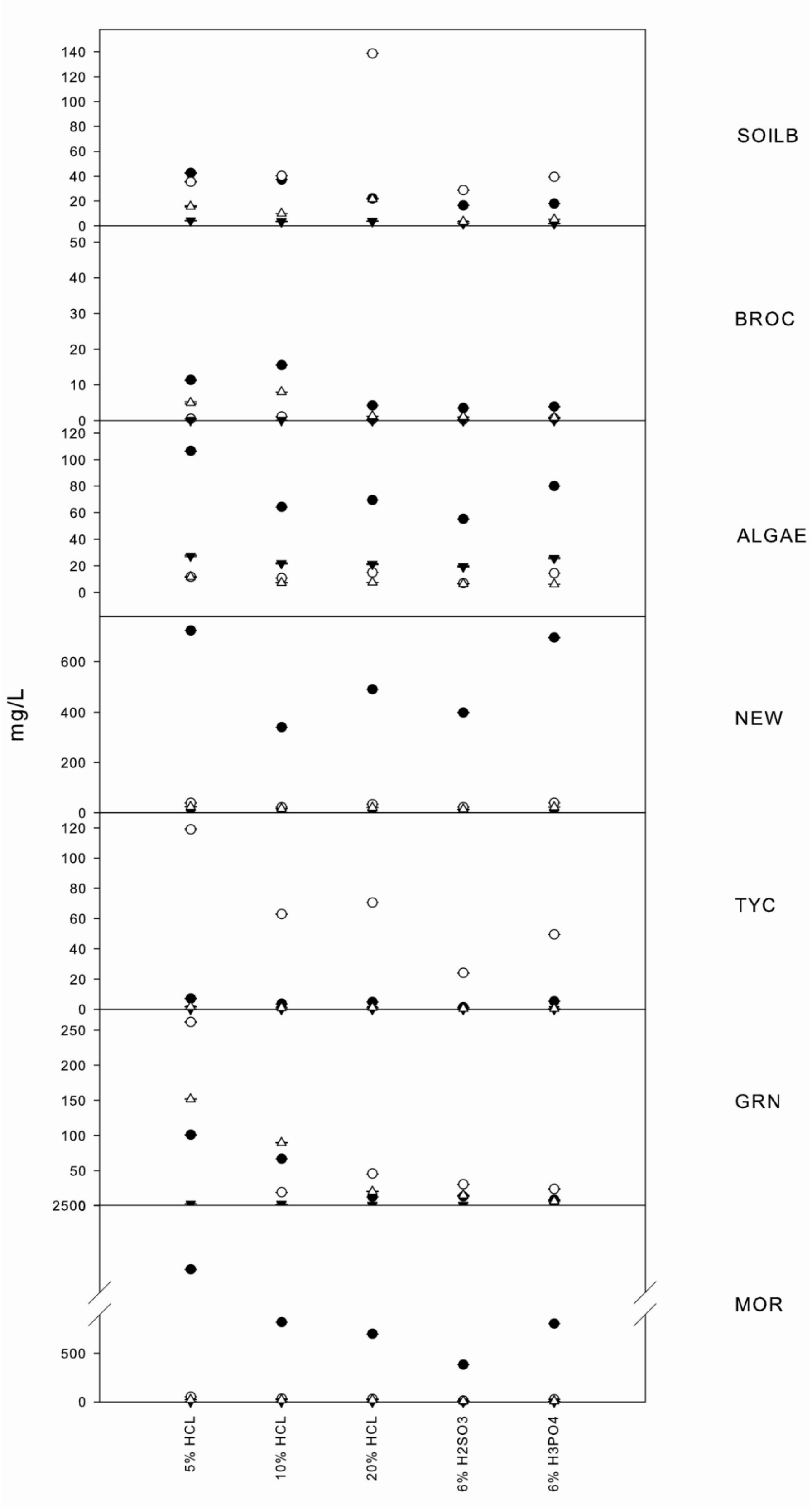

Figure 2.10: SOILB, BROC, ALGAE, NEW, TYC, GRN, MOR AAS values from rinse method supernatant. The graph shows Ca (black infilled circle), Fe (black outlined circle), Mn (black infilled upturned triangle) and Mg (black outlined triangle). All data are reported as mg/L.

For TYC, the highest 1σ for %C and δ^{13}C were within the fumigation method and for C/N within the capsule method (Figure 2.6). C/N values ranged from 13.8 to 78.7 (based on %N from acidified samples), though this range was significantly affected by 6% H_3PO_4 capsule due to low %N (p-value < 0.01); all other measurements lie closer to the mean value of 37.7. Using treated %C and untreated %N, C/N values ranged from 19.9 to 43.4. With the exception of the 6% H_3PO_4 capsule and 36% HCl fumigation methods, all other differences in %C, %N and C/N were statistically insignificant from one another and untreated values. The range of δ^{13}C is –16.5 to –17.9 ‰, primarily through slightly enriched rinse method data relative to other measured data, and 6% H_3PO_4 capsule and 36% HCl fumigation samples. For C/N, samples in Ag+Sn capsules showed lower values whilst for δ^{13}C there was no clear trend in the offsets. Within the fumigation method, Ag+Sn capsule samples had higher %C and %N values and depleted δ^{13}C values. Loss of OM following the rinse method ranged from 0.7 to 7.5% of the available OM pool (Figure 2.9). AAS analysis (Figure 2.10) showed Fe to be the most significant element mobilised during acidification (from 24.0 mg/l to 119.1 mg/l).

In GRN, C/N ratio and δ^{13}C showed greatest variability, with the highest 1σ from the rinse and fumigation methods (Figure 2.7). Across all methods C/N values ranged from 6.4 to 8.0 and δ^{13}C from –20.5 to –21.9 ‰. Within the rinse method, %C and %N were relatively higher (though C/N was slightly lower) with enriched δ^{13}C values. Results across all methods were significantly different for %C (p-value < 0.01), C/N (p-value = 0.01) and δ^{13}C (p-value < 0.01). There is a systematic offset between Ag and Ag+Sn samples: for %C and %N samples in Ag+Sn capsules returned relatively higher values of ~ 0.2 – 0.6% (%C) and ~0.05 – 0.1% (%N) with 20% HCl fumigation higher than the rest. For δ^{13}C, results for Ag+Sn capsules were consistently depleted by 0.3 – 1.0 ‰ (Figure 2.7). These data follow similar trends, though of greater magnitude, to those detected in NEW and SOILB. Loss of OM following the rinse method ranged from 1.2 to 15.9% of the available OM pool (Figure 2.9). AAS data (Figure 2.10) indicate Ca and Mg were mobilised in small concentrations.

Finally, %C, C/N and δ^{13}C data for MOR were highly variable within and between methods, with the highest 1σ within the fumigation method (Figure 2.8). C/N values ranged from 8.1 to 113.0 across all methods, most notably for 6% H_2SO_3 capsule and 20% HCl fumigation. δ^{13}C ranged from –20.1 to –27.2 ‰ and varied most notably within the capsule and fumigation methods (p-value < 0.01). Acid reagents between methods showed clear significant differences (e.g. 20% HCl; p-value < 0.05). The effect of capsule type on $\delta^{13}C$ showed depleted isotopic values by as much as ~7 ‰ for Ag+Sn samples treated with HCl. The loss of OM following the rinse method ranged from 0.8 to 3.0% of the available OM pool (Figure 2.9). The AAS results (Figure 2.10) showed very high levels of Ca (from 382.2 mg/l to 2279.1 mg/l).

2.9 Discussion

2.9.1 Method Offsets

It is an implicit assumption of the acid methods investigated in this study that (any) alterations during sample preparation to the C and N pools are systematic and proportional regardless of acid reagent or method used. Any alterations that do occur should be in the same direction (i.e. gain or loss of both C and N). It therefore follows that, within instrument precision, results from each method should be indistinguishable from one another. Our results show significant variations within and between methods. The reliability of results within specific environments (materials) are also highly variable. Measurements of background C and N concentrations from capsules and acid reagents were insignificant suggesting contamination did not contribute to variability within our results (except for 6% H_3PO_4). The reproducibility of standard reference materials for C/N and $\delta^{13}C$ within and between analytical runs indicates that the variability shown is real bias associated with the acid method.

In general, samples treated with HCl in the capsule method appear relatively coherent, though internal imprecision on C/N and $\delta^{13}C$ was still significant in some environments (e.g. ALGAE, NEW, GRN, MOR). The 6% H_3PO_4 in the capsule method generally produced aberrant results with losses of %C and %N across all sample materials ranging from 51 to 60%, and 38 to 94% respectively. This appears to be the case on samples with no, or low, IC content (e.g. SOILB, BROC, ALGAE) but appears a more effective reagent on high IC samples (e.g. NEW and MOR). The difficulty in volatilising H_3PO_4, and therefore completely drying the sample material prior to analysis, appears to be the primary cause of bias in low IC samples. The results from 6% H_3PO_4 capsule are given no further consideration in this discussion and I do not recommend this as a suitable pre-treatment reagent for samples intended for OM analysis in the capsule method on low IC materials. Capsule method results on ALGAE were significantly lower for %C, %N and C/N relative to the rinse and fumigation methods. The capsule and fumigation methods largely circumvent the loss of OM compared with the rinse method (Verardo et al, 1990; Nieuwenhuize et al, 1994a, 1994b; Harris et al. 2001) though volatile organic carbon and nitrogen losses can occur (up to 78% and from 11% to 40% respectively) during the acid treatment and the drying down process (Cutter and Radford-Knoery, 1991; Newton et al. 1994; King et al. 1998; Lohse et al. 2000; Ryba and Burgess, 2002). It is possible that ALGAE contained a greater proportion of readily volatile OC compounds that were lost through volatilisation in the capsule method drying phase (e.g. Ryba and Burgess, 2002; Komada et al. 2008), which is longer in the capsule method relative to the fumigation method. This loss will likely vary depending on the amount and state of lignin and cellulose compounds in the sample bulk OM (e.g. Turney et al. 2006; Gani and Naruse, 2007) and their response to acidification and heating, though a concomitant shift in $\delta^{13}C$ was not evident. In the capsule and fumigation methods, salt formation during the drying down phase was noted (cf. Larson et al. 2008). This phenomenon is common to all our samples with IC content, apparently increasing with increasing amounts of sample IC.

In the rinse method, all sample materials showed a loss of OC likely due to solubilisation (Figure 2.9), though this did not necessarily translate into lower %C or %N values, or indeed a shift in $\delta^{13}C$. For BROC, losses in OC during the decanting phase of the rinse method were significant in our HCl treatments. However, these samples indicated an elevation in %C after treatment of ~4%, and a depletion of ~1.2 ‰ in $\delta^{13}C$ (an ~ 4.5% offset relative to known values). This may be an artificial apparent elevation of C and N in the treated material due to the loss of inorganic components (e.g. fine colloids (organic and inorganic)) to the supernatant (e.g. Froelich, 1980; Harris et al, 2001). It has been shown that different fractions of sample material can have significantly different organic compositions (e.g. Basiden et al 2002), and therefore the loss of fine materials could ultimately bias the acquired data towards the signal from the coarser fraction. Therefore, our UV-Vis data indicating a loss of water-and acid-soluble fractions (e.g. some lipids, amino acids, proteins, polysaccharides; hydrolysed labile OM e.g. Ostle et al. 1999; Schubert and Nielsen, 2000; Galy et al, 2007) that are concomitant with a consequent fractionation in $\delta^{13}C$ (~0.9 – 1.2 ‰) are most probably correct.

Similar trends are also clear in NEW, GRN and MOR, suggesting that in samples with an IC component there is potential for artificial enrichment of C and N in the sample by weight after treatment. In TYC and GRN there is a clear relative enrichment in $\delta^{13}C$ likely due to a loss of ^{12}C rich organic material, suggesting a preferential preservation of ^{13}C-depleted compounds (e.g. lipids and lignins; e.g. Benner et al; 1987). Fernandes and Krull (2008) also observed this trend in their soils and sediments. It may be possible to reduce the loss of fine colloidal particles by introducing a centrifugation step to the rinse method, though this does not imply that potential biasing towards the coarse fraction of the sample will be eliminated.

The most variable results across all samples were from the fumigation method. %C and %N results were least accurate and precise relative to other methods, resulting in least internal accuracy in C/N values and $\delta^{13}C$. Compared with the capsule and rinse methods, fumigation samples were least reproducible on our samples, though no clear trend in either elevated or depleted values was clear. However, on some samples (e.g. ALGAE and GRN) the variability was comparatively small for C/N, but not for $\delta^{13}C$. The difficulty in reproducing reliable values in this study suggests that the fumigation technique is not the most appropriate method to follow.

In contrast to Midwood and Boutton (1998) and Kennedy et al (2005), our results suggest a clear differential environmental effect from the acid method on C/N and $\delta^{13}C$ of bulk OM. There is significant variability within and between methods alongside reproducibility problems within and between samples (e.g. different environments). Using the same reagent (e.g. 20% HCl) across different methods can also produce significantly different results (e.g. BROC, ALGAE, NEW, TYC, MOR). This variability suggests that the use of the same method and reagent does not necessarily translate into reproducible and reliable results. However, HCl treated samples in the capsule method appears most accurate and precise, whereas the rinse and fumigation methods show much less internal accuracy and precision.

2.9.2 Effect of capsule

An apparent systematic pattern in $\delta^{13}C$ results for Ag+Sn samples in NEW (range ~1.8 ‰), GRN (range ~1.7 ‰) and MOR (range ~7 ‰) was clear from our aquatic samples with an IC component, particularly under HCl treatment. These samples show a depletion in δ^{13}C , with concomitant increases in both %C and %N. Whilst an increase in %C could point towards inefficient removal of an IC component from the sample (e.g. Fernandes and Krull, 2008), the shift towards depleted δ^{13}C values suggests that the observed offsets are caused by organic components. A momentary “flash” combustion of the Sn capsules, which may briefly elevate EA furnace temperatures, but a slower ‘burn’ for Ag capsules, was noted. This factor may have allowed for more complete combustion of less thermally labile compounds more depleted in ^{13}C (e.g. lignin(-like) compounds; *sensu* Benner et al. 1987; Turney et al. 2006; Gani and Naruse, 2007).

2.9.3 Small versus Normal sample size

Significant differences between ‘small’ and ‘normal’ sample size data (Table 2.3) suggest an acidification induced offset in sample bulk OM. The ‘small’ sample sizes consistently overestimated %C and %N, producing relatively inaccurate results (see SOILB and BROC results). This variability cannot be explained by sample size (i.e. enough C and N was weighed out for analysis before acid treatment) but is more likely a function of the loss of measurable OM during the acid treatment. This loss increased the difficulty with which subsequent CO_2 and N_2 concentrations could be differentiated from baseline conditions. However, some ‘small’ samples produced reliable results, which suggest a non-systematic and non-linear response between different environments to acid treatment. This acid-induced bias is likely to be amplified in small samples, which may be problematic given that the capsule and fumigation methods begin with a limited amount of starting material. Thus the simultaneous measurement of %C, %N and δ^{13}C (and even δ^{15}N) from the same sample (“dual-mode” analysis) could be analytically problematic.

2.9.4 Proportionality

A comparison between sample materials (Figure 2.11) suggests that the accuracy and precision of methods between environments are highly variable and can respond in different proportions (i.e. significantly outside instrument precision). The proportions of %C and %N lost within and between samples are highly variable within and between methods, with no clearly emergent trend. This non-linear, disproportional offset under different acid methods is clearly evident in SOILB and BROC, our standard materials. Calculated %C and %N losses for SOILB are estimated at 1 – 23% and 2 – 24%

respectively, and are larger in the capsule and fumigation methods than for the rinse method for this sample and calculated losses of %C and %N for BROC are estimated at 8 – 51% for %C and 4 – 38% for %N and were greatest in the capsule and rinse methods. Internal incoherencies are also evident within and between sample types (e.g. BROC, GRN, TYC), and the offsets between methods and between sample types are significantly disproportionate. However, some methods appeared to produce relatively reproducible results (e.g. BROC and ALGAE in the capsule method under HCl, NEW in the rinse method and possibly in Midwood and Boutton, 1998; Kennedy et al, 2005). However, the emergence of repeatability is unpredictable and *not* subject to correction. Alterations in % C and % N, or both, are not always in the same direction (gain or loss) or of the same proportion, nor does either one preferentially control C/N values.

2.9.5 Dissolution of IC

A comparison between mean values of C/N and δ^{13}C for acidified and untreated samples could not be made on NEW, TYC, GRN and MOR due to the likely presence of IC in these sample materials. Our AAS data indicates elevated Ca in NEW and MOR, probably indicative of IC in the form of calcium carbonate (Figure 2.10) that vary considerably in their concentration between acids suggesting a nonlinear leaching. Consistency of results in NEW suggests a robust IC removal, though in MOR there may be some bias in δ^{13}C from residual IC. The elevated values of Ca and Mg in GRN suggest the presence of calcium carbonate and dolomite in the sample. Disproportionate removal of dolomite may be a factor in the enrichment of δ^{13}C in this sample. For SOILB, BROC, ALGAE and TYC, the leaching of metals is relatively low, though Ca is slightly high in ALGAE and Fe in TYC. In these samples, nearly 100% of C is in OC. We suggest that this indicates leaching from sample OM or an inorganic component within the sample matrix (e.g. clays) though the concentrations are comparatively small.

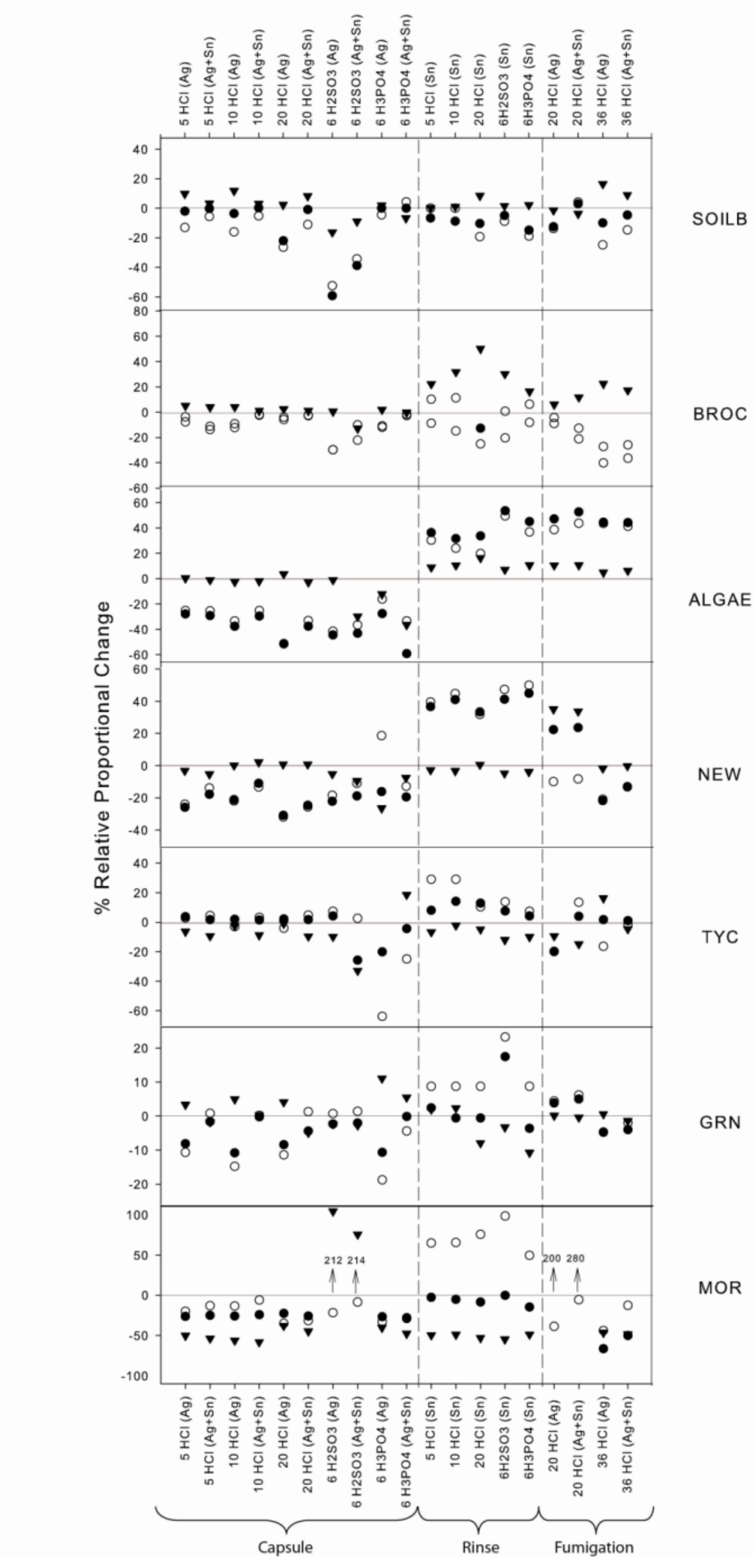

Figure 2.11: Relative proportional offset in %C, %N and C/N for all sample materials. Infilled black circle represents %C, void circle %N and infilled triangle C/N. SOILB and BROC are relative to known values based on long term untreated values. ALGAE, NEW, TYC, GRN and MOR are plotted relative to their overall means of all measured acidified samples.

2.9.6 C/N ratio

It has been shown that changes of C/N values in bulk OM can vary through acid treatment methods. This variability biases C/N values at 1σ for SOILB (~ 14 to 18; proportional change of –14% to +3%), BROC (~ 7 to 13; proportional change of –27% to +11%), ALGAE (~6 to 11; proportional change of –36% to +4%), NEW (~7 to 13; proportional change of –26% to +2%), TYC (~ 14 to 79; proportional change of –32% to +110%), and MOR (~ 8 to 113; proportional change of –25% to +104%). C/N values can vary substantially when calculated from %N from treated or untreated samples (e.g. SOILB, BROC, ALGAE), significantly influencing interpretation. These different ranges illustrate the direct response of the OC to acidification that varies within and between methods. This finding is important as there is no consensus in the literature on whether %N (and indeed N isotopes) should be measured from treated or untreated samples (e.g. Newton et al. 1994; King et al. 1998; Kennedy et al. 2005; Lu et al. 2010).

These offsets could be a function of the amount, type and nature of refractory OC (and its subsequent lability) within sample material that is a function of the environmental setting; the heterogeneity of C and N within the sample OM; and the homogeneity of sample material. Further, the bias on C/N values from %C and %N determined on the same acidified sample will vary depending upon the degree to which C and/or N concentrations are altered in the OM by acid type and method. This variability raises cause for concern on the interpretative nature of C/N ratios and their support for carbon isotopic concentrations, but also for the comparability of C/N ratios between laboratories (different preparation methods), environmental settings (type and nature of OM) and their representation within and between down-core studies (changing amounts and types of OM down-core). C/N ratios, as indicators for OM source and, in down-core studies, could easily produce significant scatter as an artefact of method rather than environmental process.

Carbon bi-plots have been used to interpret OM provenance by cross plotting C/N ratio and δ^{13}C (e.g. Thornton and McManus. 1994; Meyers, 1997; Meyers, 2003; Lamb et al. 2006; Zong et al. 2006; Mackie et al, 2007) to determine a terrestrial (e.g. C_3/C_4 land plants) or aquatic (marine/lacustrine algae) source. Figure 2.12 shows carbon bi-plots of SOILB and BROC that clearly demonstrate procedural bias on data that is equal in magnitude to shifts between terrestrial and aquatic environments. SOILB is more coherent than BROC, indicating a differential environmental response to acidification. The need to fully understand (at the molecular and macromolecular level) the nature of the sample material and system from which it was derived is imperative. In addition, offsets in C/N are not necessarily concomitant with shifts in δ^{13}C and can add significant bias to bi-plot interpretation. Shifts in C/N and δ^{13}C across different environments and different types of OM can therefore be difficult to predict. This suggests that the implicit assumption that bulk C and N of sample OM responds linearly and proportionally to acidification is flawed.

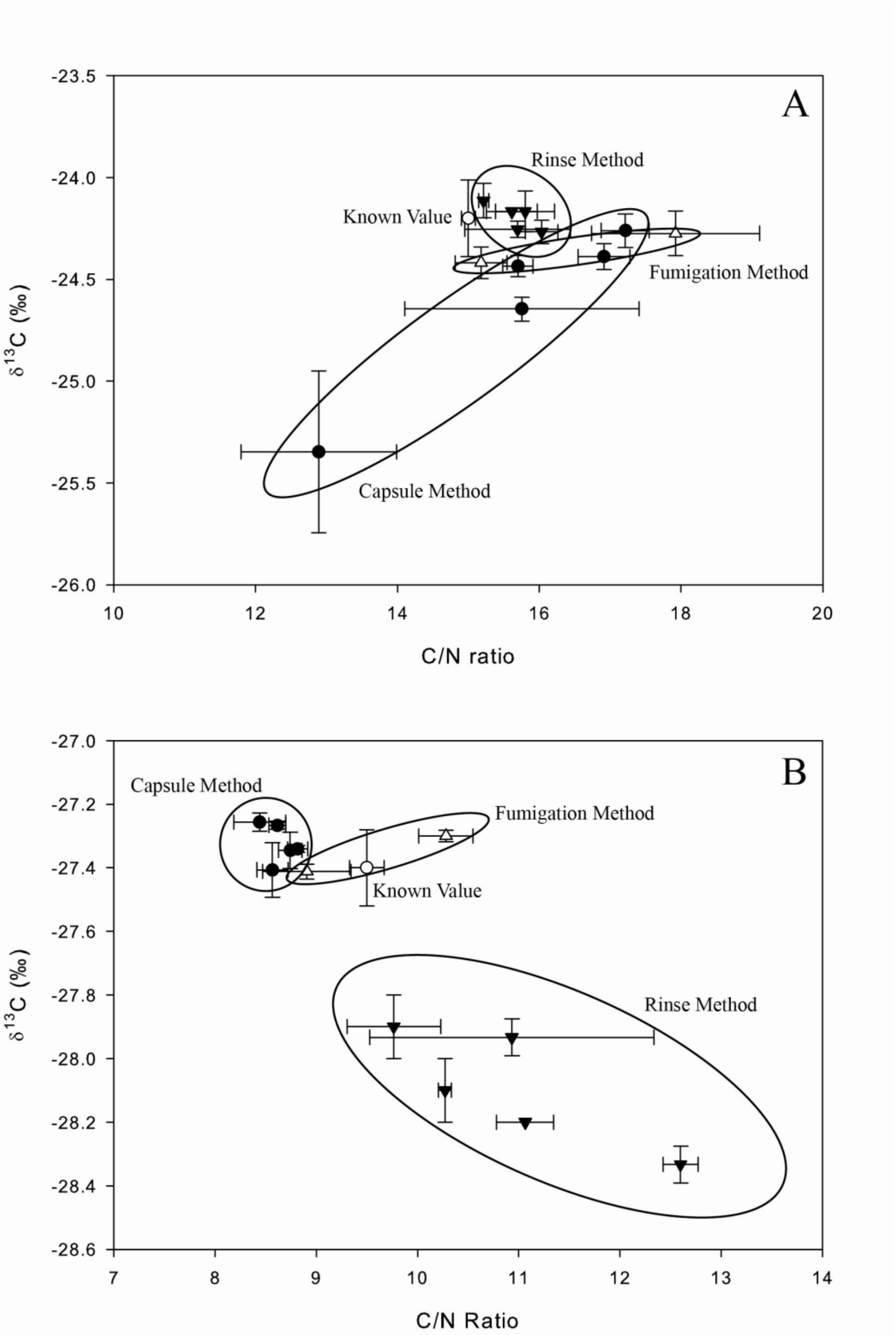

Figure 2.12: Bi-plot of δ^{13}C and C/N values of SOILB(A) and BROC(B) data (mean ± 1σ) for rinse, capsule and fumigation methods

2.10 Summary and Recommendations

This study is the first systematic comparison of the three most common acid treatment methods on a range of terrestrial and aquatic materials, from modern and geological settings. The findings of this study are important to a cross-disciplinary audience of investigators analysing C and N concentrations, and $\delta^{13}C$ from OM, to understand environmental processes and mechanisms. The key findings are summarised below:

1. We identify that the %C, %N, C/N and $\delta^{13}C$ values of OM show significant non-linear and disproportionate variability within and between acid treatment methods and sample materials. These findings strongly suggest that comparisons between laboratories are highly problematic, particularly in light of an inability to correct for these offsets and identify the underlying mechanisms. Additionally, an alteration in %C does not necessarily manifest itself in fractionation of $\delta^{13}C$, though specific methods can induce such fractionation (e.g. rinse method in BROC, TYC, GRN). This indicates the implicit assumption that the effect of acidification on sample OM is either negligible or systematic is flawed.
2. Of the methods tested, the capsule method with HCl appears to provide the most coherent and consistent results. However these still show significant within and between sample variability. For different capsule types, HCl treated materials showed a clear systematic offset in $\delta^{13}C$, though further research is required to elucidate the underlying causes of these capsule associated offsets. Additionally, the use of H_3PO_4 in the capsule method appears to consistently produce aberrant results, especially on low IC materials, due to difficulties volatilising the acid residue.
3. The rinse method can artificially elevate %C and %N values, and also significantly offset $\delta^{13}C$. This occurs due to the loss of fine-grained materials (e.g. such as clays) and the removal of IC. Losses of the soluble organic fraction from the sample material also occur (which varies significantly from sample to sample, and therefore within and between environmental settings). Differences in %C and %N are not necessarily systematically related to shifts in $\delta^{13}C$.
4. The variability in our results from the fumigation method, within and between sample materials, is too significant to produce consistently reliable results (see method summary in Table 2.4).
5. Small sized samples *after* acidification can lead to the production of unreliable data.
6. The interpretation of C/N values and their support for the interpretation of $\delta^{13}C$ values is significantly affected by acid method (Figure 2.12). This additional

imprecision from acid-treated samples (even when using untreated %N) should preclude the use of C/N ratios as an indicator for OM provenance and alteration, especially where the amount, type, nature and origin of sample OM differs significantly (*sensu* Fernandes and Krull, 2008). These findings have important implications for down-core studies of C/N and $\delta^{13}C$ especially, where the type of organic matter and matrix change. For example, the amount of acid/water soluble and acid/water insoluble compounds may vary from sample to sample leading to highly unpredictable offsets. The application of one, or more, acid methods, without an understanding of the nature of C and N within the sample material or system involved has clear inherent limitations. I re-iterate that the use of a consistent method and acid reagent does not guarantee reliability of results in changing environmental settings (e.g. across down-core sedimentary units).

2.10.1 Recommendations

I provide recommendations for researchers investigating C and N concentrations and $\delta^{13}C$ of organic materials:

1. Avoid the use of H_3PO_4 in the capsule method and avoid the fumigation method.
2. For the rinse method, it could be beneficial to include a centrifugation step to minimise the loss of fine colloidal components of the sample material (e.g. fine organic fragments and clays) and reduce potential biasing towards coarser grained fractions.
3. It is important that sample sizes be significantly above the machine baseline conditions prior to acidification, to ensure that any alterations to the sample OM fraction do not result in sample peaks becoming near indistinguishable from baseline conditions. This does not imply subsequent data are accurate and precise in the context of the method offsets discussed here.
4. Exercise extreme caution in the interpretation of C/N values, and in their use in support of $\delta^{13}C$ value interpretation in the context of OM provenance (e.g. aquatic versus terrestrial source) where acidification methods are used to derive C/N and $\delta^{13}C$ of OM.
5. To avoid the issues identified here with the acid methods, investigators can measure total C by elemental analyzer (yielding N also), and IC by colourometry, and derive OC by difference. Note, however, this is only appropriate for %C and %N (and hence C/N values), and not for $\delta^{13}C$. This assumes a negligible influence on %N from inorganic nitrogen.

Table 2.4: Summary of limitations and recommendations identified for each acid treatment method

Methodology	**Limitations**	**Justification**	**Possible solutions**
Rinse	Sample material can remain in suspension and/or remain attached to meniscus;	Visual observation (e.g. BROC, NEW, GRN);	Filter (e.g. 50 µm or less) material attached to meniscus. Very fine colloids may still be washed away, however.
	Leaching of acid and water soluble organic components;	UV-Vis data (Figure 3);	Measure C and N content of rinse (e.g. Caughey et al, 1995; Galy et al, 2007);
	Loss of non-organic components to supernatant (e.g. fine colloids);	Visual observation (e.g. BROC, NEW, GRN);	Consider introducing a centrifugation step;
	Artificial concentration of C and N (possibly due to loss of colloidal components).	Elevated C and N values (e.g. BROC).	Consider use of capsule method (if sample is not high in IC).
Capsule	Limited amount of starting material in capsule;	Capsule dimensions (commonly 5x9 mm);	
	Prone to spits and spills, especially on high IC samples (e.g. MOR);	Visual observation;	Initially add 10-20 µl deionised water. Make several small additions of acid in the first instance(e.g. 10µl, 20µl);
	Formation of CO_2 bubble within sample on materials with IC leading to "protection" of material from acid;	Visual observation (eg. NEW, MOR);	Make several small additions of acid in the first instance(e.g. 10µl, 20µl);
	On drying, significant hygroscopic salts build up (e.g. $CaCl_2$), increasing with IC	Visual observation (e.g. NEW, MOR);	This is an unavoidable by-product of the acidification

	content (Van Iperen and Helder, 1995; Larson et al. 2008)		
	Losses of C and N concentrations during acidification can significantly influence results;	‘small’ versus ‘normal’ sample size comparison.	Avoid using close to the minimum amount of C and N concentrations.
	H_3PO_4 is difficult to volatilise, particularly on low IC materials;	Visual observation (e.g. BROC, TYC); aberrant data;	Avoid H_3PO_4;
	Ag capsule tends to ‘burn’ slowly relative to Sn capsules.	Visual Observation.	Further wrap Ag capsules in Sn capsules.
Fumigation	Limited amount of starting material in capsule;	Capsule dimensions (commonly 5x9 mm);	
	On drying, significant hygroscopic salts build up (e.g. $CaCl_2$), increasing with IC content;	Visual observation (e.g. NEW, MOR);	This is an unavoidable by-product of the acidification;
	Inefficient IC removal, especially on samples with >30% IC (e.g. Harris et al, 2001), but not linked with lack of acid;	Investigated using quality control batch which was treated with 10% HCl after fumigation cycle to check for effervescence (e.g. NEW, MOR);	Consider processing high IC samples with the rinse or capsule method (cf. Harris et al, 2001);
	Ag capsules tend to ‘burn’ slowly relative to Sn capsules;	Visual observation;	Further wrap Ag capsules in Sn capsules;
	Accuracy and precision of results on very low IC samples is poor.	SOILB, BROC and ALGAE data.	Consider rinse or capsule method.

CHAPTER 3

Evidence for bias in measured $\delta^{15}N$ values of terrestrial and aquatic organic materials due to pre-analysis acid treatment methods.

Brodie, C.R., Heaton, T.H.E., Leng, M.J., Kendrick, C.P., Casford, J.S.L., and Lloyd, J.M. (2011) Evidence for bias in measured $\delta^{15}N$ values of terrestrial and aquatic organic materials due to pre-analysis acid treatment methods. Rapid Communications In Mass Spectrometry. 25, 1089 – 1099.

3.1 Introduction

The analysis of stable isotope ratios of nitrogen ($\delta^{15}N$) provides valuable information on the complex processes within the global nitrogen cycle. $\delta^{15}N$ has been used to understand trophic pathways in food webs (e.g. Bunn et al, 1995; Pinnegar and Polunin, 1999; Ng et al, 2007; Kolasinski et al, 2008), organic matter (OM) provenance and degradation (e.g. Thornton et al, 1994; Meyers, 1997; Hu et al, 2006; Barros et al, 2010), denitrification in the water column and nitrate utilisation in ocean sedimentary records (Altabet et al, 1995) and eutrophication (Owens, 1987; Voss et al, 2005). C/N ratios (weight ratios of the elements) have been widely used to support $\delta^{15}N$ (and $\delta^{13}C$) by broadly distinguishing between terrestrial and aquatic sourced OM. The N composition of aquatic derived OM (protein and lipid rich) is considerably greater than for that of terrestrial OM (cellulose and lignin rich) dependent upon the availability of N in the environment. In addition, $\delta^{13}C$ of OM has been employed to identify carbon sources and photosynthetic pathways in plants (e.g. C_3 and C_4 plant differentiation; Meyers, 1997; 2003; Sharpe, 2007), assess C dynamics in soil systems and study trophic levels in environmental systems (Bunn et al, 1995; Pinnegar and Polunin, 1999; Kolasinski et al, 2008; Harris et al, 2001), and understand C mineralisation processes (Midwood and Boutton, 1998; Freudenthal et al, 2001; Leng and Marshall, 2004).

These interpretations assume that C/N ratios, $\delta^{13}C$ and $\delta^{15}N$ of OM can be reliably determined. For C/N ratios and $\delta^{13}C$, this relies upon the complete removal of inorganic carbon (IC) from the sample total carbon pool, typically achieved through acid pre-treatment, without alteration of sample OM (see Chapter 2; Brodie et al, 2011a). In contrast, measurements of %N and $\delta^{15}N$ are commonly made on untreated sample material, on the assumption that inorganic nitrogen (IN) does not contribute to the total sample N (though this may not be valid in all environments (Muller, 1977; Schubert and Calvert, 2001; Sampei and Matsumoto, 2008)). However, it is becoming increasingly common to measure C/N ratios, $\delta^{13}C$ and $\delta^{15}N$ as part of a single, “dual-mode” analysis (Kolasinski et al, 2008; Kennedy et al, 2005; Jinglu et al, 2007; Bunting et al, 2010). In this case, if IC must be removed by acid treatment, it is necessary to establish that this treatment does not affect the %N or $\delta^{15}N$ of OM.

The effect of pre-analysis acid treatment methods on %N and $\delta^{15}N$ can be significant (Bunn et al, 1995; Ng et al, 2007). Losses in %N have been reported in the range of 0 –

50% (King et al, 1998; Lohse et al, 2000; Ryba and Burgess, 2002; Brodie et al, 2011a) alongside artificial gains of ~ 20 % (see Chapter 2; Brodie et al, 2011a). In addition, and like known variabilities in δ^{13}C previously reported (see Chapter 2; Brodie et al, 2011a), results for shifts in δ^{15}N are variable, indicating an increase of 0.1 – 3 ‰ (Bunn et al, 1995), a decrease of 0.2 –1.8 ‰ (Bunn et al, 1995; Midwood and Boutton, 1998; Kennedy et al, 2005; Ng et al, 2007; Fernandes and Krull, 2008), and no significant change (Jaschinski et al, 2008; Serrano et al, 2008), with no apparent trend in the size of offset related to the type of material (i.e. modern or ancient, terrestrial or aquatic). In addition, disproportionate and non-systematic offsets in C and N of OM due to acid treatment contribute to this variability (Schmidt and Gleixner, 2005; Brodie et al, 2011a), and could preclude interpretation of sedimentary δ^{15}N records with a range of ~ 1 – 4 ‰ (Waples, 1985; Schubert and Calvert, 2001; Altabet, 2007; Galbraith et al, 2008). An investigation into the effects of pre-analysis acid treatment methods on δ^{15}N of OM is therefore justified.

This chapter aims to investigate the effect of pre-analysis acid treatment methods on measured δ^{15}N values of OM. We test the hypothesis that the measured δ^{15}N values are not different between pre-analysis acid treatment methods. I compare untreated material, and material acid treated in the two most common methods; (i) the capsule method and; (ii) the rinse method; and use HCl as the acidifying reagent. I also independently investigate the effect of capsule type. These methods all use different capsules; the rinse method and untreated method use tin (Sn) capsules, whereas the capsule method uses silver (Ag) capsules; thus an investigation into the influence of different capsules is necessary (see Brodie et al, 2011a). Specifically, the following research questions are addressed:

1. Are there significant differences in measured δ^{15}N values of OM between methods?

2. Does capsule type affect measured δ^{15}N values?

3. Does acid treatment method influence environmental interpretation of measured δ^{15}N values?

3.2 Sample materials and Acid treatment methods

3.2.1 Sample materials

A recent comprehensive study into the effects of acid treatment methods on OC in OM of different sample materials showed significant differences in C/N and $\delta^{13}C$ of sample materials that were prepared in different ways (see Chapter 2; Brodie et al, 2011a). As a follow on from this study, three sample materials were selected for this study from those previously analysed which represent different environments and which showed considerably different treatment effects for C/N and $\delta^{13}C$ values between them. These samples are BROC, SOILB and TYC (a plant, a modern soil and an ancient lake sediment, see Table 2.1). As these sample materials represent three very different environments, and hence different amounts and composition of OM (e.g. terrestrial, freshwater, marine, plant or animal; modern or ancient), and show differences in C/N and $\delta^{13}C$ between acid treatment methods (Brodie et al, 2011a), $\delta^{15}N$ might also be expected to be biased by acid treatment. All sample materials were freeze dried and freeze milled to a flour (grain size$\leq$ 63μm) prior to analysis. None of these sample materials contain an IC component (so a comparison between untreated and treated sample aliquots could be made).

3.2.2 Acid treatment methods

Prior to sample preparation, all sub-sampling equipment and glassware were thoroughly washed in 1% nitric acid, rinsed in deionised water, followed by a wash in 2% neutracon® solution, a final deionised water rinse and then fired at 550°C for 3 h. Ag capsules were fired at 550°C for 3 h prior to use. HCl was the only reagent selected for removing IC, because it produced more coherent $\delta^{13}C$ and C/N data within and between methods than 6% H_2SO_3 and 6% H_3PO_4 (Brodie et al, 2011a). Two strengths of HCl were tested, 5% w/w and 20% w/w, based on findings in (Brodie et al, 2011a). Sample materials were prepared as follows:

Untreated samples: Samples were weighed directly into Sn capsules.

Capsule method: Samples were weighed into open Ag capsules, transferred to a metal tray on a hotplate and 10 μl of distilled water was added to moisten the samples. After moistening, 10 μl of the chosen acid reagent was added to the cold sample before the hotplate temperature was slowly increased to ~50°C. Additional acid was then added in steps of 10 µl, 20 µl, 30 µl, 50 µl and 100 µl, followed by a final 200 µl, without allowing the sample to dry out between additions.

Rinse method: Sample material was mixed with excess acid in a beaker and allowed to stand for 24 h. The beaker was topped up to 500 mls with deionised water and the sample material allowed to settle for a further 24 h. Once settled, the supernatant was decanted, ensuring minimal disturbance of the remaining material, and the beaker then topped up again to 500 mls with deionised water. Dilution was repeated 3 times in total with an overall minimum of 1200 mls of deionised water used. After the final decanting, the excess water (50 – 100 mls) was allowed to evaporate off in a drying oven at ~50°C, and the sample transferred to a Sn capsule.

The capsule method uses Ag capsules, because they are resistant to acid attack whereas Sn capsules disintegrate under acidification, especially with HCl. Unlike Sn, however, Ag does not oxidise exothermally in the elemental analyser, so that sample combustion temperatures in Ag are lower than in Sn. I therefore also analysed samples with their Ag capsules further wrapped in tin (Ag+Sn) to test whether this significantly affected $\delta^{15}N$ values. The rinse method traditionally uses Sn capsules, and these were replicated by wrapping in silver (Sn+Ag). All treatments were performed in triplicate.

3.3 Analytical method

Nitrogen isotope analyses were performed using an elemental analyser linked to an isotope ratio mass spectrometer (EA-IRMS). Samples were loaded into an autosampler and dropped into a 1.6 ml sec^{-1} stream of helium in a FlashEA 1112 elemental analyser. The combustion column contained copper oxide and silvered cobaltous oxide at 900°C, and combustion products were cleaned of oxygen and nitrogen oxides by passage through copper at 680°C, and of water and carbon dioxide by passage through magnesium perchlorate and carbosorb before passage through the GC column. The helium stream with sample N_2 was led via a Conflo III interface to a Delta+XL mass spectrometer for determination of the $^{15}N/^{14}N$ ratio. In order that all treatments of a particular sample material could be analysed in a single run, correction of the measured sample $^{15}N/^{14}N$ ratios to $\delta^{15}N$ values was not based on comparison with internal standard samples (the normal procedure) but rather on comparison with a reference gas whose $\delta^{15}N$ value versus atmospheric N_2 had been determined in separate runs. The quoted $\delta^{15}N$values are therefore correct relative to one another for the same sample material, but only approximately correct in absolute terms versus atmospheric N_2. Limits on analytical precision are mainly determined by conditions of combustion and chromatography in the elemental analyser. For organic materials containing a few %N (e.g. BROC) within-run precision for $\delta^{15}N$ is better than 0.3‰ (1σ for n = 10 samples). Measurements of background C and N concentrations from capsules and acid reagents were below instrument detection limits, suggesting that contamination did not contribute to variability within our results (Brodie et al, 2011a).

3.4 Data analysis

All data are plotted as mean ± standard deviation (1σ). Our data were analysed by One-Way ANOVA using Minitab 15.0 (MINITAB Inc. 2007). Data were tested for normality using an Anderson-Darling normality test (all p-values > 0.05) and homogeneity of variances using a Bartlett's Test (assumes normality within each factor level) and Levene's Test (does not assume normality within each factor level) (Fox et al, 2007; Terwilliger et al, 2008). For our data, the p-value for the Bartlett and Levene tests were all above 0.05, indicating that the variances are the same for each factor. These tests validate the use of ANOVA on our data. I test the null hypothesis that there is no significant difference in measured $\delta^{15}N$ values between treatment methods, capsule type and acid reagent strength (i.e. within method variability). The results for C/N and $\delta^{13}C$ have been previously reported (Brodie et al, 2011a) and were measured on different sample aliquots than those for $\delta^{15}N$.

3.5 Results

Results for $\delta^{15}N$ for SOILB, BROC and TYC are presented in Figures 3.1 – 3.3 and are reported as mean ± standard deviation (Table 3.1), alongside previously reported C/N and $\delta^{13}C$ (see Chapter 2; Brodie et al, 2011a). Results from the one-way ANOVA are presented in Table 3.2. There is a statistically significant difference between pre-analysis acid treatment methods, and within and between sample materials (Table 3.2) that is significantly greater than instrument precision (~0.3 ‰). In SOILB and TYC, measured values of $\delta^{15}N$ in acid treated are lower than for untreated samples (Figures 3.1 and 3.3; Table 3.2). For SOILB, the precision of $\delta^{15}N$ determinations was better for untreated and rinse method samples than for capsule method samples (value represented graphically by horizontal grey bars on Figure 3.1). In TYC precision was marginally better for acid treated samples than for untreated samples (untreated sample in the Ag capsule significantly influenced this; see Figure 3.3). There is a slight depletion in $\delta^{13}C$ and lower C/N in SOILB, with a relatively depleted $\delta^{15}N$ (to untreated samples). In TYC, the rinse method show enriched $\delta^{13}C$ and higher C/N values, concomitant with a relatively depleted $\delta^{15}N$.

In BROC, the measured $\delta^{15}N$ values were generally better for acid treated samples than for untreated samples (value represented graphically by horizontal grey bars on Figure 3.2), though the rinse method samples produced the lowest $\delta^{15}N$ values of all methods for this material. This poor sample precision contributed to no statistical differences being detected between untreated and acid treated sample means. However a significant difference between data in the capsule and rinse methods of ~ 1.2 ‰ exists (Figure 3.2), with the rinse method data showing relatively higher $\delta^{15}N$, concomitant with depleted $\delta^{13}C$ and higher C/N relative to known values (Brodie et al, 2011a).

Comparisons of results within the same method but combusted in different capsules showed significant differences (Table 3.2). In particular, untreated samples analysed only in Ag capsules showed significantly lower results in all materials (see unfilled circles in Figures 3.1 – 3.3). In the capsule method, there was no common trend in data for samples further wrapped with a Sn capsule, though for TYC $\delta^{15}N$ were depleted by ~0.5 ‰ relative to other samples within the capsule method. For the rinse method, across all sample materials, samples further wrapped in an Ag capsules showed higher $\delta^{15}N$ values of between 0.4 – 0.8 ‰.

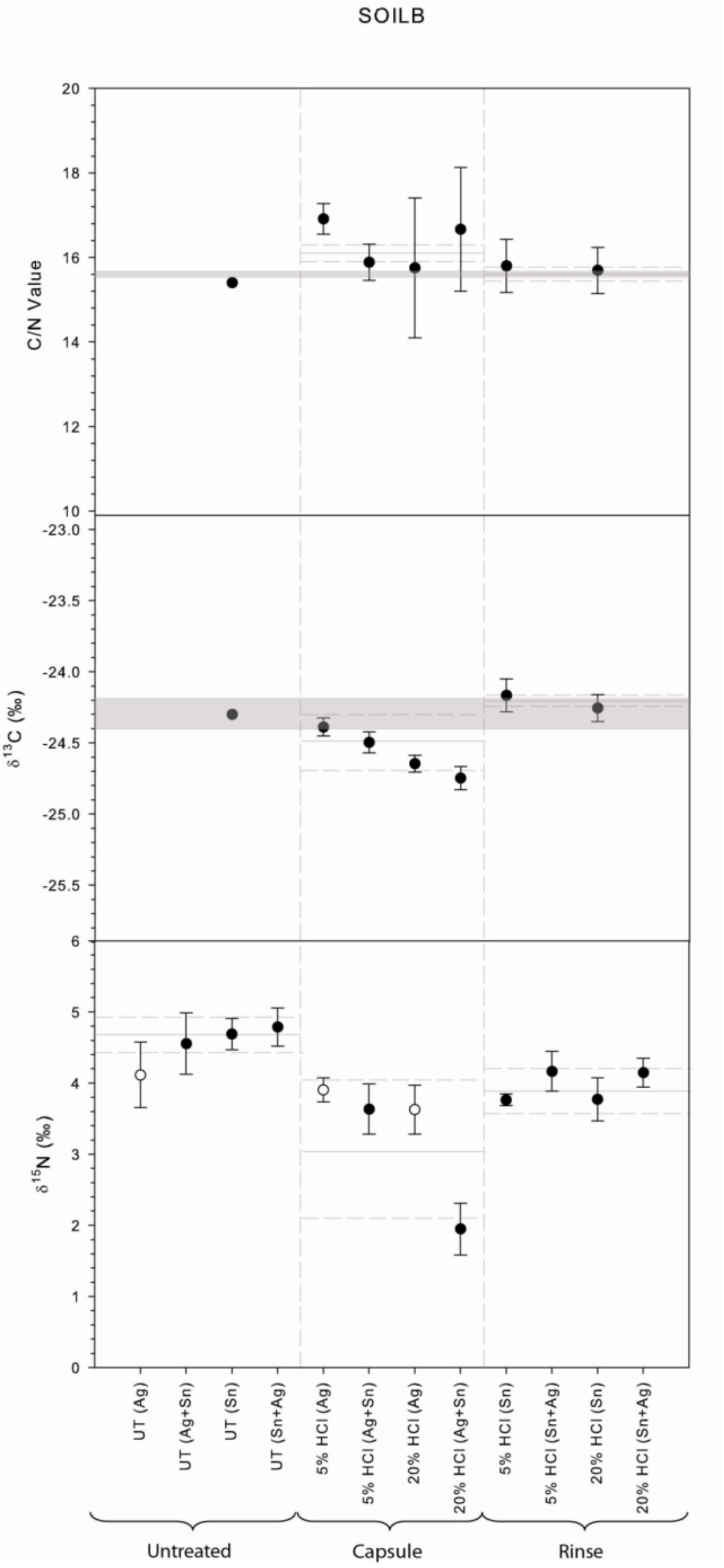

Figure 3.1: SOILB C/N, $\delta^{13}C$ and $\delta^{15}N$ values for each method and acid. Horizontal solid grey lines indicate mean values for each method, and perforated grey lines 1σ. Vertical perforated lines split the untreated, capsule and rinse methods. The horizontal grey bar on the C/N and $\delta^{13}C$ plots represents known values. Error bars are calculated as one standard deviation (1σ) of replicate measurements. Unfilled circles represent samples analysed in Ag capsules only.

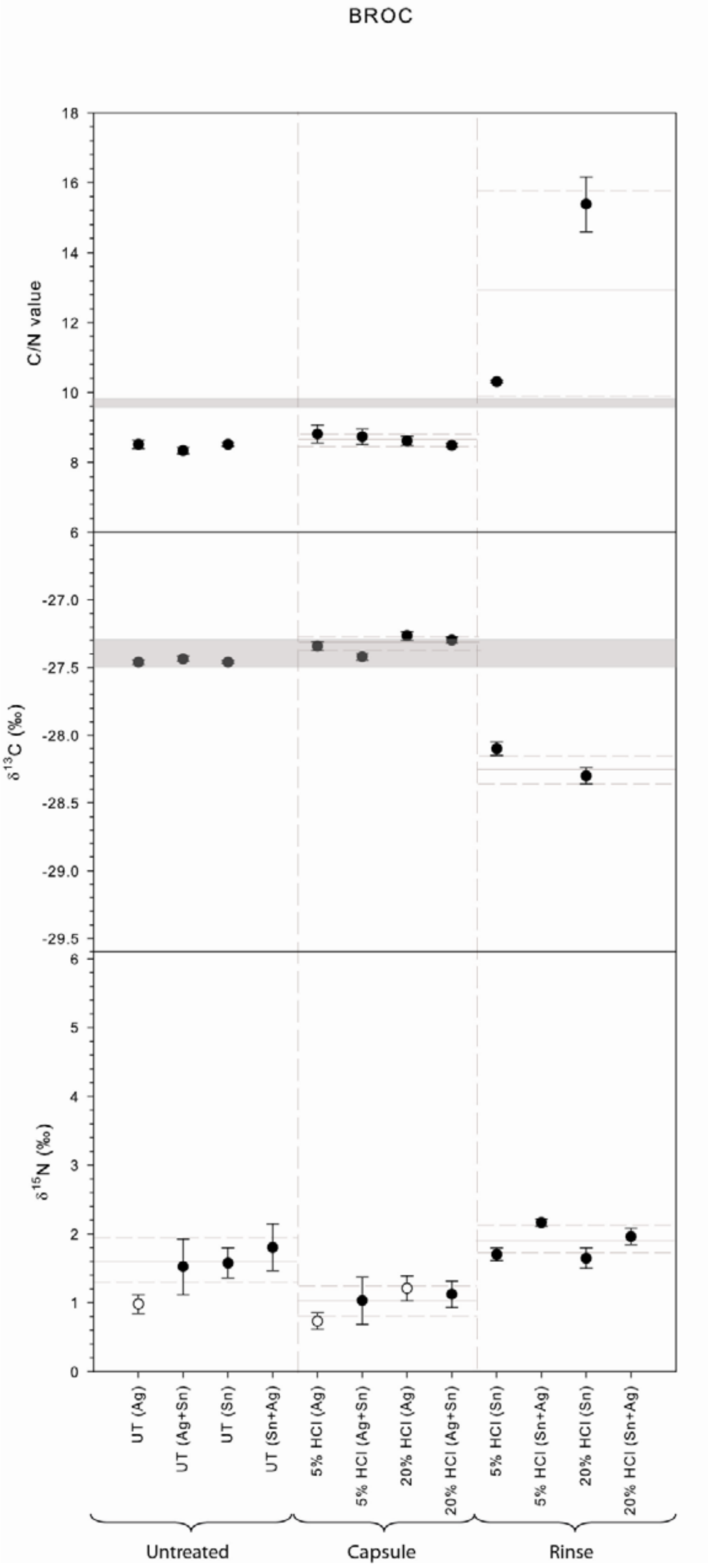

Figure 3.2: BROC C/N, δ^{13}C and δ^{15}N values for each method and acid. Horizontal solid grey lines indicate mean values for each method, and perforated grey lines 1σ. Vertical perforated lines split the untreated, capsule and rinse methods. The transparent grey bar on the C/N and δ^{13}C plots represents known values. Error bars are calculated as one standard deviation (1σ) of replicate measurements. Unfilled circles represent samples analysed in Ag capsules only.

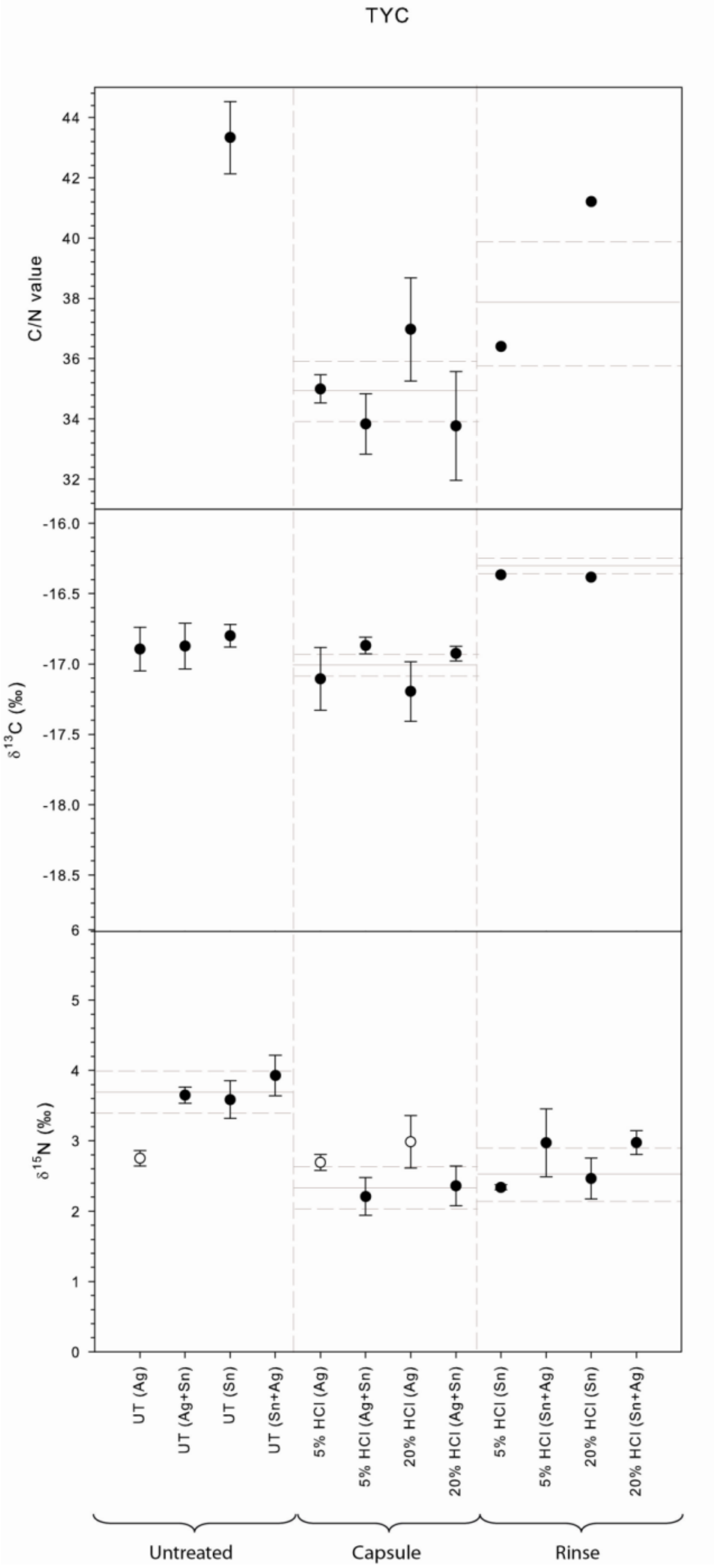

Figure 3.3: TYC C/N, δ^{13}C and δ^{15}N values for each method and acid. Horizontal solid grey lines indicate mean values for each method, and perforated grey lines 1σ. Vertical perforated lines split the untreated, capsule and rinse methods. Error bars are calculated as one standard deviation (1σ) of replicate measurements. Unfilled circles represent samples analysed in Ag capsules only.

Table 3.1: Mean and standard deviation (1σ) for δ^{15}N values in SOILB, BROC and TYC.

	SOILB	**BROC**	**TYC**
Untreated (Ag)	4.11 ± 0.46	0.98 ± 0.14	2.75 ± 0.11
Untreated (Ag+Sn)	4.56 ± 0.43	1.52 ± 0.40	3.65 ± 0.11
Untreated (Sn)	4.69 ± 0.22	1.58 ± 0.22	3.59 ± 0.27
Untreated (Sn+Ag)	4.79 ± 0.27	1.80 ± 0.34	3.93 ± 0.29
5% HCl Capsule (Ag)	3.90 ± 0.17	0.73 ± 0.12	2.69 ± 0.11
5% HCl Capsule (Ag+Sn)	3.63 ± 0.35	1.03 ± 0.34	2.21 ± 0.27
20% HCl Capsule (Ag)	3.62 ± 0.34	1.21 ± 0.18	2.99 ± 0.37
20% HCl Capsule (Ag+Sn)	1.95 ± 0.36	1.12 ± 0.19	2.36 ± 0.28
5% HCl Rinse (Sn)	3.76 ± 0.83	1.70 ± 0.92	2.34 ± 0.36
5% HCl Rinse (Sn+Ag)	4.16 ± 0.28	2.16 ± 0.06	2.97 ± 0.48
20% HCl Rinse (Sn)	3.77 ± 0.30	1.65 ± 0.15	2.46 ± 0.29
20% HCl Rinse (Sn+Ag)	4.14 ± 0.20	1.96 ± 0.12	2.98 ± 0.17

Table 3.2: Results of ANOVA analysis for each sample material for untreated, capsule and rinse methods. Data were tested at the 0.05 significance level.

		SOILB		BROC		TYC	
Analysed Factor	**ANOVA Parameter**	**Statistical Results**	**Difference**	**Statistical Results**	**Difference**	**Statistical Results**	**Difference**
METHOD	P-value	0.03	Capsule method lover $\delta^{15}N$ values than untreated	0.06	Capsule method $\delta^{15}N$ values lower than rinse and untreated method values	0.02	Untreated $\delta^{15}N$ values higher than samples from both acid treatment methods
	R-Squ (%)	42.59		61.26		47.84	
ACID	P-Value	0.07	nd	0.97	nd	0.02	Untreated values produce higher $\delta^{15}N$ than 5% HCl and 20% HCl in either acid method
	R-Squ (%)	33.42		0.00		48.17	
CAPSULE	P-Value	0.53	nd	0.00	Samples in Ag and Ag+Sn capsules produce lower $\delta^{15}N$ values compared to samples in Sn and Sn+Ag capsules	0.652	nd
	R-Squ (%)	0.00		78.84		0.00	

3.6 Discussion

3.6.1 Methodological differences in $\delta^{15}N$

As reported for C/N and $\delta^{13}C$ data (Chapter 2; Brodie et al., 2011a), the measured $\delta^{15}N$ values show evidence of significant within (effect of acid reagent strength and capsule type) and between (untreated versus capsule method versus rinse method) method differences. Across all sample materials, the differences in sample data between methods (up to ~1.5 ‰) are significantly greater than the instrument precision (~ 0.3 ‰). The untreated method is the most common approach in the literature (Kennedy et al, 2005; Kolasinski et al, 2008), though simultaneous $\delta^{13}C$ and $\delta^{15}N$ measurements ("dual-mode" analysis), which require acid removal of carbonate, are increasingly common (Jinglu et al, 2007; Galbraith et al, 2008; Kolasinski et al, 2008; Bunting et al, 2010). Our results show significant differences in measured $\delta^{15}N$ value between acid treatment methods *and* within untreated samples (Figures 3.1 – 3.3). For example, data for SOILB and TYC from acid pre-treated samples were significantly different from untreated by up to ~1.5 ‰, with the overall range in the untreated method ~0.5 ‰ (excluding the samples combusted only in Ag capsules). In the rinse method, $\delta^{15}N$ may be biased by the loss of soluble organic and/or inorganic N species (Froelich, 1980; Bebout et al, 2006), or very fine particles (Froelich, 1980; Ostle et al, 1999; Schubert and Nielsen, 2000; Harris et al, 2001; Galy et al, 2007; Brodie et al, 2011a). For example, the loss of ^{14}N rich species (e.g. protein; ammonium) would increase the $\delta^{15}N$ value (Bebout et al, 2006). This suggests problems of reliability on $\delta^{15}N$ measurements, particularly from acid treated samples. This has implications for the applicability of any one method in a short or long core, where type, amount and nature of OM can vary significantly, and on modern organic materials.

These findings partly agree with Kennedy et al (2005) and Fernandes and Krull (2008), who find that the precision of acid treated samples was equal to or less than that of untreated samples. Interestingly, Kennedy et al (2005) find no significant difference between results, and suggest that measurements of $\delta^{15}N$ on acid treated samples as an appropriate method, whereas Fernandes and Krull (2008) report differences of up to 2 ‰ (offsets due to volatilisation (capsule method) and solubilisation (rinse method)), and suggest measurement on untreated material. Such variability suggests the different organic chemical composition of sample materials from different environments can influence the reliability of isotopic C and N values obtained using these acid treatment procedures, necessitating an understanding of the complexities of sample OM within and between environments (Fernandes and Krull, 2008; Brodie et al., 2011a). This has significant interpretative implications for δ^{15}N in sedimentary records. Published studies have reported δ^{15}N data ranges in the order of ~1 – 5 ‰, on surface samples, short cores (Schubert and Calvert, 2001; Hu et al, 2006; Jinglu et al, 2007; Lambert et al, 2008; Lu et al, 2010), and long cores (Waples, 1985; Yoshii et al, 1997; Wolfe et al, 1999; Freudenthal et al, 2001; Altabet et al, 2007; Bunting et al, 2010). The differences reported here for BROC (~ 0.1 – 1.2 ‰), SOILB (~ 0.2 – 1.3 ‰) and TYC (~ 0.8 – 1.6 ‰) are only a function of pre-analysis acid treatment (i.e. an artefact), and therefore have the potential to significantly influence environmental interpretation of the data. Where different sample preparations (e.g. untreated versus acid treated) or analytical methods (e.g. “single” versus “dual” mode isotope analysis) are followed, this will preclude the comparison of δ^{15}N from different down-core records.

3.6.2 Effect of capsule type

It has been shown that there is a systematic depletion in δ^{13}C in aquatic material within the capsule method for samples further wrapped in Sn (Ag+Sn)(Brodie et al, 2011a). I therefore test whether capsule type influenced measured δ^{15}N results. For all sample materials, untreated sample aliquots wrapped only in an Ag capsule showed significantly lower δ^{15}N values in comparison to all other untreated sample aliquots (unfilled circles on Figures 3.1 – 3.3). The absence of Sn in the combustion process has an influence on the overall combustion temperature as there is no additional exothermal heat supply through the Sn oxidative reaction. This, combined with the 900°C combustion temperature, which is lower than traditionally used in C/N and δ^{13}C analysis of OM (~≥ 1000°C), likely has a direct influence on the ease with which labile and recalcitrant components of the sample materials react. The presence of Sn appeared to have less marked influence on results for acid treated samples, but this might be due to the acidification process obscuring differences between labile and recalcitrant components (Fernandes and Krull, 2008; Brodie et al, 2011a).

Alongside the potential for offsets in elemental and isotopic C and N due to the acid reagent and/or method followed, it appears that the capsule material, in which the sample is combusted, may also influence data distribution. This has implications for the comparison of data between methods, and between laboratories (because the rinse method uses Sn capsules and the capsule method Ag capsules) in addition to the likelihood for offsets linked to the type, amount and nature of OM (Fernandes and Krull, 2008).

3.6.3 Coupled offsets in $\delta^{13}C$ and $\delta^{15}N$

A comparison of $\delta^{13}C$ and $\delta^{15}N$ within and between methods clearly indicates that method-induced alterations of the sample OM can influence measured $\delta^{13}C$ and $\delta^{15}N$ values in a disproportionate and non-linear fashion. $\delta^{13}C$ and $\delta^{15}N$ shifts are not consistent or in the same direction across the methods in any one material analysed (Figures 3.1 – 3.3). For BROC, relative to untreated samples, the capsule method showed a slight enrichment in $\delta^{13}C$ of ~0.2 ‰ (and slight increase in C/N value) coupled with a depletion in $\delta^{15}N$ of ~0.6 ‰ relative to untreated. This is in contrast to the results in the rinse method, which show a depletion in $\delta^{13}C$ of ~1.2 ‰ (C/N value increased by ~3 – 6), and an enrichment in $\delta^{15}N$ of ~0.7 ‰ relative to untreated. For the capsule method, the results suggest a loss of ^{15}N enriched compounds and no significant change in $\delta^{13}C$ but for the rinse method, a loss of ^{13}C enriched compounds, but no differential loss of ^{15}N compounds (which is not too dissimilar to untreated values).

The differential loss of ^{15}N rich compounds has previously been reported from pre-analysis acid treatment methods (Bunn et al, 1995; Pinnegar and Polunin, 1999; Ng et al, 2007; Kolasinski et al, 2008), through solubilisation or volatilisation (Goering et al, 1990; Lohse et al, 2000; Ryba and Burgess, 2002; Fernandes and Krull, 2008; Brodie et al, 2011a). It has been proposed that losses or alterations to proteins, nucleic and amino-acids are the primary cause (Goering et al, 1990; Lohse et al, 2000). These compounds also tend to be relatively deficient in ^{13}C, suggesting the trends noted in BROC in the rinse method are from these nitrogenous compounds with losses greater than for the capsule method. Fernandes and Krull (2008) also reported greater losses in the rinse method by at least double. The capsule method showed a depleted $\delta^{15}N$ signature, but no significant change in $\delta^{13}C$ from known values. This clearly indicates that both $\delta^{13}C$ and $\delta^{15}N$ can be significantly affected by acid pre-treatment, but more importantly can also vary independently of one another (i.e. in significantly different proportions). The different types of N (and C) within a sample (organic and inorganic, and there relative proportions) can respond variably suggesting that the magnitude of the method affect will vary considerably between sample materials (i.e. different environments representing different OM provenance and composition). I therefore warn of the dangers of using ‘dual-mode’ analysis without a robust understanding of sample OM in the context of pre-analysis acid treatment effects on N (and C). Additionally, where sample size of C and N of OM is small, acid treatment induced alterations of OM can promote less reliable data, which further undermines a “dual-mode” analysis approach (Brodie et al, 2011a). Sample mineralogy may also influence the precision of C and N data (Fernandes and Krull, 2008).

3.6.4 $\delta^{13}C$ and $\delta^{15}N$ cross-plots

Cross plots of $\delta^{13}C$ and $\delta^{15}N$ have been used to indicate OM provenance (Meyers, 1997; Hu et al, 2006) in a similar fashion to C/N and $\delta^{13}C$ (Wilson et al, 2005; Zong et al, 2006; Yu et al, 2010), though the extent to which acid treatment method could influence the distribution of data on these plots has not been discussed. Brodie et al (2011a) reported this method bias on C/N and $\delta^{13}C$ cross-plots, illustrating the method and acid used could dictate the spread of data and subsequent environmental interpretation. This provides justification for examining $\delta^{13}C$ against $\delta^{15}N$. Our $\delta^{13}C$ and $\delta^{15}N$ cross-plots for each material similarly illustrate this bias (Figure 3.4). This may consequently preclude a robust interpretation, especially in environments where the amount, type and nature of OM varies and, there is more than one OM end member (i.e. rivers, estuaries, lakes, marine environments).

3.6.5 Inorganic nitrogen

An important assumption underpinning the interpretation of %N, C/N and $\delta^{15}N$ values of OM is that all sample N is OM bound, and that any IN component is insignificant in terms of error on data and subsequent interpretation (Sampei and Matsumoto, 2008). However, it is not common place to quantify IN of sample materials, despite the potential influence on organic %N and C/N values, especially in samples containing low OC (Stevenson et al, 1972; Muller, 1977; Waples, 1985; Schubert and Nielsen, 2001; Schmidt and Gleixner, 2005; Sampei and Matsumoto, 2008). For example, Schubert and Calvert (2001) reported C/N values of Arctic Ocean surface sediments from total N ranging from 4 – 8, and from organic N from 8 – 15. This represents a clear shift in interpretation from OM dominated by aquatic biomass to OM with an increasing terrestrially sourced component. Despite this, measurements for %N and $\delta^{15}N$ are commonly reported, whether on treated or untreated samples.

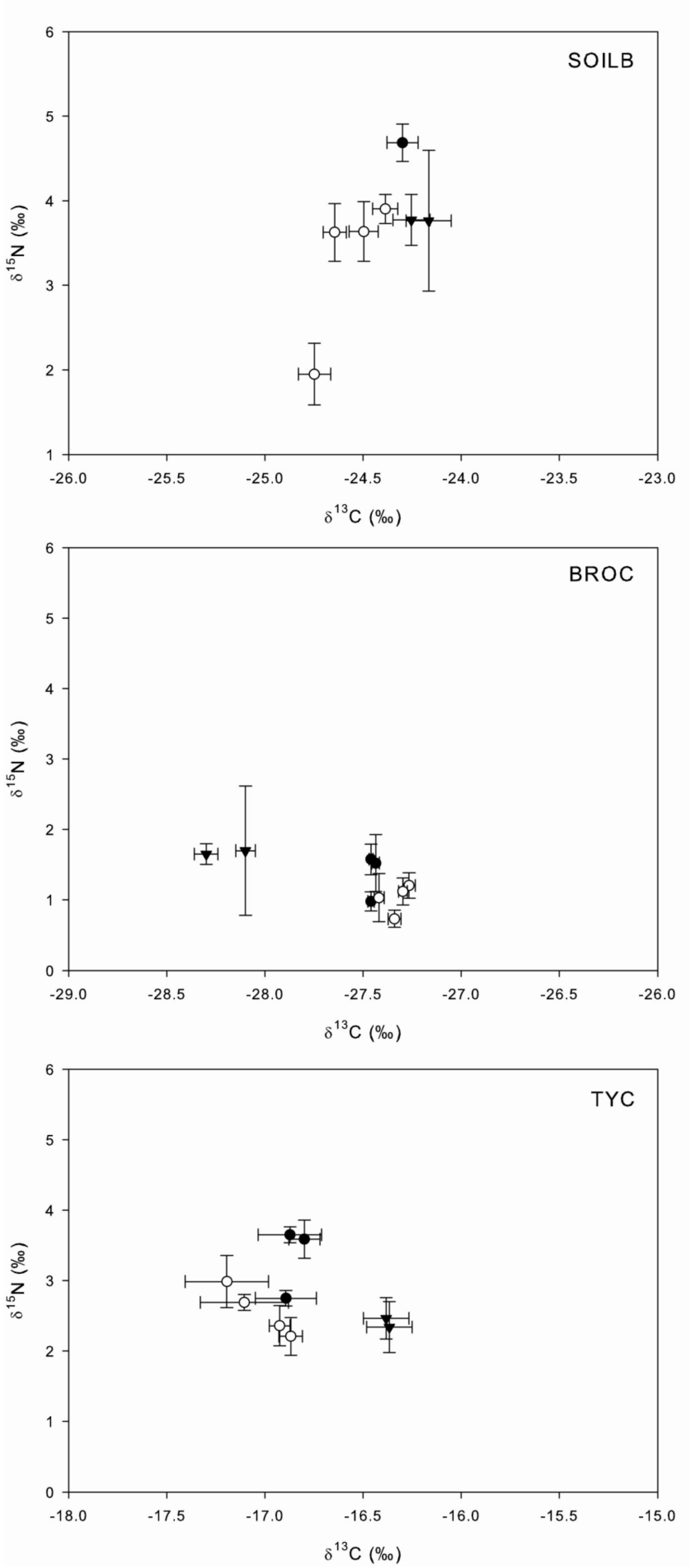

Figure 3.4: Bi-plots of δ^{13}C and δ^{15}N values of SOILB, BROC and TYC. The filled circle represents untreated samples; the unfilled circle represents rinse method samples and; the filled triangle capsule method samples. Error bars represent the standard deviation (1σ) of triplicate treatments for δ^{13}C and δ^{15}N.

In lieu of IN quantification, it has been proposed that the IN content can be estimated through a regression of %C and %N values, assuming a perfect linear relationship and using the calculated r^2 value. The estimation of IN content as a percentage deviation from that perfect linear relationship is calculated from $(1 - r^2) \times 100$ (Muller, 1977; Meyers, 1997; Hu et al, 2006). The approach of Muller, Meyers and Hu et al is the regression of a number of samples within a large system (e.g. lacustrine and estuarine surface samples), whereas my approach is sample specific (i.e. one sample rather than numerous spatial distributed samples). This IN estimation method is employed here for the analysed sample materials by linearly regressing data from all methods for each material (providing one r^2 statistic for the data – the "best fit") and then bootstrapping the data (i.e. computing 2000 iterations of the linear regression model on the data to assess the distribution of the r^2 statistic across the data set; this allows an assessment of the influence of acid treatment method on the spread of the data relative to the "best fit"). If acid treatment method has little to no influence on the spread of the %C and %N data, there should be little deviation from the "best fit" scenario, and hence little to no change in the estimation of IN.

Based on our bootstrapped r^2 estimates, and subsequent calculation of percentage IN, ~60 – 86% of BROC, ~27 – 49% of SOILB and ~ 55 – 75% of TYC may be attributed to IN (i.e. variation in %N explained by the regression model). The spread of data shown in Figures 3.5 – 3.7 represents (i) method bias and (ii) the true C and N distribution, and indicates a limitation to the interpretation of C/N values. These estimation ranges for IN content point toward an emergent linearity within our sample data, suggesting that the data be non-normally distributed either by nature, or by bias due to acid treatment method. This violates the key assumption of normality in the linear regression model and suggests an analysis of numerous spatially distributed samples (Muller, 1977; Hu et al, 2006) will propagate significant (but unrecognised) bias onto the interpretation of %C, %N and C/N values.

The overall statistical approach is misleading, and assumes (i) a dependence of %N on %C in sample OM within and between environments; (ii) a systematic and proportional co-variability of both pools within sample OM during sample pre-treatment and; (iii) the offsets from this are related to intrinsically non-linear IN processes. In the context of different formation, transportation and diagenesis processes, across significantly different environments, an emergent linearity from a complex C and

N system is unlikely to be real, particularly across diverse systems where the OM composition and structure varies. There is no apparent mechanism promoting linearity of C and N in a specific sample or indeed in a system, suggesting that the emergent linearity reported here can be substantially dictated by method. In addition, the disproportionate and non-systematic variability in elemental C and N concentrations previously reported (Brodie et al, 2011a) suggests that this procedure of estimation is further undermined, even if a non-linear relationship is assumed (which would likely lead to significantly greater bias). The idea that the emergent linearity can be used to derive an understanding of the non-linear IN pool based on the deviation from the presumed perfect linear relationship is incorrect, especially in the context of a down-core profile. Further, it does not reliably improve the understanding of the sample OM. Even if the prescribed linear fit was correct, the assumptions made are seriously flawed. It is concluded that the application of this statistical technique for IN estimation, in the context of method bias and the complexity of C and N in the environment, is an aberration and should be abhorred. I recommend that IN be quantified following an organic N digestion process (e.g. KOBr-KOH: Schubert and Calvert, 2001; Sampei and Matsumoto, 2008).

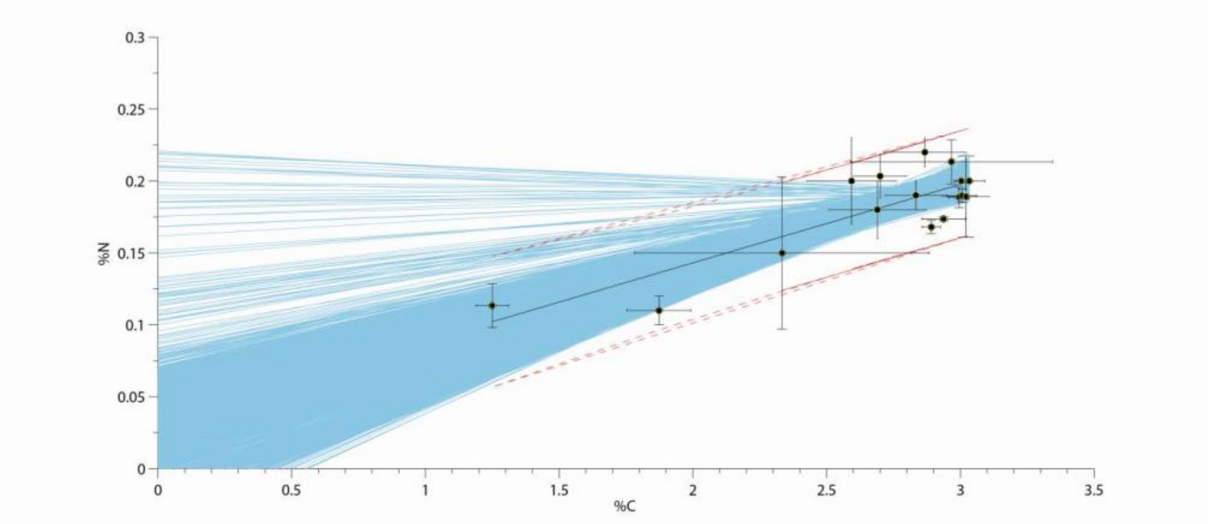

Figure 3.5: Bi-plot of %C and %N values of SOILB data for untreated (diamond); capsule (square) and; rinse methods (circle), with error bars representing 1σ. Blue lines are bootstrapped estimations of the data and red-dashed lines 95% confidence intervals.

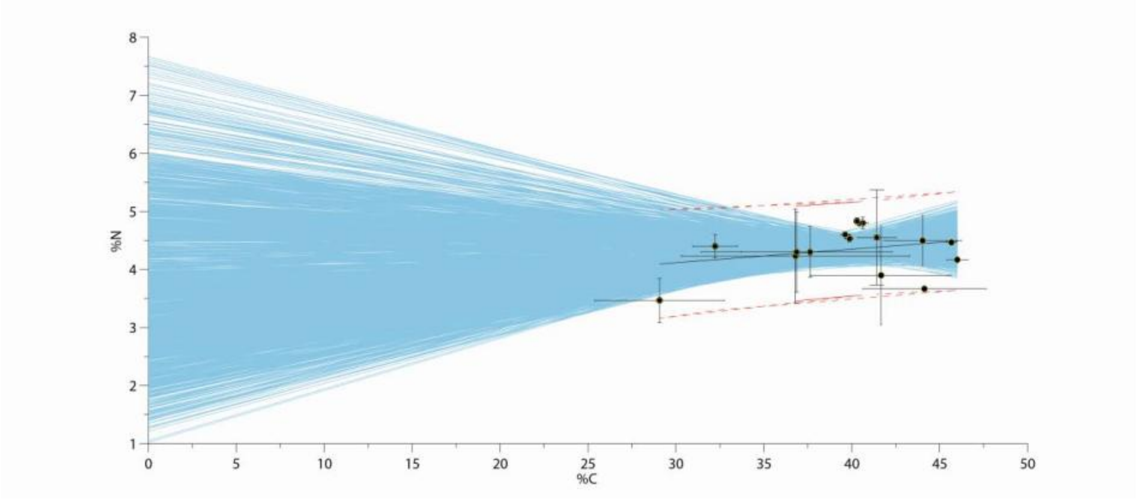

Figure 3.6: Bi-plot of %C and %N values of BROC data for untreated (diamond); capsule (square) and; rinse methods (circle), with error bars representing 1σ. Blue lines are bootstrapped estimations of the data and red-dashed lines 95% confidence intervals.

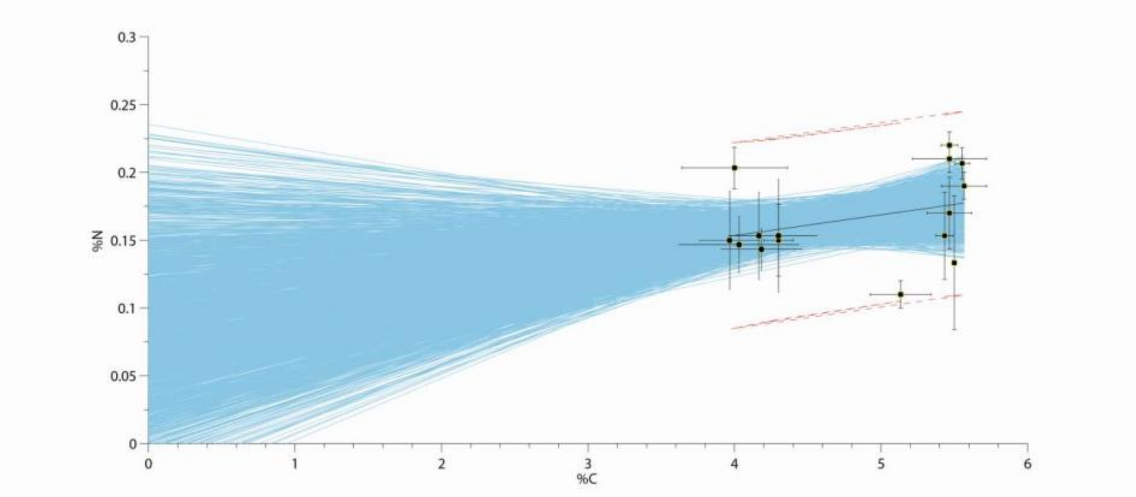

Figure 3.7: Bi-plot of %C and %N values of TYC data for capsule (square) and rinse methods (circle), with error bars representing 1σ. Blue lines are bootstrapped estimations of the data and red-dashed lines 95% confidence intervals.

3.7 Summary and Recommendations

1. These results show clear evidence for significant differences in measured $\delta^{15}N$ values between pre-analysis acid treatment methods and between untreated samples. The bias is of the order of ~1.5 ‰.
2. Differences between $\delta^{13}C$ and $\delta^{15}N$ on acid treated samples are non-linear and disproportionate. This implies that the type, amount and nature of OM, and its potential alteration during pre-analysis acid treatment methods, is an important factor underpinning the reliable determination of C/N, $\delta^{13}C$ and $\delta^{15}N$ of sample OM. Importantly, these offsets can significantly undermine environmental interpretation of $\delta^{15}N$ values.
3. Capsule type can have a significant influence on the reliability of $\delta^{15}N$ in sample OM. Untreated samples combusted only in Ag capsules particularly produce aberrant results (exclusive of bias linked to acidification). I therefore recommend further wrapping capsule method samples (which traditionally only use Ag capsules) in Sn capsules after acid treatment, as this increases the combustion temperature in the reactor column. This is recommended with the codicil that the affect of acidification could obscure the affect of the capsule.
4. I do not recommend “dual-mode analysis” of sample materials due to these unpredictable, non-linear differences, which suggest its inapplicability. Samples should be processed and analysed for C and N on separate aliquots, in the knowledge of the potential for acid-induced offsets. It should be noted that measurement of N on untreated samples does not guarantee reliable results.
5. The estimation procedure used for IN, namely linear regression, is seriously flawed, and provides no sensible or reliable information on the influence of IN on measured %N (and hence influence on C/N values) or $\delta^{15}N$ values of OM. IN should therefore be quantified on separate sample aliquots, and a correction applied (Schubert and Calvert, 2001; Sampei and Matsumoto, 2008).

Chapter 4

Evidence for bias in C/N, δ^{13}C and δ^{15}N values of bulk organic matter, and on environmental interpretation, from a lake sedimentary sequence by pre-analysis acid treatment methods.

Brodie, C.R., Casford, J.S.L., Lloyd, J.M., Leng, M.J., Heaton, T.H.E., Kendrick, C.P., Zong, Y.Q. (In Press) Evidence for bias in C/N, δ^{13}C and δ^{15}N values of bulk organic matter, and on environmental interpretation, from a lake sedimentary sequence by pre-analysis acid treatment methods. Quaternary Science Reviews

4.1 Introduction

Bulk organic matter (OM) in lacustrine sediments is a heterogeneous composition of organic materials derived from aquatic (e.g. phytoplankton; macrophytes) and terrestrial origins (e.g. trees; shrubs; grasses; animals)(see reviews in Meyers and Ishiwatari, 1993; Meyers, 1997; Sharpe, 2007). A number of factors contribute to the structure and isotopic composition of OM in lake sediment: the contribution of C and N from different source end-members; the state and availability of C and N in the environment; carbon fixation pathways; lake productivity; pre- and post-burial diagenetic processes (aerobic and anaerobic); dissolved CO_2 concentration and; changes in palaeoenvironmental controls on OM C and N budgets (e.g. Stuiver, 1975; Meybeck, 1982; Hedges et al, 1986; Hayes, 1993; Meyers and Ishiwatari, 1993; Meyers, 1994, 1997; Krishnamurthy et al, 1999; Turney, 1999; Lehmann et al, 2003; Lucke et al, 2003; Perdue and Kopribnjak, 2007). Collectively, these factors make the evaluation of the palaeoenvironmental and palaeoclimatic influence on sedimentary OM difficult. However, the investigation of lake sediment sequences with highly resolved age-depth models and high signal-to-noise ratios can still provide high amplitude palaeoenvironmental information (e.g. Lucke et al, 2003; Wei et al, 2010).

Despite the complexity of these processes on sediment OM, weight ratios of elemental carbon to nitrogen (C/N), and stable isotope ratios of C and N ($\delta^{13}C$ and $\delta^{15}N$) from bulk OM, have been successfully and widely used to interpret OM provenance (e.g. aquatic versus terrestrial source) and vegetation type (e.g. C_3 versus C_4 plants; Meyers and Ishiwatari, 1993; Thornton and McManus, 1994; Meyers, 1997; Sampei and Matsumoto, 2001; Lamb et al 2004, 2006; Street-Perrott et al. 2004; Wilson et al. 2005; Zong et al. 2006). These proxies have subsequently underpinned palaeoenvironmental research and been used as a tool for understanding biogeochemical processes in a range of sedimentary sequences (Talbot and Johannessen, 1992; Street-Perrot et al., 1997; Turney, 1999; Huang et al, 2001; Fuhrmann et al., 2003; Lucke et al., 2003; Baker et al, 2005; Lamb et al., 2007; Galy et al., 2008; Mampuku et al., 2008; Domingo et al., 2009; Langdon et al., 2010; Scholz et al., 2010; Yu et al, 2010; Wei et al, 2010).

In general, C/N ratios of OM tend to range from 3 – 9 (dominated by aquatic biomass; protein rich, lignin poor), 10 – 20 (admix of aquatics, including emergent aquatics, and terrestrial sources) and > 20 (dominated by terrestrial biomass; protein poor; lignin rich) (e.g. Meybeck, 1982; Hedges et al, 1986; Tyson, 1995; Meyers, 1997; Sharpe, 2007). The δ^{13}C of OM is broadly used as an indicator for carbon sources, productivity and photosynthetic pathways in plants. Values for land plants range from –6 to –35 ‰ (see overviews in Tyson, 1995; Meyers, 1997; Sharpe, 2007), and can differentiate between C_3 plants (δ^{13}C ≈ –22 to –35 ‰) and C_4 plants (δ^{13}C ≈ –6 to –15 ‰) in certain environments (e.g. estuaries, sea floors, lakes, soils; e.g. Smith and Epstein, 1971; O'Leary, 1988; Tyson, 1995; Meyers, 2003; Street-Perrot et al, 2004; Sharpe, 2007; Mampuku et al, 2008; Scholz et al, 2010). The δ^{13}C of OM has also been used for a range of other investigations including; (1) assessment of carbon reservoir turnover times and soil C dynamics (Harris et al, 2001); (2) determination of trophic levels in environmental systems (Bunn et al, 1995; Pinnegar and Poulnin, 1999; Kolasinski et al, 2008); (3) primary productivity reconstructions and estimation of carbon burial rates and; (4) to understand mineralisation processes (Midwood and Boutton, 1998; Freudenthal et al, 2001; Leng and Marshall, 2004). δ^{15}N has been used to understand trophic pathways in food webs (Bunn et al, 1995; Pinnegar and Polunin, 1999; Ng et al, 2007; Kolasinski et al, 2008); OM provenance and degradation (Thornton and McManus, 1994; Meyers, 1997; Hu et al, 2006; Barros et al, 2010); denitrification in the water column (Altabet et al, 1995; Ganeshram et al, 2000); nitrate utilisation (Calvert et al, 1992; Teranes and Bernasconi, 2000); N_2-fixation (Haug et al, 1998) and; eutrophication (Owens, 1987; Vob et al, 2005). In addition, C/N values are used to support δ^{13}C and δ^{15}N, for example through bi-plots providing a structure within which OM provenance and type can be broadly identified (e.g. Talbot and Johannessen, 1992; Thornton and McManus, 1994; Meyers, 1997; Meyers and Teranes, 2001; Krull et al, 2002; Lucke et al, 2003; Wilson et al, 2005; Lamb et al. 2006; Zong et al. 2006; Mackie et al. 2007; Sharpe, 2007; Yu et al, 2010). Investigators have subsequently deduced changes in environmental and/or climatic processes through interpretation of changing states of the system under investigation (e.g. terrestrial vs. aquatic biomass; C_3 vs. C_4 vegetation).

However, interpretations of C/N, δ^{13}C and δ^{15}N are predicated on the production of reliable proxy data, and the ability to disentangle the complex processes leading to OM preservation in the sedimentary record. This necessitates a complete understanding of the precision of the raw data, which, for C/N, δ^{13}C and δ^{15}N values from bulk sediment OM, are not widely discussed in the literature beyond instrument precision (reported as the standard deviation (σ) of replicate runs of standard reference materials). Further, the instrument precision on C/N values is rarely (if at all) discussed.

The accurate determination of C/N and δ^{13}C composition of OM requires the complete removal of any IC from the total carbon, commonly achieved through acid treatment. There is a variety of pre-analysis acid treatment methods that have been used in the published literature, from which it is clear there is no consensus on standard practice. Research has shown significant non-linear bias on measured C/N, δ^{13}C and δ^{15}N values directly associated with pre-analysis acid treatment methods, which can undermine an environmental interpretation of the data (Froelich, 1980; Yamamuro and Kayanne, 1995; Bunn et al, 1995; King et al. 1998; Lohse et al. 2000; Schubert and Nielsen, 2000; Ryba and Burgess et al, 2002; Kennedy et al, 2005; Schmidt and Gleixner, 2005; Galy et al, 2007; Fernandes and Krull, 2008; Brodie et al, 2011a). For example, Brodie et al. (2011a) noted a C/N value range of ~6 – 13 for a terrestrial land plant (Broccoli) across pre-analysis acid treatment methods. These C/N values suggest OM derived largely from aquatic sources, or from an admixture of aquatic and terrestrial sources. More importantly, these offsets have been shown to be non-linear and unpredictable within and between pre-analysis acid treatment methods (Brodie et al, 2011a).

Differences in %C have been reported at 5 – 78 % and for %N at 0 – 50% on modern and ancient sedimentary materials, either as a loss of C and N (Froelich, 1980; Yamamuro and Kayanne, 1995; Bunn et al, 1995; King et al. 1998; Lohse et al. 2000; Schubert and Nielsen, 2000; Ryba and Burgess et al, 2002; Schmidt and Gleixner, 2005) or as an artificial gain in C and N (Brodie et al, 2011a). Shifts in δ^{13}C are variable, ranging from enrichment in δ^{13}C of 0.2 – 8.0 ‰ (e.g. Schubert and Nielsen, 2000; Kolasinski et al. 2008; Brodie et al, 2011a), a depletion in δ^{13}C of 0.1 – 1.9 ‰ (Kennedy et al; 2008; Komada et al. 2008; Brodie et al, 2011a) and no change (e.g. Midwood and Boutton, 1998; Kennedy et al, 2005). This is similar for δ^{15}N, where results range from an enrichment of 0.1 – 3 ‰ (Bunn et al, 1995; Brodie et al, 2011b), to a depletion of 0.2 –1.8 ‰ (Bunn et al, 1995; Harris et al, 2001; Kennedy et al, 2005; Ng et al, 2007; Fernandes and Krull et al, 2008), and no significant change (Serrano et al, 2008). The bias on OM from acid treatment, alongside the complex processes that can influence OM prior to, and during, sedimentary preservation, suggests that reliance on the commonly reported instrument precision alone is unrealistic for robustly interpreting measured C/N, δ^{13}C and δ^{15}N values.

4.2 Unresolved Issues

Despite the considerable potential for acid treatment method to alter the bulk OM signal prior to C/N, $\delta^{13}C$ and δ ^{15}N analysis, the potential bias in a sedimentary sequence of samples has hitherto never been investigated. In addition, the influence of inorganic carbon (IC) and inorganic nitrogen (IN)(Hoefs, 1973; Sharpe, 2007); sample homogenisation (Baisden et al, 2002; Hilton et al, 2010) and sample size (Brodie et al, 2011a) can contribute additional inaccuracy and imprecision to measured data. There is an increase in the application of "dual-mode" isotope analysis (where C/N, $\delta^{13}C$ and δ ^{15}N are measured simultaneously from the same pre-treated sample), implying an acidification of sample material prior to analysis. It is not common to acidify samples prior to δ ^{15}N analysis, but acidification is required for dual $\delta^{13}C$ and $\delta^{15}N$ analysis. It is clear, therefore, that the assumption that instrument precision alone accounts for the absolute imprecision on measured C/N, $\delta^{13}C$ and δ ^{15}N values is questionable. Moreover, assumptions on the accuracy of the measured C/N, $\delta^{13}C$ and δ ^{15}N are also questionable.

The aim of this study was to compare, for the first time, the effect of pre-analysis acid treatment methods on C/N, $\delta^{13}C$ and δ ^{15}N of OM from a sedimentary sequence. An ancient lake cored sequence is analysed using the capsule and rinse methods alongside that of untreated materials. I test the null hypothesis that there is a significant difference between methods on the same sample horizon, implying that data precision exceeds the commonly discussed instrument precision. Specifically, the following research questions are addressed:

1. Are there significant differences between the results of pre-analysis acid treatment methods for C/N, $\delta^{13}C$ and $\delta^{15}N$ of bulk OM on a stratigraphical sequence of samples?

2. Do pre-analysis acid treatment methods add negligible imprecision to measured C/N, $\delta^{13}C$ and $\delta^{15}N$ values?

3. Can different pre-analysis acid treatment methods influence environmental interpretation of C/N, $\delta^{13}C$ and $\delta^{15}N$ of bulk OM?

4.3 Materials and Methods

4.3.1 Core material

A sedimentary sequence was extracted from Lake Tianyang (20°31'1.11" N, 110°18'43.02" E), south China, in January 2008, for multi-proxy palaeoenvironmental reconstruction, including C/N, $\delta^{13}C$ and $\delta^{15}N$ of OM. For this comparison, 20 horizons were sub-sampled in the core from 7.00 – 10.24 m (16 cm resolution). This section of the core material was selected due to the significant change in the lithology (Figure 4.1) from a brown clayey silt unit, with few very fine sands and silts, and a low organic content (10.24 m to 8.06 m), to an organic rich (amorphous) clay unit (8.06 m to 7.09 m). In addition, the $\delta^{13}C$ of bulk OM derived from some pilot samples showed that this section produced an overall $\delta^{13}C$ range of ~ 15 ‰ and, in particular, there is a ~12 ‰ shift across the lithologic boundary. Unfortunately, low levels of N precluded a full $\delta^{15}N$ record across the selected sample horizons so $\delta^{15}N$ values are only reported from 7.00 m to 7.46 m.

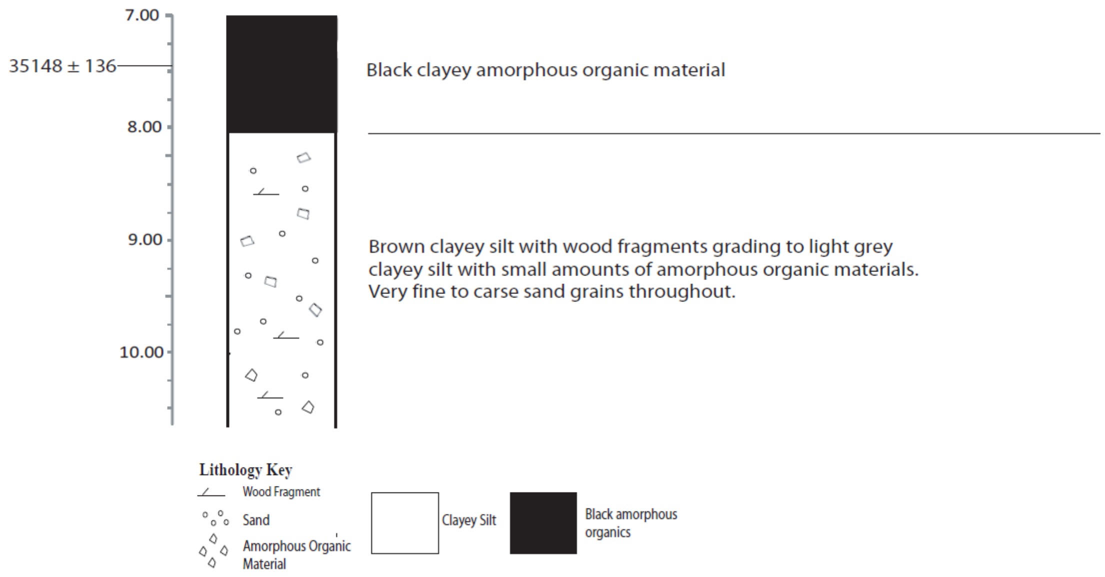

Figure 4.1: Lake Tianyang core lithology and description from 7.00 m to 10.20 m. The ^{14}C age is reported in ^{14}C yrs BP (uncalibrated).

4.3.2 Preparation methods

4.3.2.1 Cleaning Protocol

Prior to sample preparation, all sub-sampling equipment and glassware were thoroughly washed in 1% nitric acid, rinsed in deionised water, followed by a wash in 2% soap solution (neutracon®), a final deionised water rinse and then fired at 550°C for 3 h. Ag capsules were fired at 550°C for 3 h prior to use and Sn capsules were submerged in methanol for 24 h and then air dried. Cleaned capsules were then sealed in pre-cleaned containers and stored until use.

4.3.2.2 Rinse Method

The rinse method involves the acidification of sample materials for ~ 24 h followed by sequential rinsing with deionised water (See section 2.3.1).

4.3.2.3 Capsule Method

The capsule method is an in-situ acidification of sample material in a silver capsule, followed by drying down (See section 2.3.2).

4.3.2.4 Untreated

Sample δ^{15}N is traditionally measured on untreated sample material (e.g. Muller, 1977; Altabet et al, 1995; Schubert and Calvert, 2001; Sampaei and Matsumoto, 2008), assuming a negligible influence from inorganic nitrogen (e.g. nitrates, ammonia; e.g. Sampei and Matsumoto, 2008). Therefore, in addition to the rinse and capsule methods untreated sample materials for C/N, δ^{13}C and δ^{15}N analysis were also prepared, which involved directly weighing an untreated sample aliquot (500 μg for C/N and δ^{13}C and 15 μg for δ^{15}N) into a prepared Sn capsule, crimping and analysing.

4.3.3 Analytical methods

4.3.3.1 C/N and δ^{13}C

The %C, %N and δ^{13}C values of sample OM were analysed using an online system comprising a Costech ECS4010 elemental analyser (EA), a VG TripleTrap, and a VG Optima mass spectrometer at the NERC Isotope Geosciences Laboratory (NIGL), with data reduction carried out using DataApex Clarity ver 2.6.1 software package. See section 2.4.1 for full details.

4.3.3.2 $\delta^{15}N$

Nitrogen isotope analyses were performed using a FlashEA 1112 elemental analyser linked to a Delta+XL isotope ratio mass spectrometer (EA-IRMS) via a Conflo III interface. Samples were combusted at 900°C with all samples acidified in the capsule method further wrapped in Sn capsules. Limits on analytical precision are mainly determined by conditions of combustion and chromatography in the elemental analyser. For organic materials containing a few %N (e.g. BROC), within-run precision for $\delta^{15}N$ is better than 0.13 ‰ (1σ for $n = 13$ samples). See Section 3.2 for further details.

4.3.4 Data Analysis

The data were compared using a one-way ANOVA, at the 95% confidence limit, to determine differences within (i.e. acid reagent) and between (i.e. untreated versus capsule method versus rinse method) the pre-analysis treatment methods, and take a p-value < 0.05 to indicate a significant difference. All data were tested for normality using an Anderson-Darling normality test, and tested for homogeneity of variances using a Bartlett’s test (which assumes data are normally distributed) and a Levene’s test (which assumes data are non-normally distributed). Comparisons were not made between acid treated and untreated samples for C/N and $\delta^{13}C$.

4.4 Results

The %C, %N, C/N and $\delta^{13}C$ data are presented in Figure 4.2 and ANOVA comparisons for C/N and $\delta^{13}C$ data from each method and reagent investigated are presented in Table 4.1.

4.4.1 %C and %N

From 7.00 to 7.52 m, the core material is characterised by high %C and %N values relative to the sample horizons below 7.52 m, where %C and %N are very low. For %C and %N, the rinse method samples above 7.52 m are consistently ~20% higher than capsule and untreated method samples. With the exception of the 5% HCl capsule method samples at 8.76 m for %C, and 20% HCl capsule method sample from 7.80 – 8.60 m for %N, the data below 7.52 m are relatively coherent.

4.4.2 C/N and δ^{13}C

C/N ratios between methods are highly variable within specific sample horizons, especially within the capsule method samples (e.g. 7.48 m, 8.76 m, 9.24 m for 5% HCl capsule method; 8.12 m, 8.60 m for 20 % HCl capsule), and between the capsule method samples and rinse method samples. An overall range of ~1 – 100 was evident between methods on some sample horizons. For example, at 8.76 m the capsule method samples returned C/N values of 81 to 122, whilst the rinse method samples returned C/N values of ~34. At 9.08 m, samples in the capsule method return C/N values of ~19, and rinse method samples ~ 11. In general, data from the rinse method appear more coherent than data from the capsule method.

δ^{13}C data from samples between 7.00 m and 7.64 m across all methods tested are indistinguishable from one another (i.e. appear to be within instrument precision limits). Similar coherence between the methods is evident in samples between 9.00 m and 9.24 m. However, our data also show sample horizons with incoherency between the methods (i.e. greater than instrument precision by a minimum of ~0.2 ‰), in particular from 7.64 m to 8.12 m and 8.60 m to 9.00 m. The greatest divergence in the data are from 7.64 m to 8.12 m and between the 20% HCl capsule method and 20 % HCl rinse method (~2.5 ‰ (7.64 m)), and from 8.60 m to 9.00 m which is caused by the 5 % HCl capsule method (~6 – 7 ‰ (8.60 m)). Between the remaining three methods at 8.60 m, the difference range is between 0.4 – 3.5 ‰. The divergence in δ^{13}C data, within and between methods, appears to become more evident in samples with relatively lower %C, but not in all instances (e.g. 9.00 m to 9.24 m). In general, given the differences between methods on any one sample horizon, a general trend in C/N and δ^{13}C values between methods is apparent.

4.4.3 δ^{15}N

δ^{15}N values were only measureable between 7.09 m and 7.46 m due to extremely low %N. The δ^{15}N data and ANOVA comparisons for each method and reagent are shown in Figure 4.3 and Table 4.2 respectively. Our results show that all acid treated samples produced lower δ^{15}N in comparison to untreated samples, with the largest range in values between methods of ~0.8 ‰ (at 7.16 m). In general, capsule method samples produced lower values than rinse method samples, with the exception of 5% HCl capsule samples at 7.09 m and 7.16 m. Overall, the rinse method samples produced more coherent results than the capsule method (< 0.2 ‰ overall range for all rinse method samples). ANOVA results indicated statistically significant differences between all methods for all sample materials, but highlighted no differences within the rinse method (i.e. no difference between samples acidified in 5% HCl or 20% HCl within the rinse method). We note a fractionation in δ^{15}N in all sample horizons, within and between methods, but no concomitant change in mass %N.

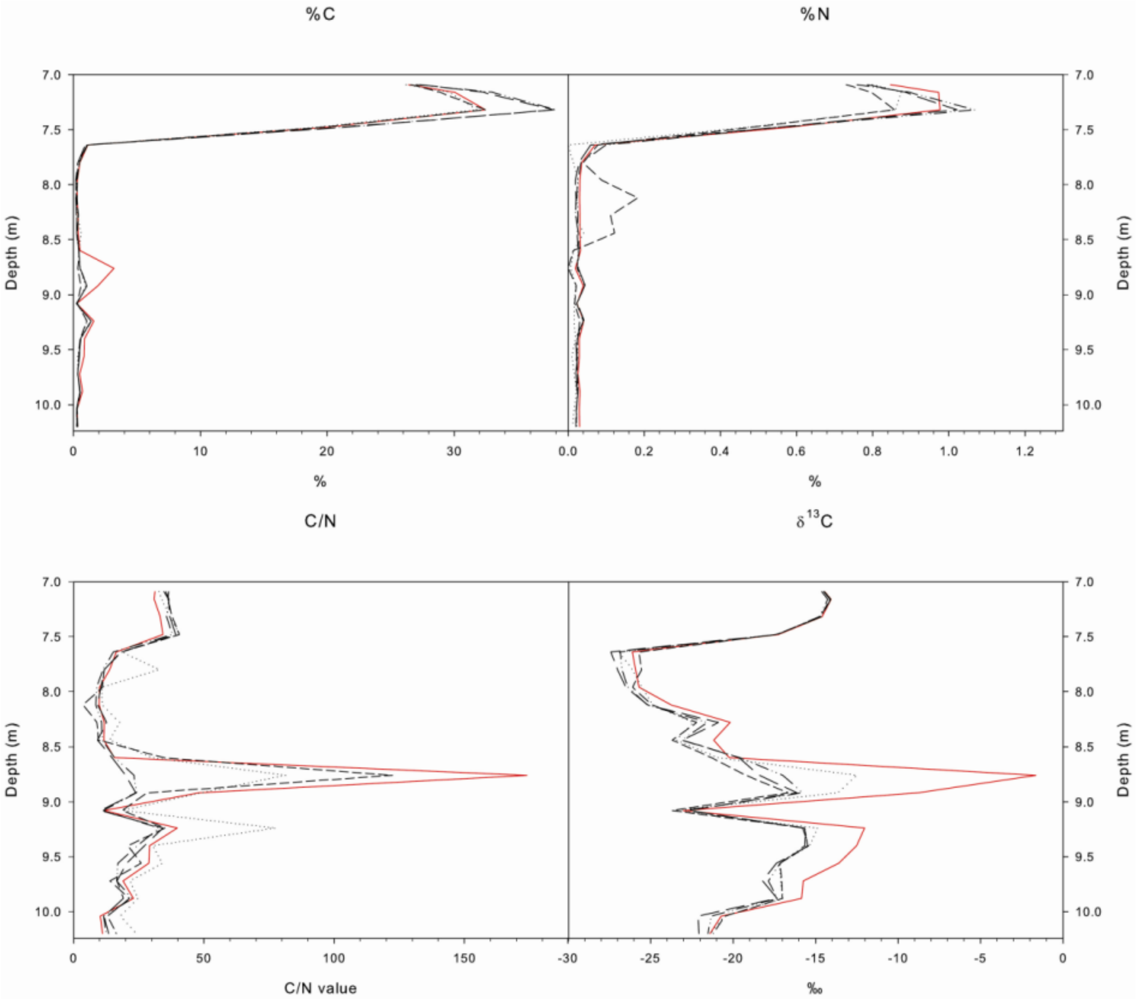

Figure 4.2: Down-core plots of %C, %N, C/N and δ^{13}C for data derived from the capsule method, rinse method and untreated samples. The solid red line represents untreated sample materials, the black dotted line represents 5% HCl capsule method data, the black short perforated line represents 20% HCl capsule method data, the black perforated and dotted line represents 5% HCl rinse method data and the black long perforated line represents 20% HCl rinse method data.

Table 4.1: ANOVA comparison results for C/N and $\delta^{13}C$ for all tested sample horizons.

	$\delta^{13}C$			**C/N**		
Depth (m)	**P-value (R-Squ)**	**Difference (‰)**	**Cause**	**P-value (R-Squ)**	**Difference**	**Cause**
7.09	0.197 (20.98)	nd	-	0.00 (74.05)	3 – 4	5% and 20% HCl capsule higher than 5% HCl rinse
7.16	0.183 (22.52)	nd	-	0.18 (23.18)	nd	-
7.32	0.04 (49.01)	0.2	5% HCl more enriched than 20% HCl in rinse method	0.29 (11.69)	nd	-
7.48	0.55 (0.00)	nd	-	0.143 (27.67)	nd	-
7.64	0.00 (94.69)	1.0	20% HCl capsule sample more enriched than 20% HCl rinse sample	0.97 (0.00)	nd	-
7.80	0.00 (98.25)	0.6 – 1.5	All samples differ over 1.5 ‰ range, with more enriched values in the capsule method.	0.00 (95.63)	22	5% HCl capsule higher than all other samples
7.96	0.01 (64.38)	0.3 – 0.7	5% HCl capsule more enriched than all other methods	0.94 (0.00)	nd	-
8.12	0.01 (60.68)	0.4	Capsule method samples more enriched than rinse method samples	0.02 (58.67)	4 – 6	5% and 20% HCl capsule method different from 20% HCl rinse samples
8.28	0.00 (87.85)	0.2	Capsule method slighted more depleted than rinse method	0.08 (38.60)	nd	-
8.44	0.01 (65.66)	0.4 – 0.6	20% HCl capsule more enriched all other samples	0.52 (0.00)	nd	-
8.60	0.00 (98.83)	0.4	5% HCl capsule more enriched than 20% HCl capsule, and	0.00 (87.59)	16	Capsule method samples higher than rinse method

			both rinse samples			samples
8.76	0.00 (95.72)	1.2 – 6.8	5% HCl capsule more enriched than all other samples. 20% HCl capsule most depleted.	0.00 (66.52)	98 – 103	5% HCl and 20% HCl capsule method higher than rinse method samples.
8.92	0.01 (81.77)	2.6 – 3	5% HCl more enriched than all other samples.	0.00 (94.19)	20 – 25	5% HCl capsule higher than other samples
9.08	0.00 (97.53)	0.6 – 1.0	Capsule samples more depleted than rinse samples. 5% HCl rinse more enriched than 20% HCl rinse.	0.00 (87.87)	7	Capsule method samples higher than rinse method samples
9.24	0.00 (97.71)	1.0	5% HCl capsule more enriched than all other samples	0.04 (47.69)	20	5% HCl capsule higher than other samples
9.40	0.07 (40.58)	nd	-	0.03 (54.35)	10	5% and 20% HCl capsule method samples different
9.56	0.74 (0.00)	nd	-	0.31 (9.77)	nd	-
9.72	0.00 (88.05)	1.0 – 1.2	Rinse method samples more depleted than capsule method samples. 20% HCl capsule more enriched than all other samples	0.06 (41.74)	nd	-
9.88	0.09 (35.93)	nd	-	0.04 (49.52)	7	5% HCl capsule different from 20% HCl rinse
10.02	0.00 (94.86)	1.0 – 1.8	Rinse samples more depleted than capsule samples. 5% HCl rinse most depleted	0.04 (49.95)	8	5% HCl different from both rinse samples
10.20	0.00 (94.72)	0.3 – 0.6	Rinse method sample more depleted than capsule samples	0.00 (74.84)	6 – 8	5% HCl capsule higher than other samples

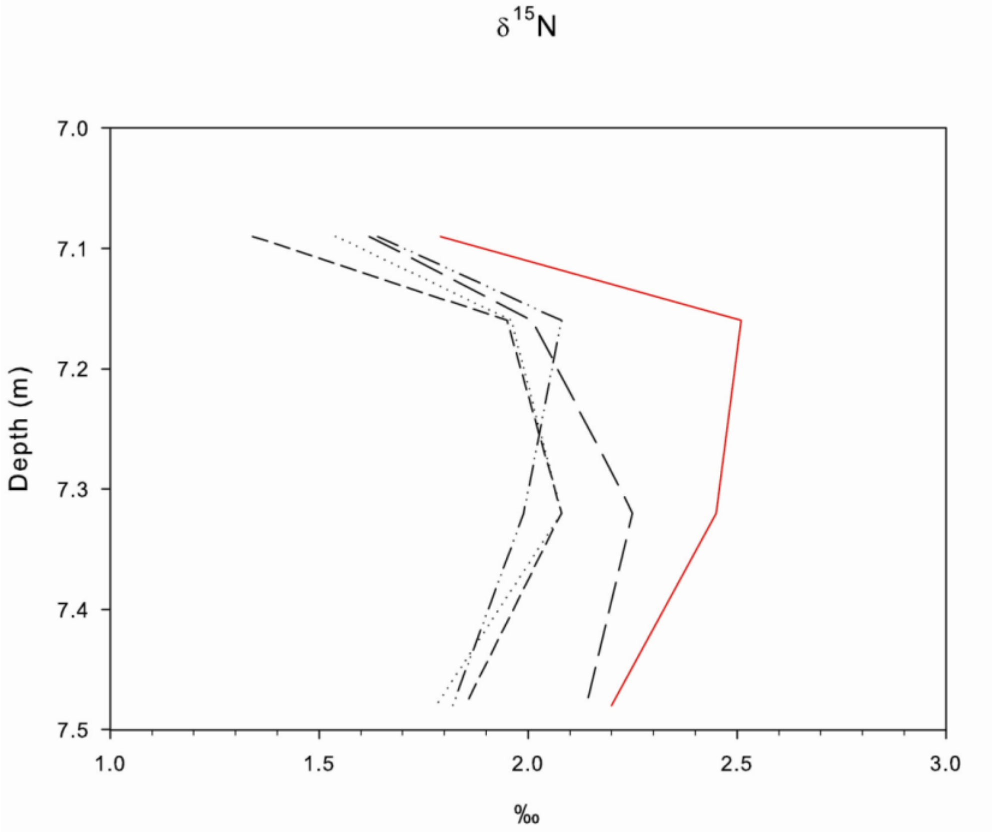

Figure 4.3: Down-core plots of $\delta^{15}N$ for data derived from the capsule method, rinse method and untreated samples. The solid red line represents untreated sample materials, the black dotted line represents 5% HCl capsule method data, the black short perforated line represents 20% HCl capsule method data, the black perforated and dotted line represents 5% HCl rinse method data, and the black long perforated line represents 20% HCl rinse method data.

Table 4.2: ANOVA comparison results for $\delta^{15}N$ for all tested sample horizons.

	$\delta^{15}N$		
Depth (m)	**P-value (R-Squ)**	**Difference (‰)**	**Cause**
7.09	0.00 (84.07)	0.46	Acid treated samples lower than untreated samples. 20% HCl rinse lowest.
7.16	0.00 (89.14)	0.77	Acid treated samples lower than untreated samples
7.32	0.02 (51.33)	0.46	Acid treated samples lower than untreated samples. Capsule method samples lowest.
7.48	0.00 (79.94)	0.42	Capsule method and 5% HCl rinse lower than untreated samples and 20% HCl rinse.

4.5 Discussion

4.5.1 Methodological differences

The pre-analysis acid treatment approach is underpinned by the assumption that the OM fraction is either unaltered during the process, or that any changes are at least systematic and proportional (i.e. predictable). This clearly suggests that, within instrument precision, results from any method followed should be indistinguishable from one another. Our results from the Lake Tianyang sedimentary sequence indicate an inconsistency in the application of any single pre-analysis acid treatment method in a down-core context for C/N, δ^{13}C and δ^{15}N. There is evidence for significant differences in measured C/N, δ^{13}C and δ^{15}N values within and between pre-analysis acid treatment methods (Tables 4.1 and 4.2). Differences between each acid treatment method in C/N, δ^{13}C and δ^{15}N values within and between sample horizons are highly variable, and not always in the same direction. For some sample horizons, differences between acid preparation methods for C/N values can be as high as ~90 (e.g. at 8.76 m) and as low as 0.2 (e.g. at 7.32 m; 8.44 m). Likewise, differences in δ^{13}C between acid treatment methods can be as high as 6.8 ‰ (e.g. 8.76 m) but for other horizons be within instrument precision (e.g. < 0.2 ‰; 7.09 m – 7.48 m). This may, in part, be a function of the %C and %N of the sample material. For example, our δ^{13}C data are generally in good agreement with high %C. However, the imprecision on the data tends to increase within and between methods as %C in the sample material becomes lower (e.g. 7.64 m to 9.00 m), but this is not always the case (e.g. 9.00 m to 9.24 m). This suggests sample materials with low %C may be more susceptible to acid method bias (and of greater magnitude), but this is not a general rule (Brodie et al, 2011a). The type of organic compounds in each sample and how they vary between samples, or within and between samples after acidification, have not been characterised.

Where there is a high range of C/N values apparent between methods, this can fundamentally alter the support for δ^{13}C and δ^{15}N from cross-plots of these data. For example, at 7.80 m, the 5% HCl capsule method points towards an environment dominated by terrestrially sourced OM (C/N value ~32), whereas C/N values from all other methods suggest an environment with a significant aquatic biomass contribution to total OM (C/N value ~12). This contradictory position clearly indicates a serious discrepancy regarding the interpretation of elemental and isotopic C and N proxies of OM from these cross–plots and in a down-core context. It also suggests that the assumptions underpinning acid pre-treatment methods are invalid (Brodie et al, 2011a; 2011b). In addition, there are known biases from IN contamination, which can lower C/N values below the true organic C/N value (e.g. Muller, 1977; Schubert and Calvert, 2001; Sampei and Matsumoto, 2001; Meyers, 2003; Mampuku et al, 2008). For example, Muller (1977) reported C/N values <4 from deep sea sediments as a consequence of inorganic ammonia. Furthermore, the range of C/N values, as discussed in the context of marine versus terrestrial source, is also more complex than the standard interpretation detailed. For example, C/N values (weight ratio) of submerged aquatic macrophytes have documented ranges of 6 – 60 (e.g. Atkinson and Smith, 1983) and macroalgae can range from 16 – 68 (brown macroalgae; Fenchel and Jørgensen, 1977). Brodie et al. (2011a) also report C/N range of ~ 6 – 13 for broccoli (a terrestrial plant) which has a typical C_3 δ^{13}C value of –27.4 ‰. Collectively, these factors point to a serious problem in the general theory on OM provenance as interpreted through C/N and δ^{13}C values.

In addition to the problems highlighted for C/N values, at 8.60 m, the 5% HCl capsule method returned a δ^{13}C value of –12.5 ‰, ~6.8 ‰ more enriched than data from all other acidification methods (δ^{13}C range between methods is –21.3 to –12.5 ‰). Our raw data from untreated material show that this sample material has a major IC component (δ^{13}C = –1.6 ‰), suggesting the 5% HCl capsule method is less efficient at IC removal in comparison to other methods for this sample, although it is widely assumed 5% HCl should efficiently remove calcite. Between all other methods at 8.76 m, the difference in δ^{13}C value was ~ 2 – 3 ‰. However, in the context of the overall data trend (e.g. the ~12 ‰ shift from 7.00 m to 7.52 m; see Figure 4.2), the value returned for the 5% HCl capsule method would not look out of place had this been the only method followed. This, subsequently, could have led to a misinterpretation of the core data in the context of sample OM: the 5% HCl capsule data at 8.76 m suggest an environment dominated by C_4 type vegetation (both high C/N and δ^{13}C values), whereas the three other acid treatment methods tested produced more consistent results (though still potentially imprecise), suggesting a C_3 dominated environment. I therefore do not recommend the use of 5% HCl in the capsule method. These differences between the acid reagents and methods investigated here have two possible explanations: (i) the different effect of acid treatment on the IC components within the sample material and; (ii) non-linear and unpredictable offset on the OC components within the sample material. At 8.76 m, the offset in δ^{13}C value is caused by inefficient removal of IC (see above), an offset not recorded in the other methods. This suggests that different methods and reagents (even at 5% HCl) have differential rates of removal of what is probably calcite (i.e. 5% HCl appeared to remove the IC in the beaker method, likely due to the increased time of exposure of the sample to the acid in this method relative to the capsule method). Therefore, this problem is likely to be exacerbated where less soluble forms of IC exist in sample materials, such as dolomites and siderites, which can produce as large an offset to the δ^{13}C value as calcite. Moreover, an admixture of different IC components can further complicate the digestion process due to different rates of removal (i.e. stoichiometry of each IC component and combined stoichiometry, relative to dissolution reagent) and IC component grain size (Al-Aasm et al, 1990; Yui and Gong, 2003). Where there is an IC contamination on δ^{13}C values, enrichment is usually expected in the δ^{13}C value; however, some freshwater and diagenetic carbonates can have very negative δ^{13}C values (Hoefs, 1973; Sharpe, 2007). In addition, our data illustrate offsets in the opposite direction (i.e. a depletion of the δ^{13}C value; e.g. 7.64 m – 7.80 m) which suggests that the data are not only affected by the inefficient (and disproportional) removal of IC from the sample, but also by the effect of acidification on the OC component. I therefore suggest that the sample IC component should be identified and quantified to ensure no residual IC remains after treatment, or, where the IC exists as a more robust form (e.g. siderite), the size of the offset can at least be partly accounted for.

The structure and composition of C and N in OM from a down-core sedimentary sequence can vary substantially (e.g. relative proportions of lipids, lignins, proteins and cellulose; Fernandes and Krull, 2008), and may subsequently respond disproportionately under different acid treatment methods. This suggests that C/N, δ^{13}C and δ^{15}N values are likely to be a relative proxy for the overall chemistry of the core material, but the degree with which it reflects the true OM value of the core is highly variable. In addition, where sample material is low in %C and %N, the effect of acidification on δ^{13}C and δ^{15}N could be significantly magnified (e.g. Brodie et al, 2011a; 2011b) which may be due to C and N isotopes becoming highly heterogeneous within the OM at these low levels. These factors add unpredictable, non-linear biasing to the dataset within sample horizons and with varying magnitude and proportions between sample horizons (i.e. suggesting the underlying trend of the data can be biased in a non-systematic fashion).

For δ^{15}N, a fractionation between untreated and acid treated samples, and between acid treated samples, is noted but with no concomitant loss in %N (no difference in values between treated and untreated data). The mechanisms for this are unclear; however, there seems to be a systematic shift across all acid treated samples towards lower δ^{15}N with samples in the rinse method tending to produce the lowest δ^{15}N. The environmental interpretation of elemental and isotopic analysis of OM can be significantly affected by both IC and IN, pre-analysis acid preparation method and the structure and composition of OM across the land-sea gradient. Additionally, the isotopic signature of IN is not significantly dissimilar to that of organic N, making the overall interpretation of the δ^{15}N of OM in the presence of IN difficult (e.g. Knies et al, 2007). This illustrates the importance of fully understanding OM structure and composition, and the IC and IN components, within the system under investigation where a bulk organic matter approach is adopted.

4.5.2 Artificial concentration of %C and %N

I also find that %C and %N are artificially concentrated (but not proportionally) in samples from 7.00 m to 7.52 m analysed from the rinse method relative to untreated values and capsule method samples. Brodie et al (2011a) suggested that this was probably a function of the loss of fine grained inorganic material (e.g. clays) in the supernatant relative to the amount of sample material treated with respect to that in other methods, despite the inherent losses of C and N through solubilisation (e.g. Schubert and Nielsen, 2000; Galy et al, 2007) and absorption onto fine grained particles. There is no concomitant shift in δ^{13}C values, though C/N values are disproportionally increased. Within the 20% HCl rinse method, and for %N only (from 8.12 m to 8.60 m), the %N values are substantially higher (Figure 4.2). Given the very low amounts of N within sample material, and the biasing effect of the acid preparation, the results are likely to be unreliable as %N is very close to machine baseline conditions.

These findings have significant implications for the comparison of records that are (i) derived in different laboratories following differing pre-treatment methods (or variations of the same method), and (ii) derived from different environments where the amounts and relative proportions of C and N in sample OM varies, and the amount, type and nature of OM and IC and IN varies. The assumption that data are reliable (and the subsequent interpretation robust) because of our ability to produce extremely high instrument accuracy and precision is a *non sequitur*. Our data suggest the necessity to account for the acid treatment bias in full and determine the size of the offset to ensure that our scientific approach is robust and acknowledge the full range of error in the analysis. It is suggested that the biasing of the true OM signature during pre-analysis acid treatment is inevitable, but unpredictable. It is imperative that the effect of pre-analysis acid treatment methods on δ^{13}C and δ^{15}N values be pursued at the molecular level to improve our understanding of the mechanisms controlling the bias evident in our data (and most likely in other down-core records).

4.5.3 Implications for the interpretation of C/N, δ^{13}C and δ^{15}N of bulk OM

Our findings have significant implications for the interpretation of measured C/N, δ^{13}C and δ^{15}N values of bulk OM in the context of the established theory in the literature (e.g. OM provenance and vegetation type). It has been shown that the interpretation of C/N and δ^{13}C data is not just dependant on an environmental shift, but can also be dependent on the bias due to pre-analysis acid treatment method. This is likely to be underpinned by the complexities in the structure and composition of OM within and between environments. Specifically, it suggests that small changes in the down-core records (i.e. < 4 ‰) may provide less reliable interpretations in comparison to much larger shifts (i.e. of the order of 10 ‰, or greater). Interpretations of C/N, δ^{13}C and δ^{15}N values have been underpinned by the assumption that we can reliably determine C/N, δ^{13}C and δ^{15}N of sample OM. This chapter has shown that this assumption is highly problematic, and that a detailed discussion and investigation on the potential source of bias, above that of the standard instrument precision, is essential for a robust interpretation of the data. It is clear that additional bias on C/N, δ^{13}C and δ^{15}N measurements in OM can derive from inorganic carbon (IC) and inorganic nitrogen (IN) content, pre-analysis acid treatment method followed and OM composition of the sample material.

However, our data also show sample horizons with no difference in results within and between methods, highlighting the inconsistency in any one method down-core. This suggests that the accuracy and precision with which C/N, δ^{13}C and δ^{15}N values from any one acid treatment method reflects sample OM is highly variable and unpredictable. Therefore, instrument precision should be interpreted as an absolute minimum precision on measured data (e.g. Brodie et al, 2011a; 2011b). The fact that pre-analysis treatment method can significantly influence the environmental interpretation of sedimentary OM is worrying, and cautions against the over interpretation of the minutiae of the data acquired. For example, here I report differences within and between methods on our down-core record in the region of 2 – 3.5 ‰ for δ^{13}C (excluding the excursion at 8.76 m which has a substantial IC contamination signal). A precision range of this magnitude can account for the overall range of some down-core studies (e.g. Turney et al, 1999; Zong et al, 2006; Scholz et al, 2010; Yu et al, 2010). It is therefore critical the extent of bias due to acid treatment on elemental and isotopic measurements in OM is understood to ensure that any interpretation is grounded on a robust dataset reflecting sample OM, especially where inferences on climate variability and mechanisms are being proposed. In addition, these findings suggest that the correlation of C/N and δ^{13}C values of bulk OM derived from different sedimentary archives is highly problematic.

Given the current drive in the community to derive annual – centennial resolution down-core records of past environmental change, and in the context of increasing use of data transformation techniques, such as spectral and wavelet transforms used to understand periodicities (e.g. Baker et al, 2005), it is imperative that the inaccuracy and imprecision of the data is fully understood and the subsequent limitations to interpretation acknowledged. For example, differences within and between methods of the order of ~2 – 3.5 ‰ significantly alter the amplitude and potentially change the frequency of a down-core record, which may be misinterpreted as being environmentally significant (i.e. the amplitude of environmental variability compared with the amplitude of variability in the data caused by inaccuracy and imprecision of the data). It may artificially cause high-frequency signals to manifest as significant periodicities in the core data during analysis, which may lead to incorrect interpretation. In addition, the bias due to acid treatment can also affect the underlying trend in the record, which can further undermine the analysis. This suggests C/N and δ^{13}C values from bulk OM are a less reliable tool for reconstructing environmental events with low amplitude variability. This is likely to have implications for the high resolution, high frequency reconstructions favoured in the recent literature. Time-series analysis was not undertaken on this data – the analysis itself, in addition to the acid treatment bias, would have been undermined by the low resolution sampling and poor dating constraint across the data in the first instance, and made *a priori* assumptions about the system and climatic processes responsible for the geochemical OM signature (e.g. Wunsch, 2010).

4.6 Implications for accuracy and precision

Based on the findings of this chapter, I preliminarily assess the inaccuracy and imprecision on C/N (Σ_E), δ^{13}C (Σ_C) and δ^{15}N (Σ_N) values from sample bulk OM as follows:

Σ_E (on individual C/N values) = $e_d + e_{pic} + e_{pin} + e_{sh} + e_{ss} + e_{an}$

Σ_C (on individual δ^{13}C values) = $c_d + c_{ic} + c_{sh} + c_{ss} + c_{an}$

Σ_N (on individual δ^{15}N values) = $n_d + n_{in} + n_{sh} + n_{ss} + n_{an}$

The inaccuracy and imprecision associated with each component of the above equations are presented in Table 4.3. The diagenesis component (e_d; c_d; n_d) can contribute a significant bias relative to the organic signal of the original source OM from pre- and post deposition processes, such as oxidation and microbial reworking (e.g. bacterial breakdown or by detritivores), the extent of which will vary depending on the length of time OM takes to reach the sediment, the productivity in the water column and dissolved oxygen concentrations (Meyers, 1994; Krull et al, 2002; Lehmann et al, 2003). For example, Meyers and Ishiwatari (1993) noted that a diagenetic decrease in C/N values could occur in lake sediments of the order of ~ 26. A loss of non-lignin compounds from a C_4 marsh plant depleted δ^{13}C by ~4 ‰ (Benner et al, 1987), though in sediments evidence for diagenetic bias is contradictory. Spiker and Hatcher (1984) noted a 4 ‰ depletion in lake sediments which they attributed to the loss of ^{13}C-rich carbohydrates, whereas Rea et al (1980) and Jasper and Gagosian (1989) noted no bias due to diagenesis. For δ^{15}N, the effect of diagenetic processes on the primary sedimentary OM signal is also contradictory. Altabet and Francois (1994) reported a 5 ‰ enrichment in δ^{15}N and Sigman et al (1999) noted an increase of ~4 ‰ in δ^{15}N from Southern Ocean sediments. However, de Lange et al (1994) reported a decrease of ~1 ‰ in δ^{15}N, and Freudenthal et al (2001) noted a ~1 ‰ bias in eastern Atlantic Ocean sediments with no clear trend towards an increase or decrease in δ^{15}N. The degradation of organic compounds, which have distinctive isotopic signatures, appears to be non-discriminatory, implying that diagenetic processes must be accounted for on a system by system basis. For example, the loss of readily degradable amino acids and hydrocarbons, relative to terrestrially sourced compounds such as lignins and lipids, would deplete δ^{15}N (loss of ^{15}N and ^{13}C). These contradictory results clearly imply that there is no emergent generalised affect on the δ^{13}C and δ^{15}N signature of bulk OM, and this can differ markedly between oxic and anoxic conditions (Tyson, 1995). However, a detailed molecular level investigation may allow the estimation of this bias on bulk OM.

The influence of IC and/or IN (e_{pic}; e_{pin}; c_{ic}; n_{in}) is dependent upon the efficiency of removal during acid treatment, and the structure and composition of the inorganic component (e.g. Al-Aasm et al, 1990; Yui and Gong, 2003; Knies et al, 2007), the bias for δ^{13}C in this study shown to be ~6.8 ‰ at 8.76 m. However, the extent of the bias on δ^{15}N is less obvious owing to the similar values in both organic and inorganic N (Knies et al, 2007). The homogeneity of the sample material (e_{sh}; c_{sh}; n_{sh}) can also contribute additional imprecision, likely increasing substantially on samples poorly homogenised or with significantly low amounts of C and N (e.g. Basiden et al, 2002). Sample size can also contribute significant bias, particularly those low in C and N before acid pre-treatment is undertaken (e_{ss}; c_{ss}; n_{ss}). Where sample size becomes very small (especially in conjunction with an acid pre-treatment), %C and %N can increase by over 50% (see Brodie et al, 2011a) and δ^{13}C and δ^{15}N values tend to become more positive, suggesting at least a ~1 ‰ deviation in the OM value (our analysis were carried out on sample sizes significantly above machine baseline conditions and therefore do not carry this additional inaccuracy). Finally, the analytical term (e_{an}; c_{an}; n_{an}), comprising the bias from acid treatment and the instrument precision. Pre-analysis acid treatment has been shown here, and elsewhere, to substantially bias the elemental C and N values of sample OM through degradation of the OC fraction and/or inefficient removal of the IC fraction (and differential rates of removal linked to IC stoichiometry). For this core, the error is estimated to be in the region of ~ ± 2 – 3.5 ‰ associated with the OC fraction and ~6.8 ‰ (enrichment) associated with the IC fraction. The instrument precision, which is inherent to all measurements in this study, is of the order of ± 0.5 for C/N values, ± 0.1 ‰ for δ^{13}C values and ± 0.15 ‰ for δ^{15}N values.

I caution, however, that whilst this equation is more representative of the absolute inaccuracy and imprecision on measured C/N, δ^{13}C and δ^{15}N values than instrument precision alone, the terms are by and large inherently non-linear and unpredictable, implying that absolute inaccuracy and imprecision is unobtainable. An assumption of linearity of these terms would be seriously flawed. It is concluded that the unpredictable, non-linear biasing to the data within sample horizons and with varying magnitude and proportions within and between sample horizons can undermine a robust interpretation of the data, with the size of bias varying considerably between different cores.

Table 4.3: Summary of inaccuracy and imprecision on C/N, δ^{13}C and δ^{15}N values measured from bulk OM.

Process		**C/N Bias**	**δ^{13}C Bias**	**δ^{15}N Bias**
Diagenesis	Bias variable	e_d	c_d	n_d
	Explanation	Bias associated with breakdown, oxidation and reworking of primary OM.	Bias associated with breakdown, oxidation and reworking of primary OM.	Bias associated with breakdown, oxidation and reworking of primary OM.
	Size of Bias	~5 – 26	~ 0.2 – 4 ‰	~ 0.1 – 5 ‰
Inorganic Carbon	Bias variable	e_{pic}	c_{in}	N/A
	Explanation	Bias associated with the structure, composition and quantity of sample IC.	Bias associated with the structure, composition and quantity of sample IC.	
	Size of Bias	± 1 – 60	± 3.4 ‰	
Inorganic Nitrogen	Bias variable	e_{pin}	N/A	n_{in}
	Explanation	Bias associated with the structure, composition and quantity of sample IN.		Bias associated with the structure, composition and quantity of sample IN.
	Size of Bias	± 1 – 5		indefinable
Analytical Bias	Bias variable	e_{an}	c_{an}	n_{an}
	Explanation	Bias associated with acid treatment of sample and instrument precision.	Bias associated with acid treatment of sample and instrument precision.	Bias associated with acid treatment of sample and instrument precision.
	Size of Bias	± 0.5 – 15 (± 0.4)	± 4 ‰ (± 0.2 ‰)	± 0.7 ‰ (± 0.3 ‰)
Sample Size	Bias variable	e_{ss}	c_{ss}	n_{ss}
	Explanation	Bias associated with the amount of C and N supplied for analysis.	Bias associated with the amount of C and N supplied for analysis.	Bias associated with the amount of C and N supplied for analysis.
	Size of Bias	± 0.5 – 100	0.5 ‰ (or greater)	0.5 ‰ (or greater)
Sample Homogenisation	Bias variable	e_{sh}	c_{sh}	n_{sh}
	Explanation	Bias associated with homogenisation of sample material prior to treatment	Bias associated with homogenisation of sample material prior to treatment	Bias associated with homogenisation of sample material prior to treatment
	Size of Bias	± 0 – 0.2	± 0.0 – 0.1 ‰	± 0.0 – 0.1 ‰

4.7 Summary and Recommendations

1. This study has clearly demonstrated significant bias on bulk C/N, $\delta^{13}C$ and $\delta^{15}N$ values of OM associated with pre-analysis acid treatment method in a stratigraphical sequence of samples. I have shown that there is an inconsistency in the use of any one method within and between sample horizons and that where this bias is evident it is significantly above instrumental precision. The differences appear to be the result of (i) differential rates of removal of IC and (ii) disproportionate biasing to OC fraction of the sample material.
2. In light of my findings, it is recommended that researchers do not interpret the minutiae of the bulk $\delta^{13}C$ and $\delta^{15}N$ of OM data, but restrict interpretations and discussions to those shifts significantly greater than a robust estimate of the inaccuracy and imprecision on the data (i.e. ~ 4 ‰ on this down-core data). The estimation presented here is considerably greater than is normally assumed (i.e. standard instrument precision) and underlines the importance of determine the size of the bias on C/N, $\delta^{13}C$ and $\delta^{15}N$ data in a down-core record. Consequently, $\delta^{13}C$ data should be used as a first-order indication of potential changes in sample OM, which could be further investigated for environmental and climatic change at the molecular level.
3. The biases discussed here make the environmental interpretation of C/N values (e.g. terrestrial versus aquatic) and $\delta^{13}C$ values (C_3 versus C_4 vegetation) problematic. For example, at 7.80 m C/N values range from 12 – 32 between methods and at 8.60 m $\delta^{13}C$ values range from –21.3 to –12.5 ‰.
4. The rinse method can artificially elevate %C and %N values and significantly undermine the integrity of C/N values. I recommend including a centrifugation step in this method, but warn that this will not guarantee resolution of the problems associated with decanting.
5. The 5% HCl capsule method appears to be less efficient in the removal of IC leading to more enriched $\delta^{13}C$ values, and I therefore do not recommend the use of this reagent within the capsule method.

Chapter 5

Down core palaeoenvironmental reconstruction from Lake Tianyang, south China

5.1 Introduction

Asia is home to a large portion of the world's population and a region of central importance to the global hydrologic cycle and atmospheric circulation patterns (e.g. Ramage, 1971; Webster 1998; An et al, 2000; Wang et al, 2005; Nakagawa et al, 2008). However, the mechanisms that control palaeoenvironmental change across several glacial – interglacial cycles in Asia are poorly understood owing to a lack of long-timescale records, particularly from a terrestrial perspective (e.g. Wang et al, 2005). Research on cave speleothem records in sub-tropical China (e.g. Wang et al, 2001; Yuan et al 2004; Cheng et al, 2009), Qinghai-Tibetan Plateau ice core records (Thompson et al, 1997), loess/palaeosol sequences from central and northern China (e.g. Porter and An, 1995; Chen et al, 1999; An et al, 2000; Porter, 2000), a lake sequence from Japan (Nakagawa et al, 2008) and from sedimentary sequences from the South China Sea (Wang et al, 1999; Sun et al, 2003) has improved our understanding of orbital forcing of the Asian monsoon (AM) over the past two glacial cycles. These references broadly suggest that the summer AM precipitation pattern is dominated by a ~23 ka cycle which is synchronous with northern hemisphere summer insolation, implying a direct link to solar forcing and lend support to the theory for direct solar modulation of the AM regime by the precession cycle (~23 – 19 ka) (Kutzbach, 1981; Kutzbach and Street-Perrot, 1985; Kutzbach and Guetter, 1986; Prell and Kutzbach, 1987; Rossignol-Strick et al, 1998; Ruddiman, 2006). This is in contrast with the theory that AM variability, at the precession and obliquity cycles, is linked to latent heat transport from the southern hemisphere which lags northern hemisphere July insolation by ~ 6 ± 1 kyr (e.g. Clemens et al., 1991; Morely and Heusser, 1997; Clemens and Prell, 2003).

However, these records focus on variability controlled primarily by summer-time temperature and precipitation. Palaeoclimate reconstructions suggest that the amount of precipitation associated with the summer monsoon was significantly lower during northern hemisphere cold phases (e.g. stadial/glacial periods; Wang et al, 2001; Yuan et al, 2004; Dykoski et al, 2005; Nakagawa et al, 2008; Clemens et al, 2008). During these cooler periods, the mean annual position of the inter-tropical convergence zone (ITCZ) is proposed to have been more southerly (e.g. Hughen et al, 1996; Haug et al, 2001; Wang et al, 2004; Yancheva et al, 2007), when the strength of the winter AM wind field is proposed to have been stronger (e.g. Wang et al, 2001; Yuan et al, 2004; Dykoski et al, 2005; Yancheva et al, 2007). However, the variability of the Asian winter monsoon during these cooler periods is poorly understood for two primary reasons: (i) there is no comparable signature of the winter monsoon in the hydrological cycle and (ii) there is no robust proxy for the reconstruction of winter monsoon wind strength from terrestrial archives.

A recent study by Yancheva et al (2007) attempted to address this issue, reporting winter monsoon wind strength variability over the last 16 ka BP using magnetic properties and Titanium (Ti) concentrations in a sedimentary record from Lake Huguangyan, Leizhou Peninsula. They proposed the mechanism controlling the sediment magnetic properties and Ti concentrations were directly linked to changes in the strength of winter winds carrying Ti laden dust from the central and northern China loess plateaus. This implies Ti concentrations (and/or magnetic susceptibility) increased during times of greater winter monsoon activity (e.g. during the Younger Dryas; Middle and Late Holocene). This theory was supported by the correlation of their Ti record with redox sensitive S-ratio, χ, total OC and Fe/Mn ratio from the same core. For example, during the Younger Dryas period, Ti concentrations in the Lake Huguangyan sediment were higher, coincident with an increase in S-Ratio (indicating more magnetite suggesting preservation in oxic conditions), an increase in magnetic susceptibility (controlled by increased magnetite concentrations), an increase in Mn concentrations (suggesting oxygenation of the bottom waters) and low total OC (increased wind-driven lake mixing by winter monsoon winds also implying oxygen rich bottom waters). In addition, comparison with the well-dated Dongge and Hulu cave records (Wang et al, 2001; Yuan et al, 2004; Dykoski et al, 2005) highlighted a coincidence of periods of weaker summer monsoon (i.e. lower precipitation; identified in the cave records by higher $\delta^{18}O$ values) with high Ti concentrations in the Lake Huguangyan sediments, particularly for the Pre-Bølling – Allerød warming and the Younger Dryas period, but with a weaker overall correlation during the Holocene. This leads to the hypothesis that Ti concentrations should follow broad scale glacial – interglacial changes, with high Ti concentrations during glacial periods, implying winter AM variability may be reconstructed from lake sedimentary sequences in southern most China.

This chapter presents a palaeoenvironmental record from a sedimentary sequence from Lake Tianyang, south China, southern Leizhou Peninsula. The aim of this research was to develop a high resolution multi-proxy sedimentary record from Lake Tianyang. Specifically, the following research questions are addressed:

1. Does the Lake Tianyang sediment record preserve a climate signal over several glacial – interglacial cycles?
2. Can a robust winter monsoon wind proxy be derived from the Lake Tianyang sedimentary record and what are the implications for the Lake Huguangyan record?

5.2 Lake Setting

Lake Tianyang (20°31’1.11” N, 110°18’43.02” E) is an infilled maar crater lake located on the southern edge of the volcanic topography of Leizhou Peninsula, south China (Figure 5.1). The lake basin has a surface area of ~7.3 km^2 and sits ~80 – 100 m above sea level, with a surface outflow to the southeast of the basin (Zheng and Lei, 1999) and lies ~100 km south of the Huguangyan crater lake (Mingram et al, 2004). The lake basin is proposed to have formed in the middle Pleistocene, ~480 ka BP (Chen et al, 1990) and is underlain by Cenezoic basalts of the Zanjiang formation, which are characteristic of the Leizhou Peninsula as a whole (e.g. Ho et al 2000; Mingram et al, 2004), belonging to the Lei Qiong volcanic field. The main period of volcanic activity was during the Quaternary, ~1.4 – 0.4 Ma, when local fault zones reactivated leading to the development of a number of volcanic craters, including Tianyang (Huang et al, 1993, Ho et al, 2000).

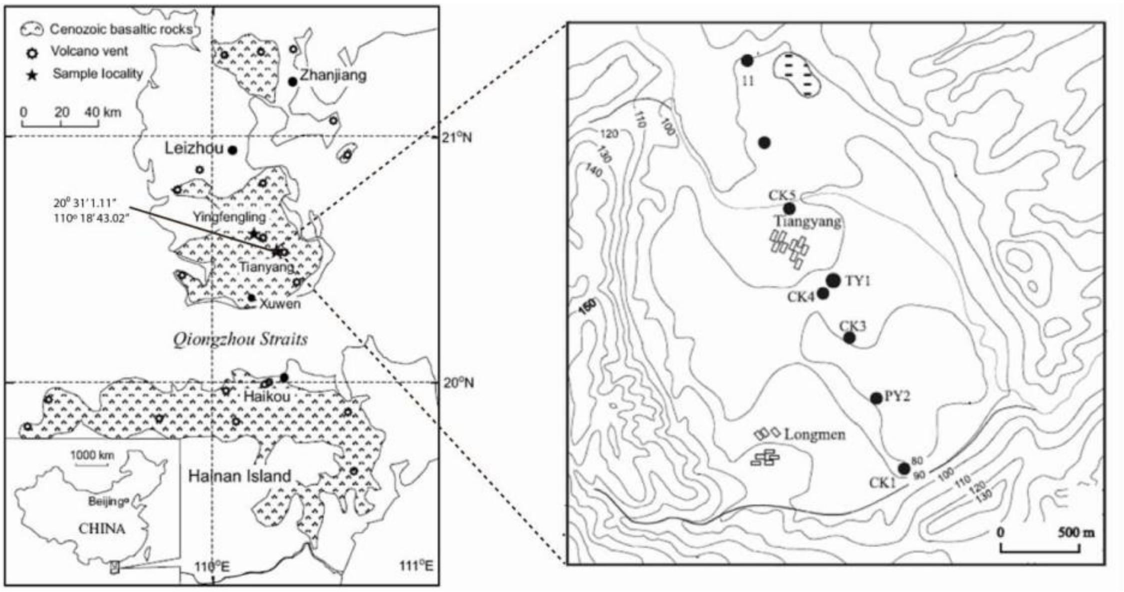

Figure 5.1: Map of Leizhou Peninsula indicating location of Lake Tianyang (black star), and Lake Tianyang contour map. Adapted from Yu et al (2006: 357) and Zheng and Lei (1999: 341)

This area has a strongly seasonal climatic signal, with an annual precipitation range of 1260 – 2280 mm as a result of the seasonal migration of the ITCZ, summer AM regime and typhoon activity. Average annual temperature range is approximately 22 – 24°C (SBG, 2000), and the natural vegetation of the region is tropical semi-evergreen seasonal rainforest (Zheng and Lei, 1999). Lake Tianyang has undergone extensive agriculture in the recent past resulting in the lake basin and crater slopes being turned over to arable pasture during the Late Holocene (Zheng and Lei, 1999).

5.2.1 Past research on Lake Tianyang

Since the 1980s, a number of cores have been sampled from Lake Tianyang for palynological and inorganic geochemical analysis (e.g. Chen, 1988; Chen and Yang, 1989; Peng, 1989; Chen et al, 1990; Lei and Zheng, 1993; Zheng and Lei, 1999). Sedimentary deposits in the centre of the lake basin reach > 220m from the surface, and ~90 – 120 m depth in the area near the centre, before rapidly thinning towards the lake margin (Figure 5.2; Zhang et al, 1980; Chen et al, 1988; Chen and Yang, 1989; Chen et al, 1990; Lei and Zheng, 1993).

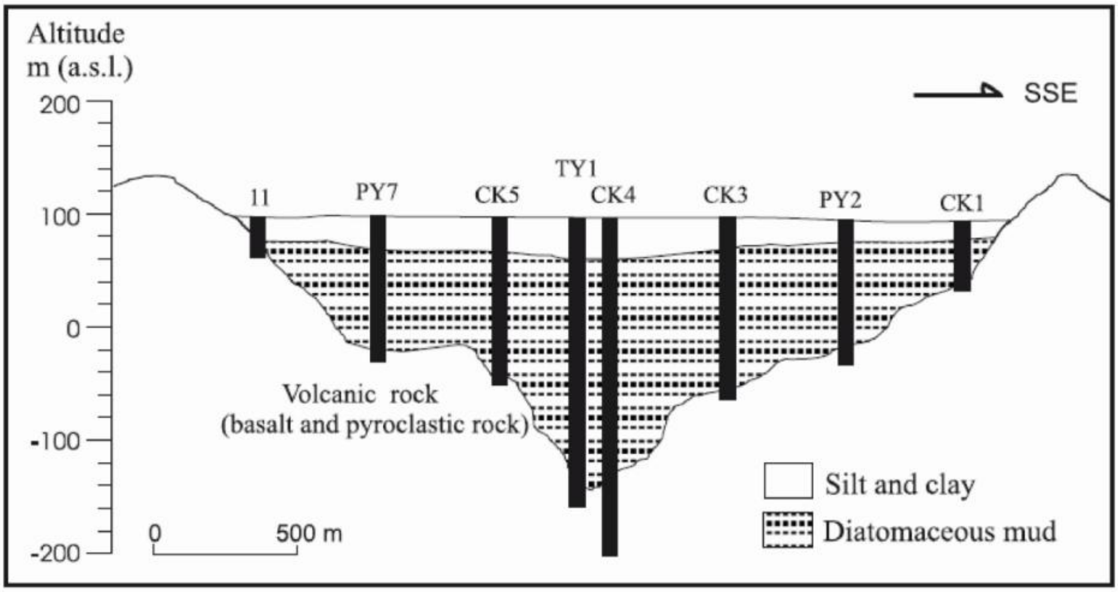

Figure 5.2: Cross section of Lake Tianyang (adapted from Zheng and Lei, 1999; 343).

There are very few high resolution records in this area beyond ~70 ka BP (e.g. Mingram et al, 2004), and in particular from Lake Tianyang (e.g. Chen and Yang, 1989; Chen et al, 1990; Zheng and Lei, 1999). Chen et al (1990) and Zheng and Lei (1999) reported low resolution geochemical and palynological records, which according to them spans the last ~400 ka BP (from a ~220 m core), which indicate that Lake Tianyang sedimentation has undergone two major changes, at ~160 m and ~53 – 37 m (Figure

5.3). Prior to the first major change, the sediment was rich in diatoms (in the range of 55 – 85%; diatomite), indicative of high lake levels relative to the catchment rim and high productivity, and very low in Al_2O_3 (an indicator of terrestrial runoff, with low values suggesting very low terrestrial sediment input). The first major change occurred at ~160 m, where the diatom assemblage became deficient in planktonic species. The sedimentology changed to diatomacious clay and Al_2O_3 increased suggesting that lake levels were lower, probably exposing the crater rim and resulting in increased terrigenous run-off, fundamentally altering the lake sedimentary regime.

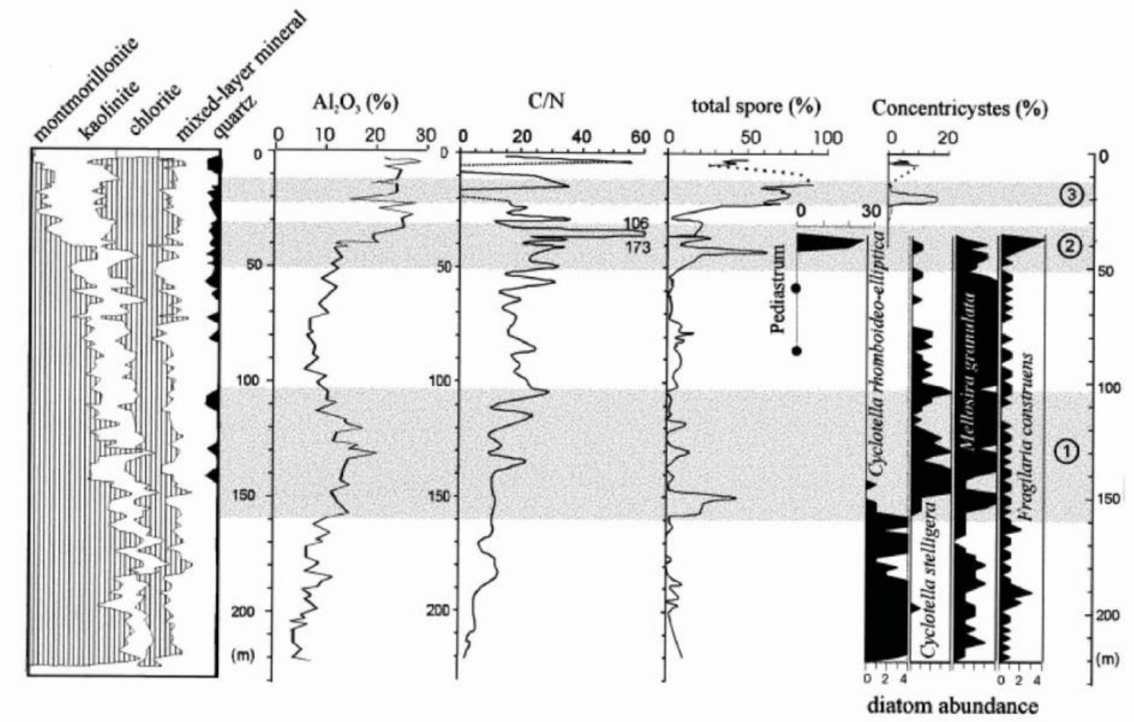

Figure 5.3: Previous reconstructions on Lake Tianyang. Clay mineral components, Al_2O_3 (%), C/N ratio, fern spore (%), Pediastrum abundance and diatom assemblages. The scale on the diatom assemblage records are; 1 = 0.1 – 4%; 2 = 5 – 19%; 3 = 20 – 49% and; 4 = > 50%. The horizontal grey shaded zones represent major changes in the lake environment: (1) first major drop in lake level; (2) shallow lake and/or woodland swamp environment with increasing minerogenic sediment flux and; (3) dominated by terrestrial run-off, through intensive catchment erosion and alluvial input. Adapted from Zheng and Lei (1999: 358).

The second major change occurred at ~53 – 37 m, and has attributed to a sudden lowering of the lake level, owing to the dramatic reduction in the abundance of littoral and planktonic diatom species (Huang, 1993; Zheng and Lei, 1999), before the eventual disappearance of diatoms in the record at ~37 m. Across this section of core, and at ~42 m, the sedimentology becomes increasingly minerogenic, with relatively high Al_2O_3 concentrations and an increase in pollen spores, particularly pediastrum (an aquatic algae commonly found in swamp-like environments)(Chen et al, 1990; Zheng and Lei, 1999). From ~40 m, the sedimentology becomes increasingly dominated by carbonized wood fragments and amorphous organic clay beds. Towards the top of the core, the sedimentology varies significantly in its minerogenic content, with significant increases in fine and coarse sands. This suggests that the environment became a woodland dominated swamp that changed gradually to an alluvial-based sediment regime. It is possible that these major changes in the Lake Tianyang sediment history are the result of neotectonic activities (e.g. Huang, 1993). These factors present an excellent opportunity for high resolution palaeoenvironmental reconstructions over several glacial cycles in Lake Tianyang, in a region where the spatial resolution of records and understanding of palaeoenvironmental change is currently lacking (Wang et al, 2005).

5.3 Materials and Methods

A 120 m long sedimentary sequence was sampled from the centre of Lake Tianyang in January 2008, from which the upper 40 m were analysed in this thesis. Cores were extracted using a Vibracorer, internally fitted with 2 mm thick PVC liner, and immediately wrapped and sealed in polythene packaging for shipping to cold storage at Durham University, UK. The upper 0.5 m of sediment was discarded due to evidence of a ploughed horizon.

5.3.1 Sedimentology

The description and macroscopic examination of the sediment is based on the classification system of Schnurrenberger et al (2003). The stratigraphic log shows significant macroscopic changes in the sedimentary regime (Figure 5.4). In general, the core material comprises homogenous grey and brown clays, interspersed with coarse-grained particles. Two significant exceptions are thick biogenic units with amorphous organic content > 25%, from 39.60 m to 36.20 m (dominated by carbonised wood fragments) and from 8.10 m to 6.90 m (dominated by amorphous organics and fine clays). In addition, there is a thick unit of clastic material, with major contributions of medium to coarse grained quartz (angular and sub-angular) and magnetite (from ~23.70 m to 21.00 m). Wood fragments are also relatively abundant in the record from 27.60 m to 26.50 m.

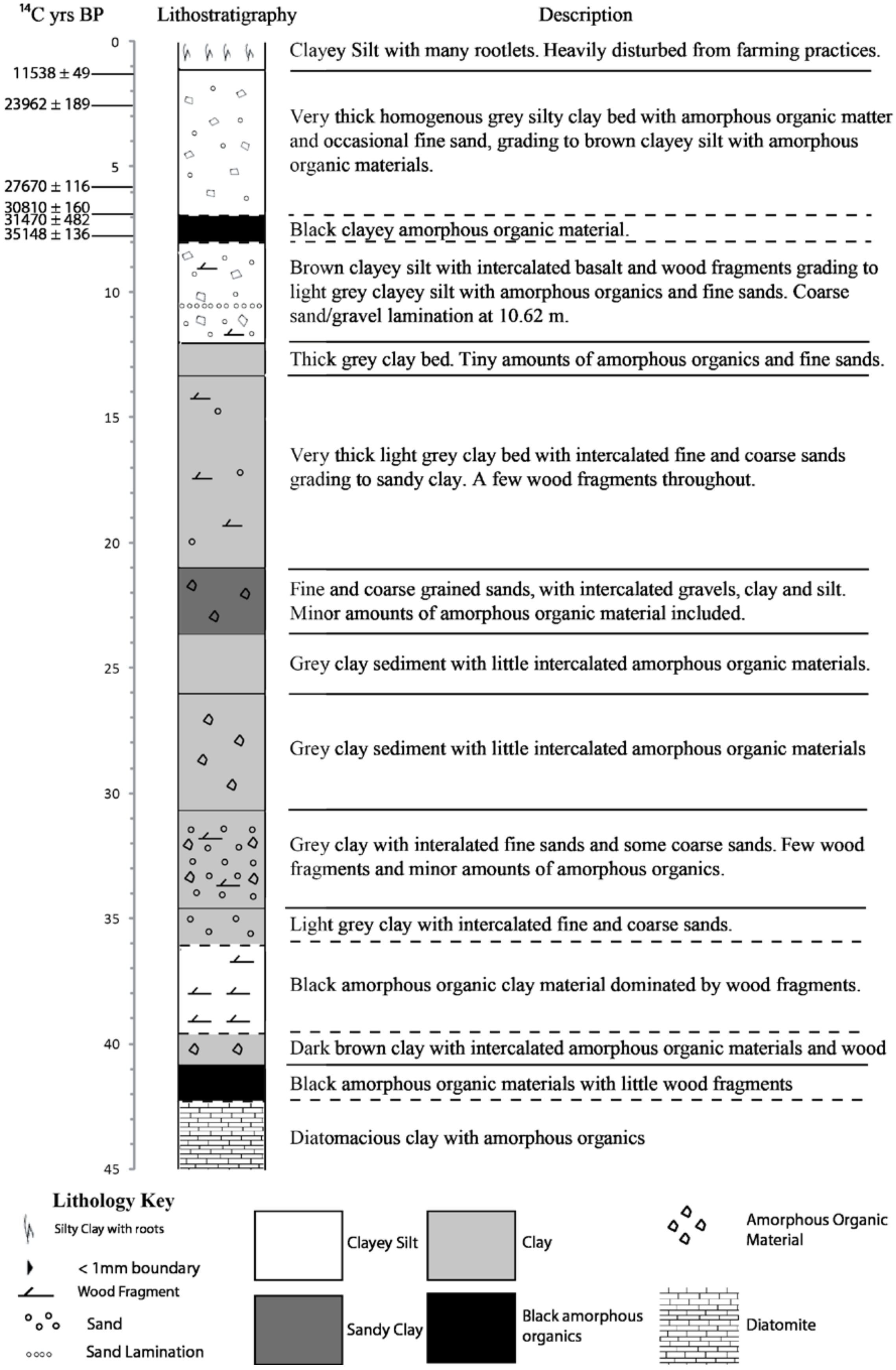

Figure 5.4: Lake Tianyang lithostratigraphy for upper 40.00 m.

5.3.2 C/N and $\delta^{13}C$ of organic matter

The sedimentary sequence was sub-sampled at 8 cm resolution from 18 – 0.5 m, giving a temporal resolution of ~640 yrs, and at 16 cm resolution from 40 – 18 m giving a temporal resolution of ~1280 yrs. Prior to $\delta^{13}C$ analysis of bulk organic matter (OM), samples were acid treated with 20% HCl to remove the inorganic carbon fraction following the capsule method (see Section 2.2.1 for cleaning protocols and Section 2.3.2 for a description of the capsule method). %C, %N and $\delta^{13}C$ values of sample OM were analysed using an online system comprising a Costech ECS4010 elemental analyser (EA), a VG TripleTrap, and a VG Optima mass spectrometer at the NERC Isotope Geosciences Laboratory (NIGL)(see Section 2.4.1 for a full description). Instrument precision was $\leq$ 0.2 ‰ (1σ). However, the accuracy and precision of $\delta^{13}C$ values of bulk OM from the Tianyang sediment archives is potentially of the order of up to ~4 ‰ on each individual sample as a result of pre-analysis acid treatment (see Chapter 4). In lieu of quantifying the inaccuracy and imprecision on each sample, we assume a conservative value of ~4 ‰ for the entire $\delta^{13}C$ record.

5.3.3 XRF elemental analysis

X-Ray fluorescence (XRF) analyses were performed on 490 samples on a Spectro X-Lab 2000 Energy Dispersive XRF (ED-XRF) in the Department of Geography, Durham University, UK. The sedimentary sequence was sub-sampled at 8 cm resolution (temporal resolution of ~600 yrs), from the same sample horizons as for C/N and $\delta^{13}C$ analysis, to quantify Al, Au, Ba, Cu, Fe, K, La, Mn, Nb, Ti. Approximately 5 g of freeze-dried and ball-milled sediment was mixed with 1 g of FluXana Hoechstwax, and pelletised under 10 tonnes of pressure for 60 seconds. Pellets were then transferred to a sample tray for analysis. Instrument accuracy (long term averages) and precision (1σ of within run standard reference materials) was determined by analysis of a range of standard reference materials, in particular modern and ancient lake sediments, and within run accuracy and precision was monitored using sandy soil (7002) and a clay based marine sediment (NCS 74301)(Table 5.1). All elements are normalised to Al, which accounts for the effect of clay on the element concentrations. In Tianyang, clay is a dominant component of the sedimentary archive and therefore the Aluminium (Al) normalisation is justified.

Table 5.1: XRF Standard values. Precision ranges are several orders of magnitude lower than range in data.

Elements	**7002**		**NCS 74301**	
	Certified values	Measured Values	Certified values	Measured Values
Al_2O_3	14.02 ± 0.5	13.7 ± 0.2	13.75 ± 0.40	13.73 ± 0.14
Ba	987 ± 40	979 ± 15	0.44 ± 0.02	0.45 ± 0.02
Cu	-	0.028 ± 0.001	424 ± 8	426 ± 9
Fe_2O_3	3.77 + 0.20	3.74 ± 0.03	6.26 ± 0.5	6.65 ± 0.1
K_2O	5.20 ± 0.20	5.23 ± 0.09	2.95 ± 0.1	2.91 ± 0.01
La	-	0.034 ± 0.0034	-	0.066 ± 0.004
Mn	0.05 ± 0.04	0.06 ± 0.01	0.43 ± 0.03	0.41 ± 0.01
Nb	-	17.6 ± 0.9	15.1 ± 1.0	13.3 ± 1.2
Ni	42.1 ± 1.80	43.2 ± 1.80	150 ± 4	154 ± 3
TiO_2	0.45 ± 0.01	0.45 ± 0.02	0.67 ± 0.02	0.68 ± 0.03

5.3.4 Core scanning

Sediment bulk density (ρ) and Magnetic susceptibility (χ) were measured on a GEOTEK multi-sensor core scanner at Durham University. The entire core length was measured at 5 mm resolution (implied sub-annual temporal resolution). χ was measured using a Bartington point sensor (MS2E), and is a measure of how easily a material can be magnetised upon exposure to a weak magnetic field (Sandgren and Snowball, 2001), and is reported in m^3/kg. The resultant signal is a function of magnetic and diamagnetic minerals in the bulk sample material. χ was density corrected and calculated from $\chi = K/\rho$, where χ = volume susceptibility; K = dimensionless measure of magnetic susceptibility (in SI units); and ρ = sediment bulk density.

5.3.5 ^{14}C analysis

AMS (Accelerated Mass Spectrometer) ^{14}C determinations were measured on plant macrofossils and on bulk sediments in the absence of macrofossil material, from the unlaminated Lake Tianyang core. AMS ^{14}C analysis was undertaken at the Gaungzhou Radiocarbon laboratory, Guangzhou, China; the NERC Radiocarbon Laboratory, UK and; BETA Analytical, USA (see Table 5.2). All samples were pre-treated following the acid-base-acid method using 1 M HCl and KOH.

Table 5.2: Summary of new AMS ^{14}C dates on sedimentary sequence from Lake Tianyang reported as ^{14}C ages BP (uncalibrated). Error ranges are reported as 2σ calculated from instrument precision alone.

Lab. No.	Depth (cm)	Analysed Material	^{14}C yr BP
SUERC – 30578	116	Bulk organics	11538 ± 49
SUERC – 30579	268	Bulk organics	23962 ± 189
GZ2665	587	Bulk organics	27670 ± 116
BETA 282395	692	Plant fragment	30810 ± 160
BETA 281924	692	Charcoal	29180 ± 140
SUERC – 30580	693	Bulk organics	31470 ± 482
GZ2666	746	Bulk organics	35148 ± 136
GZ2667	1637	Wood	38209 ± 360
GZ2668	1974	Wood	39011 ± 446
GZ2669	2693	Wood	38395 ± 165
GZ2670	2949	Plant Fragment	40010 ± 308
GZ2671	3473	Wood	39040 ± 404
GZ2672	3944	wood	38817 ± 269

5.4 Results and Discussion

5.4.1 Chronology

5.4.1.1 Radiocarbon Datings

A total of 13 new AMS ^{14}C determinations for the Lake Tianyang maar are presented in Table 5.2 in radiocarbon years before present (^{14}C yrs BP). With the exception of the datings at 1.16 m and 2.68 m, these ^{14}C determinations lie outside of the widely accepted ^{14}C age calibration range of 26 ka (Stuiver et al, 1998; Bronk Ramsey, 2001; Reimer et al, 2004), though a new, lower resolution calibration curve, INTCAL09, is available beyond 26 ka (calibration uncertainties are in the range of ±500 yrs, Reimer et al., 2009) which is used here.

The ^{14}C determinations from 1.16 m and 2.68 m may be contaminated by older and younger C as a result of sediment reworking, due to anthropogenic activities, and pedogenic processes (e.g. Peng, 1989; Chen et al, 1990; Zheng and Lei, 1999) implying the datings acquired from this material are potentially subject to greater imprecision than is quoted. In addition, these datings (along with those from 5.87 m and 6.93 m) are derived from bulk sediment OM (in lieu of terrestrial micro- or macro-fossils), and may have enhanced the uncertainty associated with (i) the hard water effect, a secondary source of ^{14}C (i.e. catchment geology) that results in the lake water body becoming depleted in ^{14}C relative to the atmosphere (e.g. Hajdas et al., 1995), (ii) influx of carbonaceous materials, such as coal, charcoal and lignite, and which would bias any resultant ^{14}C calculations towards older ages (e.g. Hajdas et al., 1995), (iii) variations in the relative proportions of OM end members and their ^{14}C composition relative to the atmospheric reservoir during the lifespan of the material (i.e. authigenic organic carbon versus allochthonous organic carbon); (iv) the potential for acid treatment to bias OM ^{14}C in a non-linear and unpredictable manner, and in a non-linear and unpredictable manner with respect to ^{13}C and ^{12}C (sensu Brodie et al, 2011a). An insight on the affect of acid treatment bias on ^{14}C datings can be gained by considering the isotope-fractionation correction of these ^{14}C datings using the Craig carbon fractionation correction (Craig, 1954). The correction is based around a δ^{13}C value of –25 ‰ (representative of wood, and implies a direct link to the atmospheric $^{14}CO_2$ reservoir and proportionality in the photosynthetic process) and is calculated from:

$$A_c = A_m \left[1 - \frac{2(25 + \delta^{13}C_{PDB})}{1000} \right]$$

where A_c is the ^{14}C activity corrected for isotopic fractionation and A_m is the measured ^{14}C activity of the sample (dpm/g of C). The constant “2” in the equation represents the difference in mass between ^{14}C and ^{12}C (representative of the fractionation factor between the two isotopes as a function of atomic mass, directly implying proportionality in the kinetic fractionation process). For a hypothetical sample of A_m = 4.0 dpm/g of C, and a measured δ^{13}C value of –25 ‰, A_c would yield no correction to the measured ^{14}C activity. However, if δ^{13}C was –15 ‰ in this hypothetical sample, A_c would reduce to 3.92 dpm/g of C which equates to a 2% reduction in the measured sample activity. This 10 ‰ difference in δ^{13}C would result in an increase in the calculated ^{14}C age by ~167 years. By simple division, this implies that every 1 ‰ shift in δ^{13}C equates to ~16 ^{14}C years (i.e. before calibration). Therefore, biasing to the δ^{13}C value by acid treatment alone (i.e. assuming no biasing to ^{14}C, but not proven) directly impacts upon the precision of ^{14}C datings, and in addition suggests that the fractionation factor of “2” may not accurately reflect the isotopic proportionality of C in the measured sample.

The ^{14}C determinations below 16.37 m are infinite, and cannot contribute directly to the age-depth model of the Lake Tianyang maar archive. Despite the potential uncertainty on the ^{14}C determinations through contamination, correction, uncertainties on ^{14}C calibration frameworks, and acid treatment bias, the datings on these horizons appear to be in stratigraphic order (i.e. 2.68 m to 7.46 m) and collectively suggest this section of the sedimentary record was deposited during Marine Isotope Stage 3 (MIS 3) with a sedimentation rate ~14 cm ka^{-1}.

The 13 new AMS ^{14}C datings reported here suggest the Lake Tianyang maar sedimentary archive is considerably older than previously reported (i.e. outside of ^{14}C dating capabilities, see Table 5.3; Peng, 1989; Chen et al, 1990). The previous chronology for Lake Tianyang maar was based on 16 ^{14}C ages (conventional measurement method; Peng, 1989; Cheng et al, 1990), 6 thermoluminescene ages (Chen et al, 1990) and low resolution palaeomagnetic data (Chen, 1988; Chen and Yang, 1989). Zheng (2008, Pers. Comm.) suggest the sample handling and measurement protocols relating to the previously reported ^{14}C determinations may have resulted in additional contamination suggesting the measurement inaccuracies are greater than reported. In addition, he also raised concerns over the reliability of the thermoluminescene ages due to the exposure of the sediment to natural light for long periods prior to sampling. In addition, the resolution of the palaeomagnetic data and lack of independent dating control, quash a potential palaeomagnetic chronology.

Table 5.3: Previously reported ^{14}C dates from Lake Tianyang sedimentary records.

Lab. No.	**Depth (cm)**	**Analysed Material**	**^{14}C yr BP**	Reference
CG-689	3.27	Black sandy clay	18030 ± 225	Peng (1989)
CG-676	4.46	Black sandy clay	25395 ± 630	
CG-678	14.67	Black mud	23445 ± 435	
CG-679	22.94	Black clay	21935 ± 435	
CG-680	24.98	Black clay	20745 ± 950	
CG-687	29.04	Black clay	22505 ± 435	
CG-681	34.12	Peat	28760 ± 880	
CG-683	35.25	Carbonized wood	28630 ± 925	
CG-684	38.10	Black clay	29635 ± 910	
CG-686	41.70	Black clay	34650 ± 1620	
GC 764	19.97 – 20.09	Black clay	15830 ± 620	Chen et al (1990)
GC 763	23.06 – 23.10	Peat	20730 ± 620	
GC 1010	28.74 – 28.83	Peat	30275 ± 1410	
SH-1	29.10 – 29.15	Carbonized wood	30310 ± 1200	
GC 1077	34.82 – 34.92	Carbonized wood	46270 ± 1480	
GC 1024	36.05 – 36.11	Carbonized wood	47700 ± 1280	

5.4.1.2 Tuned age model

In an attempt to improve the accuracy of the Lake Tianyang maar chronology in light of the new ^{14}C determinations, the newly developed NAP and AP pollen counts (both calculated as % total land pollen and provided by Prof. Zheng Zhuo, Sun Yat-sen

University, counted from sub-samples of the same core material, and sample horizons, analysed in this thesis), alongside the new $\delta^{13}C$ are correlated to the SPECMAP $\delta^{18}O$ benthic stack (Imbrie et al, 1984; Martinson et al, 1987). A principal reasoning of this tuning approach assumes that the intensity of the major palaeoclimate events proposed to be detected in the SPECMAP $\delta^{18}O$ stacked benthic record (i.e. glacial – interglacial/stadial – interstadial shifts) were expressed in a vast spatial range of different proxy archives, including this new reconstruction from Lake Tianyang maar (e.g. Tzedakis et al, 1997; Bokhorst and Vandenberghe, 2009; Blaauw et al, 2010a; 2010b). By implication, this line of reasoning, in the context of time, assumes (near) synchroneity of such events within and between the proxy archives allowing the coincidence of said events to be used as "isochrons" or "tie-points" with which to align the proxy events in the records of interest (N.B. the assumption of synchroneity diminishes an objective evaluation of relative timings of these events, precluding discussion of leads and/or lags). The "tie-points" are taken to be of equal age between the archives, and provide age-depth estimates for an undated, or poorly constrained archive (here the Lake Tianyang maar archive) based on the age model of a better dated archive (here the SPECMAP benthic $\delta^{18}O$ stack, constrained itself by orbital tuning): in essence, an event-based chronostratigraphy. The SPECMAP $\delta^{18}O$ stack has considerable chronological uncertainties *per se*, ~5000 yrs (Martinson et al., 1987) implying that the correlation to the Lake Tianyang maar record will necessarily contain larger uncertainties as a combination of the SPECMAP uncertainties, the tuning process, indefinable sedimentation rates between the tie-points (e.g. Blaauw et al, 2010) and age-depth model development.

In conjunction with the new ^{14}C age estimations reported from 2.68 m, 5.87 m and 6.92 m, which are in stratigraphic order and broadly indicate that the sediment was deposited during MIS 3 (providing some independent dating control), I establish a number of "tie-points" between the SPECMAP $\delta^{18}O$ benthic stack and the Lake Tianyang maar NAP, AP and $\delta^{13}C$ records below ~7.50 m based on the coincidence of major event horizons (see Table 5.4). This assumes (i) the NAP, AP and $\delta^{13}C$ records in Lake Tianyang maar have recorded significant shifts in vegetation from grassland to woodland that were associated and (near) synchronous with the relatively rapid shifts from glacial – interglacial conditions (Tzedikas et al, 1997; Blaauw, 2010), (ii) linearity in sedimentation rate between the established "tie-points" and, (iii) no major hiatus in sediment accumulation. The "tie-points" were defined as occurring at the point of inflection (e.g. Casford et al., 2007) in the SPECMAP $\delta^{18}O$ benthic stack at the beginning and end of major MIS changes, providing the "master" ages, and at the point of inflection in the Tianyang NAP, AP and $\delta^{13}C$ records, providing the depths across these proxies. Identifying an event stratigraphy within the Tianyang archive by multi-proxy comparison of the pollen and $\delta^{13}C$, two related proxies for vegetation which can be reasonably expected to respond similarly to change (i.e. following patterns of aridity), provides a more reliable, but not absolute, "tie-point" identification (e.g. Bokhorst and Vandenberghe, 2009). This is justified in the Tianyang archive as the pollen and $\delta^{13}C$ show striking visual similarities in their oscillations, suggesting clear identification of regional to global scale oscillations (e.g. glacial – interglacial) over local oscillations (within the Tianyang catchment).

Table 5.4: Age-depth model ^{14}C cal yrs BP and SPECMAP "tie-points"

TYC depth (cm)	Depth uncertainty (cm)	Age (ka BP)	Age uncertainty (ka BP)	Dating technique
268	1	26891	519	^{14}C
587	1	29849	400	^{14}C
692.5	2	33125	442	^{14}C
716	1	63000	5000	SPECMAP
780	1	78000	5000	SPECMAP
940	1	98000	5000	SPECMAP
1044	1	107000	5000	SPECMAP
1260	1	121000	5000	SPECMAP
1772	1	134000	5000	SPECMAP
1820	1	151000	5000	SPECMAP
2508	1	181000	5000	SPECMAP
2684	1	194000	5000	SPECMAP
2972	1	227000	5000	SPECMAP
3052	1	237000	5000	SPECMAP
3452	1	295000	5000	SPECMAP
3740	1	309000	5000	SPECMAP
3884	1	318000	5000	SPECMAP

The vegetation – climate nexus has been exploited in this manner to develop a tentative, but relatively robust, chronostratigraphy for the Lake Tianyang maar archive (Figure 5.5) because, on glacial – interglacial timescales, the vegetation pattern tends to change from woodland (i.e. C_3 vegetation cover) to open vegetation (grassland/savannah; C_4 vegetation; e.g. Tzedikas et al, 1997; 2003; Zheng and Lei, 1999; Bird et al, 2005). NAP is generally associated with cool temperate to arid environments, where precipitation is relatively low (i.e. first order indicator of aridity), whereas AP (e.g. woodland), representative of C_3 vegetation, are generally associated with humid and wet environments, where precipitation is abundant (Zheng and Lei, 1999; Bird et al, 2005; Galy et al, 2007). This implies that grass-like vegetation is more likely to dominate during glacial/stadial periods, in more arid conditions, and woodland-like vegetation during interglacial/interstadial periods. I suggest the age of the upper 40 m of the Lake Tianyang maar archive is ~325 ka (see age-depth model; Figure 5.5), which is considerably older than previous estimates (see Table 5.3: Chen et al, 1988; Peng, 1989). The age-depth model is based on a linear regression (N.B. a polynomial fit gave a near identical r^2 value) across all identified age horizons.

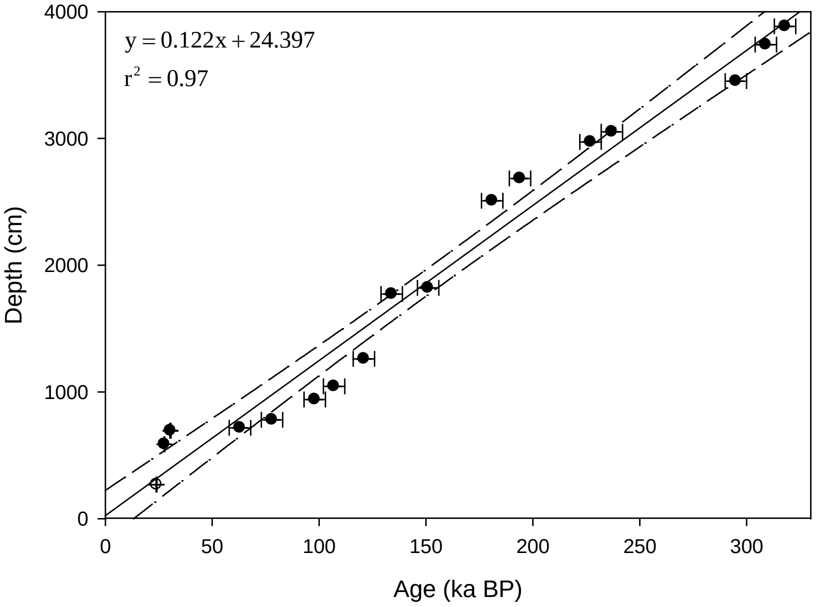

Figure 5.5: Age-depth model for Lake Tianyang maar based on data in Table 5.4. Perforated lines represent 95% confidence intervals of the linear age-depth model.

5.4.2 C/N and δ^{13}C

%C, %N and C/N values for the Tianyang sedimentary sequence are not reported based on the findings of Chapters 2 and 4. The δ^{13}C values of bulk OM are presented in Figure 5.6. The δ^{13}C record has an overall δ^{13}C value range of –11.6 ‰ to –30.2 ‰ and shows 9 major shifts throughout the record, of the order of ~10 to 15 ‰ (i.e. above the inaccuracy and imprecision of the data; between 0.2 and 4 ‰; see Chapter 4). Between ~145 ka BP m and ~65 ka BP the δ^{13}C record is highly variable relative to the entire record, with an overall δ^{13}C range of –15.4 ‰ to –30.1 ‰, the amplitude of which is internally similar with the rest of the Tianyang record. There are 3 major periods of relatively enriched δ^{13}C values, between ~290 ka BP to ~245 ka BP (δ^{13}C ≈ –17.4 to –24.8 ‰), ~210 ka BP to ~140 ka BP (δ^{13}C ≈ –13.0 to –19.5 ‰), and ~65 ka BP to present (δ^{13}C ≈ – 11.6 to –19.0 ‰). From ~290 ka BP to ~245 ka BP, the δ^{13}C values are more variable and are relatively slightly depleted in comparison with the two other major periods of enriched δ^{13}C values.

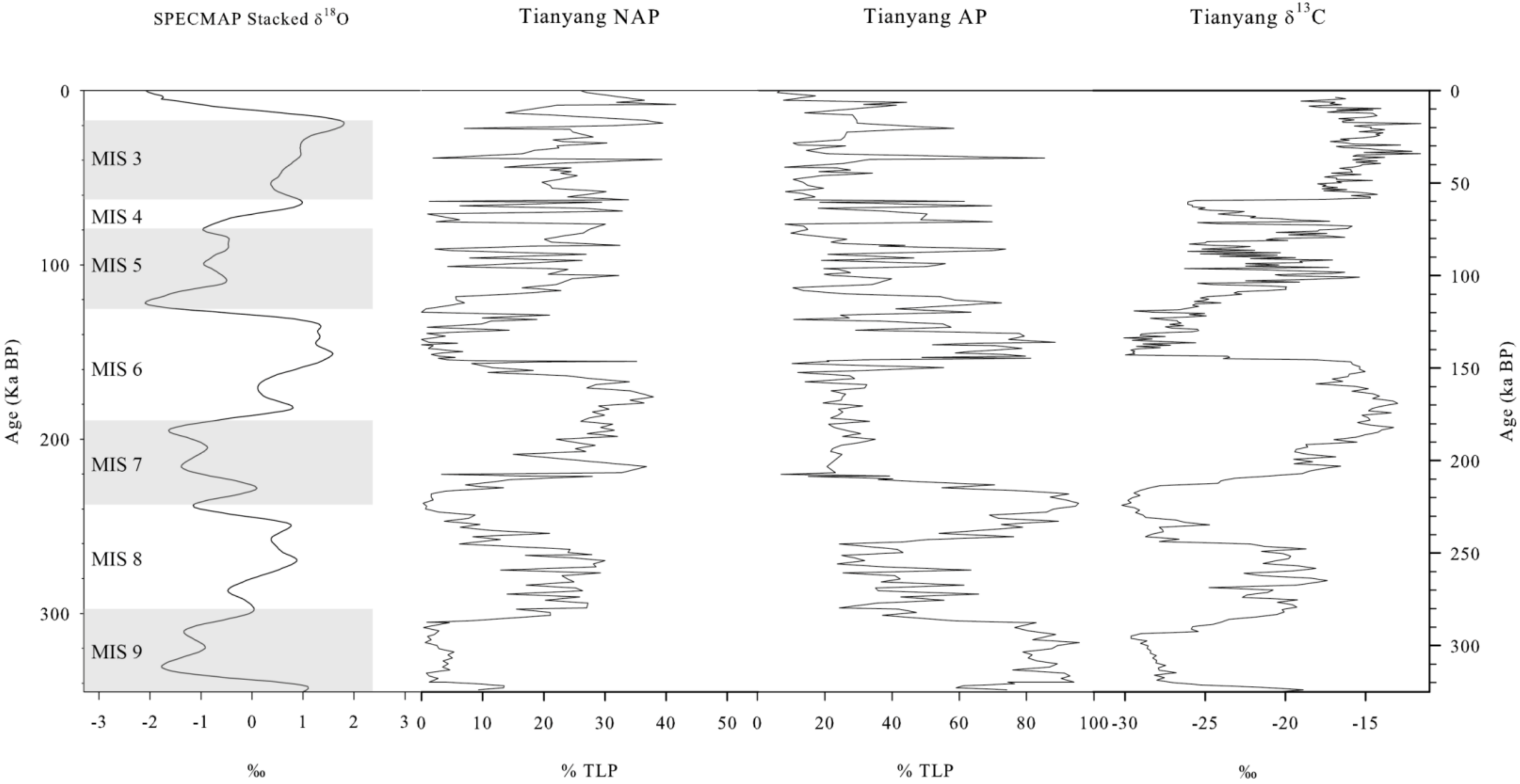

Figure 5.6: Comparison of SPECMAP stacked $\delta^{18}O$ with Lake Tianyang maar NAP and AP pollen counts, and $\delta^{13}C$ record. Greyed out sections of SPECMAP record indicates inter-glacial/inter-stadial periods.

Organic matter (OM) in lake sediments can be, and has been, used to reconstruct the palaeoenvironment of lake systems and their catchment areas (e.g. Meyers, 1984; 1997; Leng and Marshall, 2004). The source of OM in lake sediments can vary substantially, deriving from autochthonous sources (e.g. detrital fall-out of primary productivity in the water column; macrophytes) and/or allochthonous sources (e.g. terrestrial vegetation). C/N and $\delta^{13}C$ values of OM have been broadly used to identify such changes in OM provenance (e.g. Section 4.1). However, the results of Chapters 2, 3 and 4 suggest that the application of C/N values to bulk OM as a tool for OM provenance is unreliable, and highly susceptible to producing aberrant data as a function of acid treatment and OM composition. However, $\delta^{13}C$ values can still provide palaeoenvironmental information on high amplitude changes, which from bulk OM can be a function of temperature, light, moisture, pCO_2, and changes in vegetation photosynthetic pathways (e.g. Ehleringer and Monson, 1993; Ehleringer et al., 1997; Kock et al., 2004). For example, $\delta^{13}C$ has been used to broadly distinguish between C_3 and C_4 plant type's consequent of the discrimination of ^{13}C during photosynthesis, assuming a terrestrial source of bulk OM. C_3 plants utilise the Calvin-Benson photosynthetic pathway which produce depleted $\delta^{13}C$ values in the range of –22 to –35 ‰, whereas C_4 plants utilise the Hatch-Slack photosynthetic pathway which tend to produce relatively enriched $\delta^{13}C$ values in the range of –6 to –15 ‰ (Smith and Epstein, 1971; O'Leary, 1988; Meyers, 1997; Talbot et al, 2006; Sharpe, 2007; Mampuku et al, 2008), however, these ranges with respect to C_3 and C_4 vegetation are not mutually exclusive (e.g. Tyson, 1995) and may not primarily reflect photosynthetic processes (e.g. Edwards et al., 2010). In general, this natural kinetic fractionation allows an interpretation of changes in vegetation type, which in this core, is broadly consistent with the NAP and AP data (see Figure 5.6).

The NAP and AP data are indicative of two considerably different vegetation types. The NAP record is based upon pollen counts of grass-like vegetation, whereas the AP record is based upon pollen counts of woody vegetation, primarily trees. Together, these proxies can be used as a first-order assessment of changes in available moisture and humidity within the Tianyang catchment: for example, higher plants, such as trees, require an abundant source of moisture through precipitation and humidity, in order to survive. On the other hand, grasses are adapted to much lower precipitation and humidity amounts, different temperature and local – regional pCO_2 variations all of which have been argued to contribute to the evolution and spatial distribution of C_4 vegetation at intra-annual to glacial/interglacial timescales (e.g. Ehleringer et al., 1991; 1997; Cerling et al., 1993; Collatz et al., 1998; Edwards et al., 2010). However, a robust understanding of $p\mathrm{CO}_2$ changes on the Tianyang palaeovegetation is not feasible owing to the volcanic nature of the Leizhou Peninsula, and the potential for locally sourced CO_2 (by outgassing) from the geology through time.

Given the tropical setting of the Lake Tianyang maar, significant shifts in NAP and AP probably indicate a local – regional shift in the primary precipitation regime, which is intimately linked to the seasonal AM and ITCZ movements. The striking variability in the pollen records is evident in the $\delta^{13}C$ record, suggesting the underlying bulk OM signature is internally (i.e. within the Lake Tianyang maar sedimentary regime) dominated by past changes in catchment vegetation, implying broad scale changes in vegetation type (i.e. between C_3 and C_4 vegetation) are an important (and probably primary) control on the sedimentary OM isotopic signature, as a function of seasonal moisture variations. Specifically, I suggest that the new Tianyang $\delta^{13}C$ record tracks changes in aridity during glacial/stadial periods, and periods of increased humidity during interglacial/interstadial periods (e.g. Galy et al., 2007). Furthermore, and notwithstanding the uncertainties on the $\delta^{13}C$ reported here, the record shows significant variability in addition to the broad glacial-interglacial scale cycles indentified. For example, between ~285ka BP and ~250 ka BP and ~145 ka BP and ~65 ka BP, the $\delta^{13}C$ has recorded variability likely associated with stadial/interstadial change, suggesting the Tianyang record (currently sampled at ~640 year resolution from ~145ka BP to present and ~1280 year resolution from ~325 – 145 ka BP) potentially contains a centennial scale record of regional – global palaeoclimate, a record with such resolution is currently absent in south continental China.

5.4.3 XRF elemental ratios

The XRF analysis quantified 47 elements (see data tables on CD), however, only those that contribute important information on the Tianyang palaeoenvironmental are presented (Figure 5.7). Elements are presented as a ratio to Aluminium (Al) to normalise for the clay content within the samples. XRF elemental ratios may be interpreted in a number of ways, for example as catchment erosion indicators, water column reduction-oxidation (redox) processes and dust flux. The interpretation of the elemental ratios therefore requires an understanding of their geochemical behaviour in a lake environment.

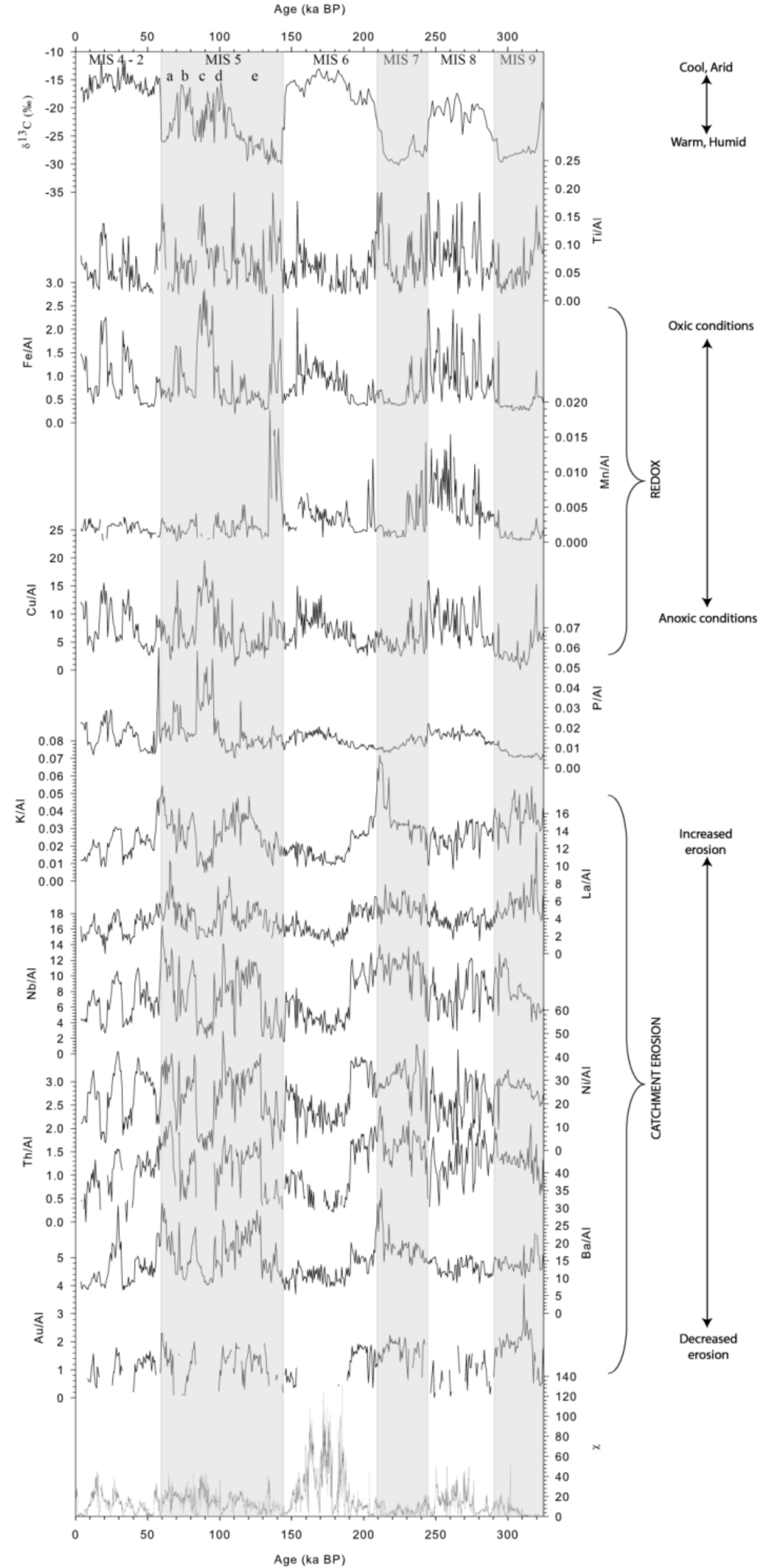

Figure 5.7: Lake Tianyang δ^{13}C, XRF and χ records. Vertical grey bars indicate inter-glacial/inter-stadial periods.

Fe and Mn concentrations in sediments of small lake catchments can be used to reconstruct transient changes in palaeo-redox conditions in both marine and freshwater systems (e.g. Edgington and Robbins, 1976; Farmer and Lovell, 1986; Davison, 1993; Matty and Long, 1995; Stumm and Morgan, 1996; Bryant et al, 1997; Schaller et al, 1997; Kolak et al., 1998; Brown et al, 2000; Boyle, 2001; Koinig et al, 2003; Yancheva et al, 2007). In freshwater systems, it has been shown that redox sensitive metals, particularly Fe and Mn, can be used as an indicator of bottom water oxygenation changes (e.g. Davison, 1993; Schaller et al, 1997; Yancheva et al, 2007). Under anoxic conditions, Fe and Mn exist in reduced states, with primarily soluble Fe^{2+} and Mn^{2+} dominant in the water column. This can result in water column eddy diffusivity (i.e. bottom water flow turbulence) carrying these reduced forms of Fe and Mn across the redox boundary and back into the oxygenated zone where they may reform oxides or oxyhydroxides. Under oxic conditions, Fe and Mn form stable oxidised states; Fe^{3+} and Mn^{3+} and Mn^{4+} forming oxide/oxyhydroxide precipitates which can become incorporated into the sediment, though Mn^{4+} in the form on MnO_2 is the thermodynamically stable form (Davison, 1993; Bryant et al, 1997). However, Fe and Mn precipitates can be diagenetically remobilised in the sediment by diffusion into sediment pore waters and then into the lake bottom waters, where anoxic conditions exist at or below the sediment – water interface. The position of this redox boundary is heavily influenced by seasonal changes in lake stratification and by changes in surface wind stress which can migrate from within the sediment into the water column and back again. Similarly, Cu is readily mobilised under changing oxygen conditions and may be reasonably expected to show some degree of coherency with Fe and Mn redox changes.

The Fe/Al, Mn/Al and Cu/Al appear to be internally consistent at the glacial to interglacial timescale, with clear evidence of high resolution variability within alternating glacial/stadial and interglacial/interstadial periods (see Figure 5.7). However this is not a pervasive feature of these records. For example, from ~285ka BP to ~250 ka BP, high concentrations of Fe, Mn and Cu suggest a well oxygenated water column, similar evidence for which occurs during MIS 6. In the upper section of the core, Fe and Cu show a number of coincident high concentrations, between ~90 ka BP and ~ 12 ka BP, whereas Mn is present in very low concentrations. This suggests that the Mn cycle may not responding as coherently to changes in water column oxygenation at these depths, and suggests a change in local processes that may not be directly consequent of broad scale glacial-interglacial expression. Specifically, the internal coherence of the redox sensitive parameters, which is evident in the lower sections of the core, and throughout for Fe and Cu appears to diminish in the Mn record (lower amplitude and different phasing). This may be a function of the reduction in delivery of Mn-rich material to the lake (i.e. no Mn available for remobilisation) suggesting that Mn from MIS 5e to present may be a less reliable recorded of changes in water column oxygen conditions.

Not all elements are susceptible to diagenetic remobilisation due to transient changes in water column oxygen levels. For example, Al, Au, Ba, K, La, Nb, Ni, P and Ti have one oxygenation state implying that their sedimentary signature is controlled by different environmental processes, such as catchment erosion and provenance (e.g. catchment versus windblown source). For example, the K/Al ratio has been used as an indicator of changes in the illite and kaolinite content of sediments (e.g. Bonatti and Gartner, 1973; Yarincik et al, 2000) and can contribute to the understanding of changes in catchment weathering (Yarincick et al, 2000; Burnett et al, In Press). Illite is commonly associated with temperate and/or arid environments (e.g. such as glacial/stadial climates) and is the product of physical weathering of source material (e.g. catchment geology), whereas kaolinite is more commonly produced in tropical and/or humid environments (e.g. such as interglacial/interstadial periods) and is a product of chemical weathering (Yarincik et al, 2000). This implies that, during interglacial/interstadial periods, where chemical weathering is more prominent due to increased humidity (implying relatively higher temperatures and amounts of precipitation), the kaolinite concentration in lake sediments is likely to increase, suggesting the K/Al ratio is low. On the other hand, during glacial/stadials, where illite input to sediment increases, the K/Al ratio should increase. In Lake Tianyang, Au, Ba, La, Nb and Ni, P and Th are used as catchment erosion indicators due to their high concentrations in catchment rocks (see Table 5.5).

Table 5.5: Selected element concentrations of Lake Tianyang averaged from a range of catchment rocks

Element	Concentration
Au	137 µg/g
Ba	179 µg/g
La	34 µg/g
Nb	54 µg/g
Ni	141 µg/g
P	0.4 %
Th	7.6 µg/g
Ti	1.3 %

Throughout the Tianyang record, Au/Al, Ba/Al, La/Al, Nb/Al, Ni/Al and Th/Al are strikingly consistent reflecting changes in sediment delivery from the catchment area. This is supported by the K/Al record, which shows a similar trend, but of lower amplitude, that may reflect changes in physical versus chemical weathering (i.e. low K/Al versus high K/Al). A striking shift common to all records occurs during MIS 6, where the concentrations of these metals synchronously decrease rapidly (in the context of the core sampling resolution, not the chronostratigraphy), concomitant with an increase in Fe/Al, Mn/Al and Cu/Al concentrations (but not Ti/Al), and also χ. At the same time, %NAP increase, and $\delta^{13}C$ shows a distinctive shift towards more depleted values. This internal coherency within the multi-proxy records suggests commonality in the process underlying the change, causing a reduction in catchment erosion, an increase in bottom water oxygen and a shift towards grass dominated vegetation. This suggests the establishment of an arid, dry environment.

Concentrations of Ti have been used to reconstruct changes in catchment erosion (e.g. Olsen et al, 2010) and dust flux resulting from changes in wind strength (e.g. Yarincik et al, 2000; Yancheva et al, 2007), with high concentrations of Ti suggesting either increased sediment delivery from the catchment or stronger winds and hence an increased dust flux to the catchment. The Ti record in Lake Tianyang is generally highly variable, and does not show an internally coherent relationship with the re-dox sensitive proxies (i.e. high concentrations to Ti are not always synchronous with high concentrations of Fe, Mn and Cu) or catchment erosion proxies. Prima facie, this indicates an internal de-coupling of the Tianyang proxy records in some sample horizons (but not all) suggesting a change in the mechanisms controlling the concentrations of these elements in the sedimemntary record. High Ti concentrations are coincident with high concentrations of the redox sensitive proxies, χ, and low concentration of catchment erosion proxies (with the exception of Ni) during MIS 8, at a time when $\delta^{13}C$ values are more depleted (i.e. C_4 vegetation), showing a relatively in-phase relationship across the sampling horizons. A broadly similar pattern is evident during MIS 6, however Ti concentrations are extremely low.

5.4.4 Magnetic Susceptibility (χ)

χ, a measure of the magnetism of the bulk sediment material, which is directly proportional to concentration and grain size of ferromagentic (e.g. haematite) and ferrimagnetic minerals (e.g. magnetite/titanomagnetite; Verosub and Roberts, 1995), is highly variable in the Tianyang sedimentary archive. The highest χ is evident during the MIS 6 glacial (Figure 5.7), with three clearly identifiable peaks (the first concomitant with a synchronous shift in the XRF, pollen and $\delta^{13}C$ records), with relatively higher values also evident during the MIS 8 glacial though much lower in amplitude than for MIS 6. The sedimentology during MIS 6 is dominated by fine- and coarse-grained clastic components, with a significant reduction in clay and silt, and is primarily characterised by quartz and magnetite (i.e. change in grain size distribution in the core). The Leizhou Peninsula, and the Lake Tianyang catchment, is dominated by basaltic geology, an igneous rock which is a primary natural source of magnetite and titanomagnetite (e.g. Dekkers, 1997), suggesting a catchment-derived source (supported by microscopic investigation from crater rock samples of intercalated magnetite minerals). The concentration of catchment erosion indicators are relatively low in comparison with the high χ during MIS 6, which is likely to be due to the dilution of the catchment weathering signal by the high influx of coarse-grained material. This is plausible in the context of the $\delta^{13}C$ record and %NAP counts, which suggest an open vegetation environment.

It appears χ within the Tianyang sedimentary archive is controlled by a number of factors, including changes in catchment erosion and transportation pathways (inplying grain size changes), aeolian influx, soil formation processes and, biogenic and authigenic mineralisation (e.g. Snowball, 1993; 1994; Dekkers, 1997; Maher, 1998; Sandgren and Snowball, 2001; Ishikawa and Frost, 2002). In lakes which have small and well defined catchments (e.g. Lake Tianyang maar), the dominant source of sediment is likely to be from the catchment (bedrock weathering and catchment soil), though aeolian sources are a plausible contributor.

5.5 Glacial – Interglacial Change: A Synthesis

Glacial – interglacial scale changes have previously been reported from cave records in central and east China (Wang et al, 2001; Yuan et al, 2004; Johnson et al, 2006; Cheng et al, 2009), from Qinghai-Tibetan Plateau ice core records (Thompson et al, 1997), loess/palaeosol sequences from central and northern China (e.g. Porter and An, 1995; Chen et al, 1999; An et al, 2000; Porter, 2000), and from sedimentary sequences from the South China Sea (Wang et al, 1999; Jian et al., 2001; Sun et al, 2003). In general (i.e.

assuming spatial homogeneity of the precipitation associated with seasonal AM regime through time), glacial/stadial periods tend to be characterised by dry, arid conditions, particularly in north and central China (e.g. Herzschuh, 2006), when the effective moisture on continental China is significantly lower as a result of the more southerly average position of the ITCZ (e.g. Wang et al., 2001; Flietmann et al., 2003; Bird et al., 2005; Yanhceva et al., 2007). In contrast, during interglacial/interstadial periods the ITCZ-AM system general encroaches continaental China and brings with it signifincat precipitation and humidity in apparent concenrt with the northern hemisphere summer insoaltion maximum (e.g. Wang et al., 2008).

The Tianyang $\delta^{13}C$ record shows a distinct glacial – interglacial palaeoenvironmental imprint, alongside the NAP and AP pollen counts, and a striking similarity with the SPECMAP $\delta^{18}O$ benthic record. In addition, these glacial – interglacial changes appear to be evident in the redox sensitive elements, catchment erosion indicators and χ record, particularly from MIS 9 to the end of MIS 6 inclusive (see Figure 5.7). This multiple proxy evidence demonoistrates internally consietency within the Tianyang records in the lower sections of the core. However, this is not an internally pervasive feature of these records, the relationship and pahsing between which changes significantly in the upper sections, particularly throughout MIS 5. This may principally be due to the silting up processes within the lake causing catchment erosion and redox proxies to respond more rapidly, and at different timescales within a smaller catchment surface area and water column depth, and therefore obscuring regional – global environmental change signatures with local signatures.

Prior to MIS 9 (age re-evaluated based on the new ^{14}C datings, pollen and $\delta^{13}C$ records presented here; Figures 5.5 and 5.6), the Lake Tianyang maar system began progressively to change from being a deep, highly productive lake towards a much shallower lake (Zheng and Lei, 1999), probably due to the reduction of sediment accommodation space in the catchment basin through silting up of the lake, which may be the direct result of localised neotectonic uplift (Huang, 1993). During MIS 9, the sedimentology (principally characterised by abundant wood macrofossils and highly organic clay(amorphous)), relatively depleted $\delta^{13}C$ values, high %AP and low %NAP point towards a wet woodland/swamp type environment (i.e. dominated by C_3 vegetation), with relatively low water levels. This marks the first major shift in the Tianyang system from a highly productive, diatom rich deep water lake to wetland. The redox parameters during this period reflect low oxygen levels in this shallow water environment, resulting in productivity driven depletion of the dissolved O_2. After depletion of the available dissolved O_2, oxidation of OM would be significantly reduced implying preservation in the sedimentary record. I propose that the local – regional environment was characterised by warm, humid conditions (implying abundant precipitation) during MIS 9, maintained by the average annual to millennial timescale position of the seasonal rain-bearing ITCZ-AM regime being sufficiently north of the equator, and traversing the Chinese mainland. This implies that the dominant palaeoenvironmental signal during this period is weighted towards the summer season variability, with no clear evidence for millennial-scale variability recorded in the multi-proxy record. This may reflect a period where winter monsoon activity was relatively weaker, with no detectable signal in the far south of China, but may also in part be a function of the sampling strategy (i.e. sampling resolution ~1280 kyr).

The transition to MIS 8 marks a major shift in the vegetation type within the catchment, from wet woodland to a more open vegetation structure, characterised by an increase in lower plants, such as grasses. This is evident in the %NAP and %AP records, and reflected in the $\delta^{13}C$ record ($\delta^{13}C \approx -17.3$ to -24.8 ‰). Collectively, these vegetation proxies are relatively variable and do not necessarily point towards stability in the climax vegetation within the catchment (see Figure 5.6 between ~290 ka BP to ~245 ka BP). This suggests a mixed vegetation assemblage during MIS 8, with alternations between more open, savannah like vegetation with periods characterised by higher plants and more woody vegetation. In particular, the most prominent such alternation appears to be centred on ~267 ka BP to ~273 ka BP (the resolution of the record at this depth is ~1280 yrs), and potentially represents one of the MIS 8 stadial/interstadial transitions, suggesting the Tianyang sedimentary archive contains a higher resolution MIS 8 record. This variability is also recorded in the higher resolution redox and catchment erosion proxies, and χ, which provide clear evidence for substantial variations in lake redox conditions, suggesting changes in surface wind-driven mixing of the lake water column, particularly when $\delta^{13}C$ are most depleted (proxies are internally “in-phase”). In addition, the catchment erosion proxies, which are in part influenced by vegetation cover (linked to changes in available precipitation and temperature) and affect the rate of delivery of sediment to the lake basin, are relatively variable (again, with peaks in-phase with higher water column oxygen levels and dominant C_4 vegetation). Together, these proxies indicate that the sedimentary record from Tianyang has recorded evidence for a relatively unstable glacial period in south China, and possibly in the wider tropics (i.e. via an ITCZ-AM teleconnection). Specifically, the %NAP, %AP and $\delta^{13}C$ provide compelling evidence from changes in available moisture (e.g. more arid conditions with high %NAP and higher $\delta^{13}C$ values) and changes in the summer/winter wind regime (higher Fe, Mn, Cu (redox) and Ti concentrations). Broad-scale changes in the average position of the ITCZ, and the subsequent landward penetration of the associated seasonal rainfall of the ITCZ-AM regime (i.e. average position located farther south during glacial/stadial periods in comparison to interglacial/interstadial periods) can account for this trend. It is difficult to assess the potential contribution to the singals from changes in winter/summer AM variability however Yancheva et al (2007) suggest high Ti concentrations concomitant with high water column oxygen levels are indicative of stronger winter AM winds during cool, dry periods. It is therefore possible that the vegetation proxies are recording a signal more closely linked to changes in available moisture, ultimately driving aridity that is directly linked to the displacement of the ITCZ-AM to a more southerly position. In contrast, the redox parameters and Ti concentrations may be reflecting changes in the winter AM wind regime at this time with winter winds, driven by the intensity of the Siberian high vortex, appear to penetrate much farther south, carrying a measureable signature from its dust loading.

A similar trend is also noted for MIS 6; however, in this case the vegetation structure appears to be more stable, with much lower % AP and an increase in % NAP, and more enriched $\delta^{13}C$ ($\delta^{13}C \approx -13.0$ to -19.5 ‰) which more clearly suggest an environment dominated by C_4 vegetation, likely to be an established savannah grassland (Figure 5.5). The transition from MIS 7 to MIS 6 is marked by a distinctive, and apparently rapid, shift in towards more arid conditions, implying a major change in vegetation cover and subsequent exposure of the catchment surface. Synchronous with this shift are increased concentrations in Ti, K/Al (chemical weathering index) and the catchment erosion indicators, suggesting an influx of catchment material to the lake basin as a function of the change in vegetation cover. However, the redox parameters (in this instance, possibly representing influx of oxygen rich freshwater leading to Fe, Cu and Mn precipitation), lag behind these proxies during this transition, indicating that the proxies are slightly “out of phase” suggesting the processes controlling there sedimentary concentrations within the Tianyang system are temporally variable.

As the vegetation assemblage begins to re-establish in this more arid environment, evidence for catchment weathering begins to reduce. A significant change in the sedimentary regime is evident, with a shift from clay domainted depsoits to fine and coarse grained sands (Figure 5.4) suggesting high energy depsoition. Prime facie, this suggests a difference in the Tianyang palaeoenvironment response to change during MIS 6, relative to other sections of the Tianyang sedimentary archive. A striking feature of the MIS 6 record is centered approximately on ~185 ka BP, where the $\delta^{13}C$, redox proxies and catchment erosion proxies show an in-phase, rapid shift, primarily indicating a dramatic reduction of catchment weathering, but an increase in precipitation of redox sensitive elemtns (Fe, Cu and Mn) suggesting greater oxygeneation of the water column. The $\delta^{13}C$ record shows a further enrichment, possibly indicative of a climax in arid conditions, suggesting that the redox sensitive elements may be controlled at this time by increased water column mixing due to wind regime (i.e. possible winter AM winds), though Ti concentrations are notably low during this glacial period, and relative to the Tianyang MIS 8 record (i.e. possible variable control on Ti record).

The greatest variability in the vegetation records ioccurs during MIS 5, where the sedimentary archive returns to a clay/silt dominated sequence. The vegetation proxies appear to fit extremely well with the MIS 5 (sub-stage) variability in the SPECMAP $\delta^{18}O$ record. MIS 5 has been documented in the loess/palaeosol records in north China (e.g. Chen et al, 1999) and the cave records in central and southern China (e.g. Wang et al, 2001; Yuan et al, 2004; Johnson et al, 2006, Cheng et al, 2009) all of which broadly follow northern hemisphere glacial – interglacial changes. For example, MIS 5e, 5b and 5a in these records collectively point towards periods of humidity, probably characterised by relatively higher amounts of precipitation, suggesting abundant rainfall delivery from the ITCZ-AM regime. This variability is evident higher %AP and lower %NAP concomitant with relatively depleted (lower) $\delta^{13}C$ values, indicating an environment dominated by C_3 vegetation. In MIS 5e the $\delta^{13}C$ are around –27 to –30 ‰, %AP is ~80%, and there is evidence of wood macrofossils in the sedimentology. These point towards a return to a wet woodland/swamp type environment, though as sub-stage 5e progresses, the system appears to dry up and move back towards an open savannah-like environment (leading into MIS 5d). However, in this section of the sedimentary record, the vegetation and redox proxy records become decoupled from one another, suggesting a change in the mechanisms controlling the concentrations of Fe, Mn and Cu in the sedimentary regime. During the interstadial periods (5e, 5c, 5a), the catchment erosion proxies and χ appear to be higher, suggesting an increase in chemical weathering in the catchment. Mn concentrations from Mis 5e towards present reduce dramatically relative to Fe and Cu. In comparison to Fe adn CU, Mn is more easily mobilsed under changing redox conditions. As the Lake Tianyang maar contined silting up, and thus reducing the sediment accommodation space, and ultimately, water depth, the redox boundary within the water column potentially became more responsive to seasonal variability (given its proximity to the sediment surface) resulting in a reduced residence time in anoxic conditions of Mn within the surface sediments. This continually, and rapid, overturing may therefore reduce the overall concentration, relative to Fe and Cu due to this rapid remobilisation.

The Ti record, however, is less coherent, and appears to show no clear trend of high concentrations with more depleted or more enriched $\delta^{13}C$ values, highlighting its decoupled nature from the vegetation trends in comparison with the lower section of the record. This suggests the mechanism(s) controlling Ti concentrations in the system have changed and may vary between catchment derived sources and windblown sources, making the overall interpretation of this record uncertain.

5.6 Winter monsoon proxy

Yancheva et al (2007) reported Ti concentrations, alongside χ, S-Ratio, Fe, Mn and total organic C, From the Holocene sedimentary record of Lake Huguangyan (adjacent to Lake Tianyang), and collectively interpreted them as evidence for changes in winter AM wind strength. This, they claimed, corresponded to changes in the transport of Ti laden dust from the loess plateaus in central and north China and changes in lake redox conditions. They proposed that, as the winter AM strengthened during cooler periods (e.g. glacial/stadials), which resulted in increased aridity and stronger, more persistent winter winds deriving from northern China, this increased the dust flux from the loess plateau leading to greater concentrations in the Huguangyan sedimentary record. The increase in Ti concentrations, concomitant with higher Fe and Mn concentrations (due to well oxygenated waters), high total organic C, χ and S-Ratio in the Lake Huguangyan Holocene sequence were interpreted as indicators for variability in the strength of the winter AM monsoon wind field (Yancheva et al, 2007). Ti was proposed as the primary proxy for the winter AM wind strength because of its insensitivity to lake redox changes.

Due to the small catchment size of Lake Huguangyan (~2.5 km^2 surface area; ~3.5 km^2 catchment area), Yancheva et al (2007) assumed the primary source of Ti and magnetic minerals was aeolian during these periods of stronger winter AM winds.

This hypothesis therefore suggests that high Ti concentrations should coincide with relatively depleted $\delta^{13}C$ values in the Tianyang $\delta^{13}C$ record, a decrease in % tree pollen and an increase in Poaceae pollen. Given the close proximity of Lake Tianyang to Lake Huguangyan (~100 km south), the small size of the Lake Tianyang catchment (~7.3 km^2), and the similarities in catchment geology (Ho et al, 2000), the Tianyang sedimentary record serves as an excellent opportunity to test the robustness of the winter monsoon wind strength proxy at the glacial – interglacial timescale and potentially extend its applicability.

In the Lake Tianyang sedimentary record, the link between high Ti concentrations and glacial/stadial periods is complicated, and does not suggest a pervasive driving mechanism (i.e. changes in winter AM wind strength). For example, during MIS 8 (northern hemisphere glacial conditions), a relatively unstable period in the Tianyang record characterised by a mixed vegetation assemblage, the Ti record appears to hold up the Yancheva et al (2007) hypothesis. This is supported by the coincidence of high Fe/Al, Mn/Al and Cu/Al concentrations and an increase in χ and relatively low concentrations of catchment erosion elements. A similar coincidence between the proxies is evident during the small excursion in MIS 7, suggesting a shift towards less humid conditions. % tree pollen rise by ~20% and $\delta^{13}C \approx -23.5$ ‰, coupled with increased chemical wreathing in the catchment and increased oxygen levels in the bottom waters of the system. It is possible this co-variability in the records is an erosion event linked with a change in the type of vegetation. However, this relationship breaks down at the transition to, and throughout, MIS 6. The increase in Ti/Al concentration at the MIS 7/6 transition, a shift from C_4 vegetation to C_3 vegetation, corresponds with higher concentrations of Nb/Al, Ba/Al and K/Al, suggesting an increase in catchment weathering. Moreover, I note the anomalously low Ti/Al concentrations throughout MIS 6, a cooler period where Ti concentrations are hypothesised to be higher. Throughout the remainder of the record, high Ti/Al concentrations appear to coincide with warmer periods, for example MIS 5e, 5c, 5a, indicating an opposite trend from the proposed hypothesis (Yancheva et al, 2007) and from the lower sections of the Tianyang core. This suggests that sedimentary Ti concentrations do not ubiquitously vary with changes in winter AM wind field position and/or strength implying its applicability for winter AM reconstruction within and between cores is questionable because (i) the dust loading during glacial periods is highly variable, (ii) the winter AM wind field does not directly cross the Leizhou peninsula during this period or, (iii) the Ti concentration does not reflect changes in winter AM wind strength.

There are two important considerations that underpin the winter monsoon wind strength interpretation: (i) The concentration of clastic material in the Huguangyan and Tianyang sedimentary record and (ii) Ti concentration from catchment geology (Table 5.4). Zhou et al (2008) argue that the weathering in south China is intensive owing to the climate regime (high temperatures and precipitation) and suggest that weathering of the Ti rich basalt and laterite in the catchment (dominant in maar lake catchments in the Leizhou Peninsula, including Lakes Huguangyan and Tianyang) is an important local source of Ti in the sediments, which may dilute any windblown Ti signal. This point is refuted by Yancheva et al (2007) in the context of their S-Ratio and χ records, despite the known presence of Ti rich minerals in the Huguangyan catchment, namely ilmenite and titanomagnetite (Ho et al, 2000; Mingram et al, 2004; Yancheva et al, 2007), and the evidence for catchment erosion (Liu et al, 2000; Zhou et al, 2008; Han et al, 2010). In addition, Ti concentrations of source rock in the Leizhou Peninsula are reported at ~1.0 – 1.5 %, and in the Loess and Palaeosol sequences from central and north China at ~0.4 – 0.5 % (Ho et al, 2000; Zhou et al, 2008). XRF analysis of the Tianyang catchment rock indicate Ti concentrations to be ~0.8 – 1.6 %. Furthermore, Zhou et al (2008) argue that the flux of lithogenic materials in Lake Huguangyan, relative to the rate of dust flux from the Loess plateau, is considerably higher, which, given the locally sourced Ti, indicates that the record does not provide a pure winter monsoon wind signal.

A recent investigation on the magnetic granulometry of the Huguangyan sedimentary record (Han et al, 2010) corroborated the findings of Zhou et al (2008), indicating that the grain size or magnetic minerals was primarily catchment sourced rather than from the Chinese loess plateau. Han et al (2010) reported that the primary magnetic mineral in Huguangyan is (titano) magnetite and showed that the grain size of the magnetic minerals in the sedimentary record was more closely correlated with the catchment geology than with loess. They did not completely rule out the possibility of a contributory source from the Chinese loess plateau, however, Han et al. clearly suggest the signal to noise ratio in the magnetic granulometry record in respect of the proposed winter AM wind strength of Yancheva et al (2007) is much lower than initially reported.

In addition, the support from the % total OC, which Yancheva et al (2007) interpret as a bottom-water oxygenation proxy, may be compromised by the presence of siderite in the lake throughout their record (Mingram et al, 2004; Yancheva et al, 2007). It is known that siderite is not readily digested (if at all) by acid treatment (Larson et al, 2008), suggesting a non-stoichiometric reaction in the sample material resulting in residual IC. Residual IC would subsequently increase the value of total organic C, indicating the quantification of presented by Yancheva et al (2007), and its support for changes in bottom water oxygenation, is highly questionable. In addition, Zhang and Lu (2008) questioned the applicability of the Ti record in the recent past by showing discrepancies with the proposed periods of stronger winter AM from the Huguangyan sedimentary record and the historical records.

This, together with the contradictory evidence from the Tianyang record, implies Ti concentrations from the Tianyang sedimentary record is probably not a robust winter AM wind proxy at the glacial – interglacial timescale. I suggest the Ti concentration in the Lake Tianyang sedimentary sequence is primarily controlled by changes in catchment hydrology (i.e. weathering/erosion signal), but that aeolian sources are evident. Given the similar geological and climatic setting of Lakes Tianyang and Huguangyan, and the complications aforementioned, I go further and suggest that the Ti concentration in Lake Huguangyan sediments does not represent a reliable proxy for dust flux from the Chinese loess plateau, which undermines its reliability as an indicator for changes in winter AM variability. The relationship between the winter AM wind strength, sedimentary geochemistry and provenance proposed by Yancheva et al (2007) is far more complex than originally thought, though the emergent understanding appears to support changes in catchment hydrology as the primary controlling mechanism. Importantly, this could be driven by changes in summer AM precipitation, which adds a further seasonal complexity to the argument.

5.7 Regional palaeoclimate comparison

At the regional scale, this new record from Lake Tianyang maar represents one of the longest terrestrial palaeoclimate records in the southern AM region, and which rivals the cave speleothem records (e.g. Cheng et al., 2006) with respect to continuity, resolution and time span. Specifically, the $\delta^{13}C$ and XRF records have a resolution of ~ 600 years (at 8 cm sampling intervals), implying a near annual resolution for the χ record (5 mm sampling interval) though the interpretation of this record at lower than multi-centennial resolution is compromised by chronological uncertainties (and hence constraint on sedimentation rates), the limitation of the Tianyang system (i.e. the resolution with which the sedimentary archive has faithfully recorded palaeoenvironmental variability) and sampling strategy. Given these constraints, only a tentative and broad regional comparison (limited to glacial – interglacial scale changes) is feasible and no investigation of the phasing of these different proxy archives (i.e. lead/lag relationships) can be undertaken.

The palaeoenvironmental records from the Chinese loess plateau (Guo et al., 2009) and from the hulu, Sanbao and Luizhiu cave speleothems (Wang et al., 2001; 2008) show distinctive glacial – interglacial scale variability, and in the case of the cave speleothem record, punctuated by stadial – interstadial scale variability. These records lend support to the theory that summer AM variability (i.e. implying broad-scale variability in precipitation regime) varies dominantly with northern hemisphere summer insolation at orbital timescales (e.g. Kutzbach, 1981; Prell and Kutzbach, 1985; Rooisgnol-Strick et al., 1998; Ruddiman, 2006). The Loess plateau records provide proxy evidence for variability in the summer and winter monsoon regime (Guo et al., 2009). Loess grain-size is interpreted as a proxy for past changes in wind strength/intensity, with much coarser grain sizes prevalent during glacial/stadial periods, which is attributed to changes in the Siberian High airmass which, in itself, influences winter monsoon wind regime and continental aridity (e.g. Porter and An, 1995; Ding et al, 1995; Guo et al., 2009). The chemical weathering indiex, derived from the Xifeng profile, reflects periods of increased soil productivity (e.g. palaeosol formation), influenced in part by the landward extent of precipitation and humidty (implying temperature) associated with the summer monsoon (e.g. Guo et al., 2000; 2009). The central China cave records are $\delta^{18}O$ measurements of calcitic stalgtites, which have been interpreted as a proxy for changes in meteoric precipitation, proposed to relate directly to the strength/intensity of the seasonal summer monsoon (e.g. Wang et al., 2001; 2008; Yuan et al., 2004; Cheng et al., 2006).

I compare the Tianyang $\delta^{13}C$ with the Loess plaeteau records and cave records to provide a preliminary understanding of the newly developed Tianyang record in the context of climate variability at glacial – interglacial timescales across continental China. This will provide a broad terrestrial gradient which may elucidate variations in land-sea thermal contrasts that are cited as integral to monsoonal climate (see Figure 5.8). Similarities between the Tianyang $\delta^{13}C$ record, the Loess plaeteau record and the cave $\delta^{18}O$ records at glacial – interglacial timescales are evident which lend support for my interpretation of changes in aridity in Tianyang. During glacial periods, the Loess grain size increases significantly, a change reflected in the Tianyang $\delta^{13}C$ by a shift towards more depleted values, followed by a reduction in soil formation processes in the Loess plateau. This broad trend appears relatively similar from MIS 9 through to the end of MIS 6, though the resolution of the Tianyang $\delta^{13}C$ is not as superior as in the cave $\delta^{18}O$, and therefore does not neccassarily detect sub-orbital scale variability. In addition, there is support for the “event” during MIS 7, around ~245 ka BP, being representative of a period of stronger winter monsoon, which sees an increase in Loess plateau grain size and a similar shift towards depleted $\delta^{18}O$ in the cave records, a slight depletion in $\delta^{13}C$, and an increase in sedimentary Fe, Cu, Mn and Ti. These collectively point towards a signifincat reduction in precipitation across China, suggesting more dominance of the winter monsoon winds.

However, this apparent similarity in the records appears to fundamentally change during MIS 5, at a time when the internally phasing of the multiple proxies measured in the Tianyang core appear to change. For example, from ~145 ka BP to ~70 ka BP, the Tianyang $\delta^{13}C$ and cave $\delta^{18}O$ records appear to be in “anti-phase” with respect to the expected trend seen during MIS 9 through to the end of MIS 6. Specifcally, during the interstadials 5e, 5c and 5a in the Tianyang $\delta^{13}C$, where it is proposed that the environment was much more humid the cave $\delta^{18}O$ suggest a dramatic reduction in precipitation (or, possibly, a shift in the moisture source region). At the same time, the Loess plateau records, compromised in part by their much lower resolution over this time period, appear to support the findings from the Tianyang archive. It is therefore possible that the cave $\delta^{18}O$ (at least at this time) may not be recording changes in intensity or amount of precipitation, but could actually be a recorded of changes in moisture source region, suggesting the land-sea thermal contrast in south China is much weaker with respect to moisture delivery, with a potential alternative source being derived from the Indian monsoon region (longer transit period of moisture would explain difference in $\delta^{18}O$ fractionation record in the cave records).

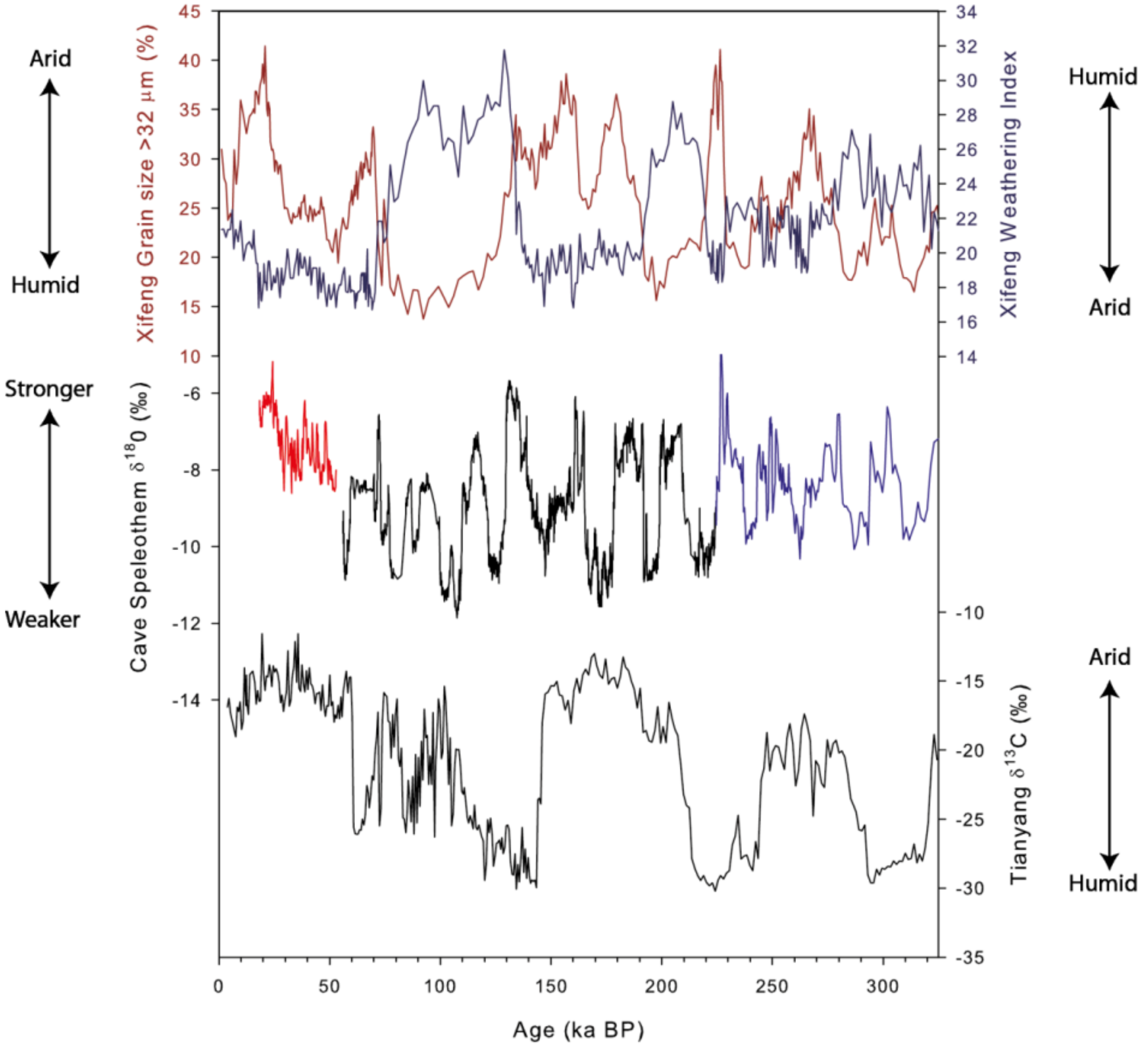

Figure 5.8: Comparison of Tianyang $\delta^{13}C$ record with loess plaeteau grain size >32 µm (%) and associated weathering indiex (Guo et al., 2009) and central and eastern Chinese cave $\delta^{18}O$ records (Wang et al., 2001; 2008; Yuan et al., 2004; Cheng et al., 2006). In the cave record plots, the red line represents data from hulu cave, the black line data from Sanbao cave and the blue line data from Luizhiu cave.

5.8 Synthesis and Conclusions

The multi-proxy geochemical record from the Lake Tianyang maar presented here is the first long-term terrestrial record detailing glacial – interglacial palaeoenvironmental changes, in the far south of continental China. Lake Tianyang has undergone major changes in its evolution, the first of which was the recorded in the reduction of diatom abundance at ~160 m, coupled with with a slight increase in minerogenic content. The second, and most notable, was between ~53 m and 37 m, where diatoms gradually disappeared and the sedimentology became increasing dominated by fine- and coarse-grained minerogenic material, alongside clear evidence for the presence of wet woodland/swamp like environment. These changes suggest Lake Tianyang began silting as a result of a reduction of sediment accommodation space and/or relatively lower lake levels. Although the mechanism(s) responsible for this major change in the system are unclear, neotectonic uplift has been proposed (Huang, 1993).

The Lake Tianyang record shows evidence for significant changes in the type of vegetation in the catchment, with an emergent glacial – interglacial and stadial - interstadial imprint in the δ^{13}C record, suggesting broad changes in temperature and precipitation patterns in south China. For example, during glacial periods (e.g MIS 8 and MIS 6), the δ^{13}C record and pollen spectra point towards a dominance of C_4 vegetation, where catchment erosion appears to be lower and bottom water oxygen levels high (i.e. huimid environment). Interglacials (e.g. MIS 9, MIS 7), however, show the opposite trend and imply a less humid environment characterised by grass-like vegetation.

In addition, XRF elemental analysis indicates changes in lake water oxygenation levels and catchment processes also with a glacial – interglacial imprint, the definition of which diminishes from MIS 6 towards present. This lower signal-to-noise ratio in the XRF elements after MIS 6 is likely due to the continued silting up of the lake towards present, with regional – global scale changes in the palaeoenvironment being significantly masked by localised processes. Furthermore, changes in the overall concentration of any one catchment erosion proxy can vary between glacial – interglacial and/or stadial – interstadial periods due to preferential erosion of catchment bedrock with a slightly different geochemical composition. Where the δ^{13}C record shows evidence for the MIS 5 stadials/interstadials, the relationship with the redox and catchment erosion proxies breaks down, suggesting the mechanism(s) controlling their sediment concentrations alters, possibly dominated by more localised processes. The key findings of this chapter are:

1. The Lake Tianyang sedimentary archive is apparently much older than previously reported. I present here an age estimation of ~320 ka BP for the upper 40m of sediment which contradicts previous estimations of ~45 – 50 ka BP for the upper 40 m (Chen, 1988; Chen and Yang, 1989; Chen et al, 1990). The new suggestion is based on the correlation of pollen and $\delta^{13}C$ data to the SPECMAP $\delta^{18}O$ stack, with a degree of independent dating control by ^{14}C dates between ~2.50 m and 7.50 m.

2. Glacial – interglacial timescale variations, and stadial – interstadial variations (i.e. MIS 5), are well expressed in the Lake Tianyang sedimentary $\delta^{13}C$ bulk OM record. This indicates that palaeovegetation patterns followed broad changes in global ice volume and associated sea-level change. Despite the limitations of the accuracy and precision of the $\delta^{13}C$ data (~ 4‰), the Tianyang $\delta^{13}C$ shows striking similarity to the % AP and %NAP data, suggesting that $\delta^{13}C$ can still provide low amplitude information on changes in vegetation (i.e. C_3 versus C_4 plants).

3. Change in the Ti/Al record does not ubiquitously represent changes in winter monsoon wind strength, as proposed by Yancheva et al (2007). Throughout the lower section of the Tianyang record (i.e. MIS 9 – MIS 6), there is a coherency between the vegetation proxies, Ti, redox sensitive parameters, χ and catchment erosion indicators, which support this theory. However, towards the end of MIS 6, and from MIS 6 through MIS 5, the coherency between the proxies capturing these processes breaks down, suggesting an increase in localised variability contributing to the elemental concentrations in the sedimentary record (e.g. catchment erosion; low lake levels), therefore diluting any regional – global scale palaeoenvironmental changes.

4. A regional comparison of the new Tianyang $\delta^{13}C$ record with palaeoenvironmental records from the Chinese Loess Plateau and central and eastern Chinese cave speleothem archives indicate broad similarities in change at glacial – interglacial timescales. During MIS 5, the relationship appears to change, and the comparison suggests a potential alteration in the strength of the land-sea thermal contrast in south China. This implies an alternative primary moisture source to the region during this time, reflected in the cave $\delta^{18}O$ records, which may be from the Indian monsoon region.

Chapter 6

Summary

6. Summary

The primary aims of this thesis were:

1. To investigate the effect of pre-analysis acid treatment methods on C/N and $\delta^{13}C$ values of OM in a range of environmental materials. (Chapter 2)

2. To investigate the effect of pre-analysis acid treatment methods on $\delta^{15}N$ values of OM in a range of environmental materials. (Chapter 3)

3. To investigate the effect of pre-analysis acid treatment methods on C/N, $\delta^{13}C$ and $\delta^{15}N$ values of OM in a down-core sedimentary sequence. (Chapter 4)

4. To develop of multi-proxy record of environmental change from Lake Tianyang. (Chapter 5)

6.1 Effect of acid treatment on C/N and $\delta^{13}C$ of organic material

Pre-analysis acid treatment methods, necessary for the measurement of C/N and $\delta^{13}C$ values of OM, carry two important inherent assumptions: (i) the influence on sample OM is either negligible or systematic and (ii) that the acid reagent and method employed completely remove IC from the sample material, which has not been previously investigated in a systematic manner. Therefore, the assumption underpinning decades of research on C/N and $\delta^{13}C$ of OM had not been validated. This implied that there was no robust understanding of the reliability or otherwise of the measured data (i.e. the proxies).

The comparative study presented in Chapter 2 was the first such systematic study on the effects of pre-analysis acid treatment methods on OM from environmental materials. It has been clearly demonstrated that the assumptions underpinning the pre-analytical methods are seriously flawed, and that C/N and $\delta^{13}C$ values of OM depended upon the acid treatment. This biasing by acid treatment can be (and normally is) several orders of magnitude higher than instrument precision (here ~0.2 for C/N and; 0.2 ‰ for $\delta^{13}C$), and was shown to be highly non-linear. Biasing in C/N was in the range of ~1 – 120 and $\delta^{13}C$ in the range of ~0.2 – 7.2 ‰, with C and N values biased in a non-proportional manner. Consequently, the environmental interpretation of the data becomes unreliable (e.g. difference between interpreting a terrestrial OM source or an aquatic OM source). The effects of acid treatment varied substantially between sample materials, within and between methods, as did the size and direction of the bias (i.e. samples from different environments). Across the methods tested, I demonstrated a lack of coherency in the application of any one method or acid reagent.

6.2 Effect of acid treatment on δ^{15}N of organic material

A progression of the comparative study to that presented in Chapter 2 was undertaken in the context of the increased application of “dual-mode” isotope analysis (i.e. the simultaneous measurement of δ^{13}C and δ^{15}N from the same sample aliquot). This implies an increase in the measurement of δ^{15}N values in OM after acid treatment of the sample, in comparison with the more common approach of measurement of δ^{15}N values in OM on untreated samples. Similarly to the findings of Chapter 2, it is shown that measured δ^{15}N values of OM between pre-analysis acid treatment methods are significantly different, and that the strength of HCl and the type of capsule the sample was combusted in (e.g. samples combusted only in Ag capsules produced lower δ^{15}N values) could contribute considerably to variability on the measured data (i.e. bias). The bias on δ^{15}N was as high as ~1.5 ‰, significantly above the instrument precision (here ~0.3 ‰). Further, it was noted that δ^{13}C and δ^{15}N values were altered within and between methods in a disproportionate and non-linear fashion. This is not unsurprising given that elemental C and N varied in a non-linear fashion under acid treatment (Brodie et al., 2011a; Chapter 2). This provides further evidence that indicates a lack of coherency in the application of any one method or acid reagent and supports the contention that the method followed can directly influence the reliability of δ^{15}N (including measurement on untreated samples).

This therefore precludes a “dual-mode” analysis approach to C and N isotopes on bulk OM and subsequently highlights the potential for different organic compounds, within and between different environmental samples and acid treatment methods, to respond in an unpredictable manner to acid treatment. It is now essential that a molecular level characterisation of acid treated materials be undertaken to develop the scientific understanding of the bias introduced to sample OM by acidification.

Additionally, it is widely assumed that IN has a negligible influence on elemental and isotopic N data, and is therefore not commonly quantified. Rather, the IN has been estimated from a bi-plot of %C and %N, with assumed linearity, and used to moderate interpretations of OM based on an offset from a perfect linear relationship between %C and %N. I showed this approach to IN estimation, and subsequent support for OM interpretations, to be an aberration. In particular, this approach is undermined by the flawed assumptions on (i) linearity and co-variability of %C and %N within bulk OM and (ii) the influence of pre-analysis acid preparation methods on elemental and isotopic C and N concentrations. IN should therefore be quantified on separate sample aliquots and a correction applied.

6.3 Effect of acid treatment on C/N, δ^{13}C and δ^{15}N on organic materials in a down core sequence

Given a more robust understanding of the biasing by acidification on elemental and isotopic C and N of organic materials derived in Chapters 2 and 3, and the emergence of reduced accuracy and precision on measured values, it was necessary to investigate the impact on the measurement and interpretation of bulk OM from a down-core sedimentary sequence. A section of sediment was analysed from the Lake Tianyang, for C/N, δ^{13}C and δ^{15}N values of bulk OM. The analysis illustrated sample horizons with no difference within and between pre-analysis acid treatment methods, and untreated samples (i.e. within instrument precision), and sample horizons with considerable differences within and between pre-analysis acid treatment methods, and untreated samples. This re-iterates the inconsistency in the application of any on particular method in a down-core context (i.e. bias on measured values is inevitable, varying in its magnitude between sample horizons). In particular, bias on the measured C/N, δ^{13}C and δ^{15}N values were evident from inefficient removal of IC, likely due to differential rates of removal between acid reagents and methods, and the bias of acidification on the organic fraction of the sample material. For IC, this is problematic as acidification is widely assumed to completely remove calcite based IC, however more robust forms of IC such as dolomites and siderites, are more difficult (if not impossible) to completely remove from samples, suggesting the extent of bias attributed to the measured values may not be clear using the methods or reagents investigated here. Bias on measured data, above that of instrument precision, was in the range of ~1 – 100 for C/N values; ~4 – 7 ‰ for δ^{13}C values; and up to ~1 ‰ δ^{15}N values. These findings are similar to those presented in Chapters 2 and 3, and makes the interpretation of C/N, δ^{13}C and δ^{15}N values, in the context of OM provenance and type, highly problematic.

6.4 Multi-proxy palaeoenvironmental reconstruction from Lake Tianyang

The multi-proxy geochemical record from Lake Tianyang is the first long-term terrestrial record detailing glacial – interglacial palaeoenvironmental changes, in the far south of continental China. I suggest a new chronostratigraphy from those previously published, proposing the upper 40.00 m of sediment in the Lake Tianyang basin is ~320 ka old. During this period, Lake Tianyang has undergone two major changes in its evolutionary history, possibly due to local neotectonic uplift, resulting in the system silting up and reducing accommodation space in the basin. Despite this change in system behaviour, the geochemical proxies show clear evidence for changes in vegetation type (pollen and $\delta^{13}C$), water column oxygen levels and catchment erosion at the glacial – interglacial scale. However, the glacial – interglacial imprint on water column oxygenation and catchment erosion diminishes after MIS 6 due to an increase in locally derived noise (i.e. local driving mechanism exerting stronger influence on record than regional – global scale mechanisms).

Moreover, despite the inherent limitations to the application and interpretation of $\delta^{13}C$ from bulk OM, I show that $\delta^{13}C$ of bulk OM can still be used to provide palaeoenvironmental information on high amplitude changes (e.g. glacial – interglacial scale shifts). These interpretations are strongly supported by coincident changes in pollen spectra derived from the same core, suggesting a major change between C_3 versus C_4 plants. Furthermore, I show that Ti/Al, proposed as a proxy for reconstructing winter AM variability, does not provide a coherent, ubiquitous signal throughout the Tianyang record, and suggest caveats to the interpretation from Lake Huguangyan. It appears that, whilst Ti may be derived from central and northern Chinese loess sequences, the local imprint of Ti from the catchment of both lakes substantially reduces the signal-to-noise ratio rendering a robust interpretation of aeolian derived Ti difficult.

Finally, a regional comparison of the Tianyang $\delta^{13}C$ of bulk OM provides tentative evidence for the change in mosiutre source during MIS 5 to China. This is corroborated by changes in the cave $\delta^{13}C$ of bulk OM fractionation suggesting a weaker land-sea thermal contrast in south China possibly leading to moisture delivery from the Indian monsoon region.

References

Al-Aasm, I.S., Taylor, B.E., South, B. (1990) Stable isotope analysis of multiple carbonate samples using selective acid extraction. Chem. Geo. 80, 119 – 125.

Altabet, M.A., Francois, R. (1994) Sedimentary nitrogen isotopic ratio as a recorder for surface ocean nitrate utilization. Glob. Biogeochem. Cycles. 8(1), 103 – 116.

Altabet, M.A., Francois, R., Murray, D.W., Prell, W.L. (1995) Climate-related variations in denitrification in the Arabian Sea from sediment ^{14}N/^{15}N ratios. Nature. 373, 506-509.

Altabet, M.A. (2007) Constraints on oceanic N balance/imbalance from sedimentary N-15 records. Biogeosci. 4, 75 – 84.

An, Z. (2000) The history and variability of the East Asian palaeomonsoon climate. Quaternary Science Reviews. 19. 171 – 187.

Atkinson, M.J., and Smith, S.V. (1983) C:N:P ratios of benthic marine plants. Limnol. Oceanogr. 28, 568 – 74.

Baker, P.A., Fritz, S.C., Garland, J., Ekdahl, E. (2005) Holocene hydrologic variation in Lake Titicaca, Boliva/Peru, and its relationship to North Atlantic climate variation. J. Quaternary Sci. 20, 655 – 662.

Barros, G.V., Martinelli, L.A., Oliveira Novas, T.M., Ometto, J.P.H.B., Zuppi, G.M. (2010) Stable isotopes of bulk organic matter to trace carbon and nitrogen dynamics in an estuarine ecosystem in Babitonga Bay (Santa Catarina, Brazil). Sci. Tot. Environ. 408, 2226.

Baisden, W.T., Amundson, R., Cook, A.C., and Benner D.L. (2002) Turnover and storage of C and N in five density fractions from California annual grassland surface soils. Global Biogeochem. Cycles. 116, 1117-1122.

Benner, R., Fogel, M.L., Sprague, E.K., Hodson, R.E., (1997) Depletion of ^{13}C in lignin and its implications for stable carbon isotope studies. Nature. 329, 708-711.

Bird, M.I., Giresse, P., Chivas, A.R. (1994) Effect of forest and savanna vegetation on the carbon-isotope composition of sediments from the Sanaga River, Cameroon. Limnol. Oceanogr. 39, 1845-1854.

Bisutti, I., Hilke, I. and Raessler, M. (2004) Determination of total organic carbon - an overview of current methods. Trend. Anal. Chem. 23 (10-11), 716-726.

Blaauw, M. (In Press) Out of tune: the dangers of aligning proxy archives. Quaternary Science Reviews.

Blaauw, M., Wohlfarth, B., Andres Christen, J., Ampel, L., Veres, D., hughen, K.A., Preusser, F., Svensson, A. (2010) Were last glacial climate events simultaneous between greenland and France? A quantitative comparison using non-tuned chronologies. Journal of Quaternary Science. 25(3), 387 – 394.

Brodie, C.R., Leng, M.J., Casford, J.S.L., Kendrick, C.P., Lloyd, J.M., Zong, Y.Q., Bird, M.I. (2011a) Evidence for bias on C and N concentrations and δ^{13}C composition of terrestrial and aquatic organic materials due to pre-analysis acid preparation methods. Chem. Geo. 282, 67 – 83. DOI: 10.1016/j.chemgeo.2011.01.007.

Brodie, C.R., Heaton, T.H., Leng, M.J., Kendrick, C.P., Casford, J.S.L., Lloyd, J.M. (2011b) Evidence for the biasing by pre-analysis acid preparation methods on $\delta^{15}N$ composition of terrestrial and aquatic organic materials. Rapid Comm. Mass. Spec. 25, 1089 – 1099.

Bokhorst, M.P., Vandenberghe, J. (2009) Validation of wiggle matching using a multi-proxy approach and its palaeoclimatic significance. Journal of Quaternary Science. 24(8), 937 – 947.

Bonatti, E., and S. Gartner, Jr. Caribbean climate during Pleistocene Ice Ages. (1973) Nature. 244, 563 – 565.

Boyle, J.F. (2001) Inorganic geochemical methods in palaeolimnology. IN: Tracking environmental change using lake sediments. Last, W.M., Smol, J.P. (Eds.). Kluwer Academic Publishers. Amsterdam. Pp. 83 – 143.

Bunn, S.E., Loneragan, N.R. and Kempster, M.A. (1995) Effects of acid washing on stable isotope ratios of C and N in penaeid shrimp and seagrass: Implications for food-web studies using multiple stable isotopes. Limnol. Oceanogr. 40 (3), 622-625.

Bunting, L., Leavitt, P.R., Weidman, R.P., Winebrooke, R.D. (2010) Regulation of the nitrogen biogeochemistry of mountain lakes by subsidies of terrestrial dissolved organic matter and the implications for climate xstudies. Limnol. Oceanogr. 55, 333 – 345.

Burnett, A.P., Soreghan, M.J., Scholz, C.A., Brown, E.T. (In Press) Tropical East African climate change and its relation to global climate: A record from Lake Tanganyika, Tropical East Africa, over the past 90+ kyr. Palaeo. Palaeo. Palaeo.

Calvert, S.E., Nielsen, B., Fontugne, M.R. (1992) Evidence from nitrogen isotope ratios for enhanced productivity during formation of eastern Mediterranean sapropels. Nature. 359, 223 – 225.

Casford, J.S.L., Abu-Zied, R., Rohling, E.J., Cooke, S., Fontanier, C., Leng, M., Millard, A., Thomson, J. (2007) A stratigraphically controlled multiproxy chronostratigraphy for the eastern Mediterranean. Paleoceanography. 22, PA4215.

Caughey, M.E., Barcelona, M.J., Powell, R.M., Cahill, R.A., Gren, C., Lawrenz, D. and Meschi, P.L. (1995) Interlaboratory study of a method for determining nonvolatile organic carbon in aquifer materials. Environ. Geol. 26, 211-219.

Cerling TE, Wang Y, Quade J (1993) Expansion of C_4 ecosystems as an indicator of global ecological change in the late Miocene. Nature 361: 344 – 345.

Chang, L.L.Y., Howie, R.A., Zussman, J. (1996) Non-silicates: sulphates, carbonates, phosphates, halides. Rock-Forming Minerals, 5B, Longman Group, London, UK. 383 pp.

Chen, J. (1988) A study on magnetic stratigraphy of Tianyang Volcanic Lake basin, Leizhou Peninsula. Marine Geology and Quaternary Geology. 8(1), 73 – 85. (In Chinese with English abstract).

Chen, J., Yang, D. (1989). Late Quaternary sedimentary features and paleoenvironmental changes in the Tiangyang volcanic lake basin, Guangdong Province. Geology and Quaternary Geology. 9, 75 – 84. (In Chinese with English abstract).

Chen, J., Huang, C., Lin, M., Jin, Q., Han, J. (1990). Quaternary geology of Tianyang volcanic lake, Guangdong Province, China. Geological Publishing House, Beijing, 256 pp. (in Chinese with English abstract).

Chen, F.H., Bloemendal, J., Feng, Z.D., Wang, J.M., Parker, R., Guo, Z.T. (1999) East Asian monsoon variations during Oxygen Isotope Stage 5: evidence from the northwestern margin of the Chinese loess plateau. Quaternary Science Reviews. 18, 1127 – 1135.

Cheng, H., et al. (2006) A penultimate glacial monsoon record from hulu cave and two-phase glacial termiantions. Geology. 34, 217 – 220.

Clemens, S., Prell, W., Murray, D., Shimmield, G. and Weedon, G. (1991) Forcing mechanisms of the Indian Ocean monsoon. *Nature.* 353. 720-725.

Clemens, S.C. and Prell, W.L. (2003) A 350,000 year summer-monsoon multi-proxy stack from the Owen Ridge, Northern Arabian Sea. Marine Geology. 201. 35 – 51.

Clemens, S.C. and Prell, W.L. (2007) The timing of orbital-scale Indian monsoon changes. Quaternary Science Reviews. 26. 275 – 278.

Clemens, S.C., Prell, W.L., Sun, Y., Liu, Z., Chen, G. (2008) Southern Hemisphere forcing of Pliocene d18) and the evolution of Indo-Asian monsoons. Paleoceanography. 23, PA4210.

Collatz, G.J., Berry, J.A., Clark, J.S. (1998) Effects of climate and atmospheric Co2 partial pressure on the global distribution of C4 grasses: present, past and future. Oecologia. 114, 441 – 454.

Coplen, T.B. (1996) New guidelines for reporting stable hydrogen, carbon, and oxygen isotope-ratio data. Geochimica et Cosmochimica Acta. 60 (17) 3359 – 3360.

Craig, H. (1954) Carbon-13 in plants and the relationship between carbon-13 and carbon-14 variations in nature. The Journal of Geology. 62(2), 115 – 149.

Cutter, G.A., Radford-Knoery, J. (1991) Determination of carbon, nitrogen, sulphur and inorganic sulphur species in marine particles. In: Hurd, D.C., Spencer, D.W. (Eds.) Marine Particles: Analysis and Characterisation. American Geophysical Union, Geophysical Monographs. 63, 57-63.

Davison, W. (1993) Iron and Manganese in Lakes. Earth Science Reviews. 34, 119 – 163.

Dekkers, M.J. (1997) Environmental magnetism: an introduction. Geologie en Mijnbouw. 76, 163 – 182.

De Lange, G.J., van Os, B., Pruysers, P.A., Middleburg, J.J., Castradori, C., van Santvoort, P., Muller, P.J., Eggenkamp, H., Prahl, F.G. (1994) Possible early diagenetic alteration of palaeo proxies, In: Carbon cycling in the Global Ocean: Constraints on the Ocean’s Role in Global Change (eg. Zhan, R. et al). NATO ASI Series, Vol 1(17), pp. 225 – 258. Springer.

Domingo, L., López-Martínez, N., Leng, M.J., Grimes, S.T. (2009). The Paleocene-Eocene Thermal Maximum record in the organic matter of the Claret and Tendruy continental sections (South Central Pyrenees, Lleida, Spain). Earth Planet. Sci. Lett. 281, 226-237.

Eaton, A.D., Clesceri, L.S., Greenberg, A.E. (eds.)(1995) Standard methods fro water and wastewater. American Public Health Association. Washington.

Edgington D. N. and Robbins J. A. (1976) Records of lead deposition in Lake Michigan sediments since 1800. Environmental Science Technology. 10, 266 – 274.

Edwards, E.J.Osborne, C.P., Stromberg, C.A.E. and C_4 grasses consortium. The origins of C_4 grasslands~: Integrating evolutionary and ecosystem science. Science. 328, 587 – 591.

Ehleringer, J.R., Sage, R.F., Flanagan, L.B., Pearcy, R.W. (1991) Climate change and the evolution of C_4 photosynthesis. Trees. 6, 95 – 99.

Ehleringer, J.R., Monson, R.K. (1993) Evolutionary and Ecological aspects of photosynthetic pathway variation. Annu. Rev. Ecol. Syst. 24, 411 – 439.

Ehleringer, J.R., Cerling, T.E., Helliker, B.R. (1997) C_4 photosynthesis, atmospheric CO_2, and climate. Oecologia. 112, 285 – 299.

Farmer J. G. and Lovell M. A. (1986) Natural enrichment of arsenic in Loch Lomond sediments. Geochimica et Cosmochimica Acta. 50, 2059 – 2067.

Fenchel, T.M. and Jørgensen, B.B. (1977) Detritus food chains of aquatic ecosystems; the role of bacteria. Adv.Microbio. 1, 1 – 58.

Fernandes, M. and Krull, E. (2008) How does acid treatment to remove carbonates affect the isotopic and elemental composition of soils and sediments? Environ. Chem. 5, 33-39.

Fox, J.F., Papanicolaou, A.N. (2007) The use of Carbon and Nitrogen Isotopes to study watershed erosion processes. J. Am. Water Res. Ass. 43, 1047 – 1064.

Freudenthal, T., Wagner, T, Wenzhofer, F., Zabel, M. and Wefer, G. (2001) Early diagenesis of organic matter from sediments of the easter subtropical Atlantic: Evidence from stable nitrogen and carbon isotopes. Geochim. Cosmochim. Ac. 65 (11), 1795-1808.

Froelich, P.N. (1980) Analysis of organic carbon in marine sediments. Limnol. Oceanogr. 25 (3), 564-572.

Fuhrmann, A., Fischer, T., Lucke, A., Brauer, A., Zolitschka, B., Horsfield, B., Negendank, J.F.W., Schleser, G.H., Wilkes, H. (2003) Late Quaternary environmental and climatic changes in central Europe as inferred from the composition of organic matter in annually laminated maar lake sediments. Geochem. Geophy. Geosys. 5(11). Q11015.

Galbraith, E.D., Kienast, M., Jaccard, S.L., Pedersen, T.F., Brunelle, B.G., Sigman, D.M., Kiefer, T. (2008) Consistent relationship between global climate and surface nitrate utilization in the western subarctic Pacific throughout the last 500ka. *Paleoceanography*. 23, PA2212.

Galy et al (2007) Determination of Total Organic Carbon Content and $\delta^{13}C$ in Carbonate-Rich Detrital Sediments Geostan. Geoanal. Res. 31(3). 199-207.

Galy, V., Francois, L., France-Lanord, C., Faure, P., Kudrass, H., Palhol, F., Singh, S.K. (2008) C_4 plants decline in the Himalayan basin since the Last Galcial maximum. Quat. Sci. Rev. 27, 1396 – 1409.

Ganeshram, R.S., Pedersen, T.F., Calvert, S.E., McNeill, G.W., Fontugne, M.R. (2000) Glacial-interglacial variability in denitrification in the world's oceans: Causes and consequences. Paleoceanogr. 15(4), 361 – 376.

Gani, A., Naruse, I. (2007) Effect of cellulose and lignin content on pyrolysis and combustion characteristics for several types of biomass. Renew. Energ. 32(4), 649-661.

Gibbs, R.J. (1977) Clay mineral segregation in the marine environment. Journal of Sedimentary Research. 47 (1), 237-243.

Goering, J., Alexander, V., Haubenstock, N. (1990) Seasonal variability of stable carbon and nitrogen isotope ratios of organics in a North Pacific bay. *Estuar. Coast. Shelf S.* 30, 239 – 251.

Guo, Z.T., Biscaye, P., Wei, L., Cheng, X.H., Peng, S.Z., Liu, T.S. (2000) Summer monsoon variations over the last 1.2 Ma from the weathering of loess-soil sequences in China. Geophys. Res. Lett. 27, 1751 – 1754.

Guo, Z.T., Berger, A., Yin, Q.Z., Qin, L. (2009) Strong asymmetry of hemispheric climates during MIS-13 inferred from correlating Chian loess and Antartica ice records. Clim. Past. 5, 21 – 31.

Hajdas, I., Zolitschka, B., Ivy-Ochs, S.D., et al. (1995) AMS radiocarbon dating of annually laminated sediments from Lake Holzmaar, Germany. Quaternary Science Reviews. 14, 137 – 143.

Han, Y.L., Tan, X.D., Chen, Z., Xiang, R., Zhang, L.L. (2010) Magnetic granulometry of recent sediments from the Huguang Maar and its implication for provenance. Chinese Science Bulletin. 55, 418 – 424.

Harris, D., Horwath, W.R. and van Kessel, C. (2001) Acid fumigation of soils to remove carbonates prior to total organic carbon or carbon-13 analysis. Soil Society of America Journal. 65, 1853-1586.

Haug, G.H., Pedersen, T.F., Sigman, D.M., Calvert, S.E., Nielsen, B., Pedersen, L. (1998) Glacial/interglacial variation in nitrogen fixation in the Cariaco Basin during the last 580 kyr. Paleoceanogr. 13(5), 427 – 432.

Hayes, J.M. (1993) Factors controlling ^{13}C contents of sedimentary organic compounds: Principles and evidence. Mar. Geo. 113, 111 – 125.

Hedges, J.I., Clark, W.A., Quay, P.D., Richey, J.E., Devol, A.H., Santos, U. de. M. (1986) Compositions and fluxes of particulate organic material in the Amazon river. Limnol. Oceanogr. 31, 717 – 738.

Hedges, J.I., Stern, J.H. (1984) Carbon and nitrogen determinations of carbonate-containing solids. Limnol. Oceanogr. 29(3), 657 - 663.

Herzshuh, U. (2006) Palaeo-moisture evolution in monsoonal Central Asia during the last 50, 000 years. Quaternary Science Reviews. 25, 163 – 178.

Hilton, R.G., Galy, A., Hovius, N., Horng, M.J., Chen, H. (2010) The isotopic composition of particulate organic carbon in mountain rivers of Taiwan. Geochim. Cosmochim. Acta. 72, 3164 – 3181.

Ho, K.-S., Chen, J.-C., Juang, W.-S. (2000) Geochronology and geochemistry of the late Cenezoic basalts from the Leiqiong area, southern China. J. Asian Earth Sci. 18, 307 – 324.

Hoefs (1977) Stable Isotope Geochemistry. Springer. Berlin.

Hu, J., Peng, P., Jia, G., Mai, B., Zhang. G. (2006) Distribution and sources of organic carbon, nitrogen and their isotopes in sediments of the subtropical Pearl river estuary and adjacent shelf, Southern China. Mar. Chem. 98, 274 – 285.

Huang, Y., Street-Perrot, F.A., Metcalfe, S.E., Brenner, M., Moreland, M., Freeman, K.H. (2001) Climate change as the dominant control on Glacial-Interglacial variations in C_3 and C_4 abundance. Science. 293, 1647 – 1651.

Hutchinson, G.E. (1957) A Treatise on Limnology. Volume 1. John Wiley and Sons, Inc. USA.

Ingalls. A.E., Aller, R.C., Lee, C., Wakeham, S.G. (2004) Organic matter diagenesis in shallow water carbonate sediments. Geochim. Cosmochim. Ac. 68(21), 4363-4379.

International Atomic Energy Agency (IAEA) (1995) Reference and intercomparison materials for stable isotopes of light elements. IAEA-TECDOC-825. Pgs 1 – 159. Vienna.

Ishikawa, N., Frost, G.M. (2002) Magnetic properties of sediments from Ocean Drilling Program sites 1109, 1115, and 1118 (Leg 180), Woodlark Basin (Papua New Guinea). Earth Planets Space. 54, 883 – 897.

Jaschinski, S., Hansen, T., Sommer, U. (2008) Effects of acidification in multiple stable isotope analyses. Limnol. Oceanogr. Meth. 6, 12 – 15.

Jasper, J.P., Gagosian, R.B. (1989) Glacial – interglacial climatically-forced sources of sedimentary organic matter to the late Quaternary northern Gulf of Mexico. Nature. 342, 60 -62.

Jinglu, W., Chengmin, H., Haiao, Z., Schleser, G.H., Battarbee, R. (2007) Sedimentary evidence for recent eutrophication in the northern basin of Lake Taihu, China: human impacts on a large shallow lake. J. Paleolimno. 38, 13 – 27.

Johnson, K.R., Ingram, B.L., Sharp, W.D., Zhang, P. (2006) East Asian Summer monsoon variability during Marine Isotope Stage 5 based on speleothem $\delta^{18}O$ records from Wanxiang Cave, central China. Palaeogeography, Palaeoclimatology, Palaeoecology. 236, 5 – 19.

Kendrick, C.P. (2009) Investigation of changes in measured %C and %N values in low concentration carbon/nitrogen materials. NERC Isotope Geosciences Laboratory, Report Series No. 268.

Kennedy, P., Kennedy, H. and Papadimitriou, S. (2005) The Effect of acidification on the determination of organic carbon, total nitrogen and their stable isotopic composition in algae and marine sediment. Rapid Commun. Mass Sp. 19, 1063-1068.

King, P., Kennedy, H., Newton, P.P., Kickells, T.D., Brand, T., Calvert, S., Cauwet, G., Etcheber, H., Head, B., Khripounoff, A., Manighetti, B. and Miquel, J.C. (1998) Analysis of total and organic carbon and total nitrogen in settling oceanic particles and a marine sediment: an interlaboratory comparison. Mar. Chem. 60, 203-216.

Kock, P.L., Diffenbaugh, N.S., Hoppe, K.A. (2004) The effects of late Quaternary climate and pCO_2 change on C_4 plant abundance in the south-central United States. Palaeo. Palaeo. Palaeo. 207, 331 – 357.

Kolasinski, J., Rogers, K. and Frouin, P. (2008) Effects of acidification on carbon and nitrogen stable isotopes of benthic macrofauna from a tropical coral reef. Rapid Commun. Mass Sp. 22, 2955-2960.

Kolak J. J., Long D. T., Beals T. M., Eisenreich S. J., and Swackhammer D. L. (1998) Anthropogenic inventories V and historical and present accumulation rates of copper in Great Lakes sediments. Applied Geochemistry. 13, 56 – 75.

Komada, T., Anderson, M.R., Dorfmeier, C.L. (2008) Carbonate removal from coastal sediments for the determination of organic carbon and its isotopic signatures, $\delta^{13}C$ and $\Delta^{14}C$: comparison of fumigation and direct acidification by hydrochloric acid. Limnol. Oceanogr-Meth. 6, 254-262.

Krishnamurthy, R.V., Syrup, K., Long, A. (1999) Is selective preservation of nitrogenous organic matter reflected in the $\delta^{13}C$ signal of lacustrine sediments? Chem. Geo. 158, 165 – 172.

Krull, E.S., Bestland, E.A., Gates, W.A. (2002) Soil organic matter decomposition and turnover in a tropical ultisol: Evidence from $\delta^{13}C$, $\delta^{15}N$ and geochemistry. Radiocarbon. 44(1), 93 – 112.

Knies, J., Brookes, S., Schubert, C.J. (2007) Re-assessing the nitrogen signal in continental margin sediments: New insights from the high latitudes. Earth Planet. Sci. Lett. 253, 471 – 484.

Kutzbach, J.E. (1981) Monsoon Climate of the Early Holocene: Climate Experiment with the Earth's Orbital Parameters for 9000 Years Ago *Science.* 214. 59 – 61.

Kutzbach, J.E., Guetter, P.J. (1986) The influence of changing orbital parameters and surface boundary conditions on climate simulations for the past 18000 years. Journal of Atmospheric Sciences. 43 (16), 1726 – 1759.

Lamb, A.L., Leng, M.J., Mohammed, M.U., Lamb, H.F. (2004) Holocene climate and vegetation change in the Main Ethiopian Rift Valley inferred from the composition (C/N and δ^{13}C) of lacustrine organic matter. Quat. Sci. Rev. 23, 881 – 891.

Lamb, A.L., Wilson, G.P., Leng, M.J. (2006) A review of coastal palaeoclimate and relative sea-level reconstructions using δ^{13}C and C/N ratios in organic material. Earth Sci. Rev. 75, 29-57.

Lamb, A.L., Vane, C.H., Wilson, G.P., Rees, J.G., Moss-Hayes, V.L. (2007) Assessing δ^{13}C and C/N ratios from organic material in archived cores as Holocene sea level and palaeoenvironmental indicators in the Humber Estuary, UK. Mar. Geo. 244, 109 – 128.

Lambert, W.J., Aharon, P., Rodriguez, A.B. (2008) Catastrophic hurricane history revealed by organic geochemical proxies in coastal lake sediments: a case study of Lake Shelby, Alabama (USA). *J. Paleolimnol*. 39, 117 – 126.

Langdon, P.G., Leng, M.J., Holmes, N. and Caseldine, C.J. 2010. Lacustrine evidence of early Holocene environmental change in Northern Iceland: a multiproxy palaeoecology and stable isotope study. Holocene, 20, 205-214.

Larson, T.E., Heikoop, J.M., Perkins, G., Chipera, S.J. and Hess, M.A. (2008) Pretreatment technique for siderite removal for organic carbon isotope and C:N ratio analysis in geological samples. Rapid Commun. Mass Sp. 22, 865-872.

Lehmann, M.F., Bernasconi, S.M., Barbieri, A., McKenzie, J.A. (2002) Preservation of organic matter and alteration of its carbon and nitrogen isotope composition during simulated and in situ early sedimentary diagenesis. Geochim. Cosmochim. Acta. 66(20), 3573 – 3584.

Lei, Z-Q., Zheng, Z. (1993) Quaternary sporo-pollen flora and palaeoclimate of the Tianyang volcanic lake basin, Leizhou Peninsula. Acta Botanica Sinica. 35, 128 – 138. (In Chinese with English abstract).

Leng, M.J., Marshall, J.D. (2004) Palaeoclimate interpretation of stable isotope data from lake sediments. Quaternary Sci. Rev. 23, 811-831.

Leng, M.J., Lamb, A.L., Heaton, T.H.E., Marshall, J.D., Wolfe, B.B., Jones, M.D., Holmes, J.A., Arrowsmith, C. (2005) Isotopes In Lake Sediments In: Isotopes in Palaeoenvironmental Research. Leng, M.J. (ed.). Springer. Netherlands.

Li, L., Bebout, G.E. (2006) Carbon and Nitrogen geochemistry of wedge sediments at ODP site 1040: Evidence for sediment sources, diagenetic history and fluid mobility. In: Morris, J.D., Villinger, H.W. (Eds.) Proceedings of the Ocean Drilling Program, Scientific Results. Volume 205.

Liu, J.Q., Lu, H.Y., Negendank, J., Mingram, J., Xiangjin, L., Wang, W., Chu, G. (2000) Periodicity of Holocene climatic variations in the Huguangyan Maar Lake. Chin. Sci. Bull. 45, 1712 – 1717.

Lohse, L., Kloosterhuis, R.T., de Stigter, H.C., Helder, W., van Raaphorst, W. and van Weering, T.C.E. (2000) Carbonate removal by acidification causes loss of nitrogenous compounds in continental margin sediments. Mar. Chem. 69, 193-201.

Lucke A., Schleser, G.H., Zolitschka, B., Negendank, J.F.W. (2003) A Lateglacial and Holocene organic carbon isotope record of lacustrine palaeoproductivity and climate change derived from varved lake sediments of Lake Holzmaar, Germany. Quat. Sci. Rev. 22, 569 – 580.

Lu, Y., Meyers, P.A., Johengen, T.H., Eadie, B.J., Robbins, J.A., Han, H., (2010) δ^{15}N values in Lake Erie sediments as indicators of nitrogen biogeochemical dynamics during cultural eutrophication. Chem. Geol. 273, 1-7.

Lukasewycz, M.T. and Burkhard, L.P. (2005) Complete elimination of carbonates: A critical step in the accurate measurement or organic and black carbon sediments. Environ. Toxicol. Chem. 24 (9), 2218-2221.

Mackie, E.A.V., Lloyd, J.M., Leng, M.J., Bentley, M.J., Arrowsmith, C. (2007) Assessment of δ^{13}C and C/N ratios in bulk organic matter as palaeosalinity indicators in Holocene and Lateglacial isolation basin sediments, northwest Scotland. J. Quaternary Sci. 22(6), 579-591.

Maher, B.A. (1998) Magnetic properties of modern soils and Quaternary loessic palaeosols: palaeoclimatic implications. Palaeogeography, Palaeoclimatology, Palaeoecology. 137, 25 – 54.

Mampuku, M., Yamanaka, T., Uchida, M., Fujii, R., Maki, T., Sakai, H. (2008) Changes in C_3/C_4 vegetation in the continental interior of the Central Himalayas associated with monsoonal palaoclimatic changes during the last 600 kyr. Clim. Past. 4, 1 – 9.

Matty J. M. and Long D. T. (1995) Early diagenesis of mercury in the Laurentian Great Lakes. Journal of Great Lakes Research. 21, 574 – 586.

McNichol, A.P., Osborne, E.A., Gagnon, A.R., Fry, B., Jones, G.A., (1994) TIC, TOC, DIC, DOC, PIC, POC—unique aspects in the preparation of oceanographic samples for ^{14}C-AMS. Nucl. Instrum. Methods Phys. Res. B 92, 162-165.

Meybeck, M. Carbon, nitrogen, and phosphorus transport by world rivers. Am. J. Sci. 282, 401 – 450.

Meyers, P.A. Ishiwatari, R. (1993) Lacustrine organic geochemistry – an overview of indicators of organic matter and diagenesis in lake sediments. Org. Geochem. 20(7), 867 – 900.

Meyers, P.A. (1994) Preservation of elemental and isotopic source identification of sedimentary organic matter. Chem. Geo. 114, 289 – 302.

Meyers, P.A. (1997) Organic geochemical proxies of paleoceanographic, paleolimnologic, and paleoclimatic proceses. Org. Geochem. 27 (5/6), 213-250.

Meyers, P.A., Teranes, J.L. (2001) Sediment Organic Matter In: Last, W.M. and Smol, J.P. Tracking Environmental Change Using Lake Sediments: Physical and Geochemical Methods. Volume 2. Kluwer Academic Publishers. Holland.

Meyers, P.A. (2003). Applications of organic geochemistry to paleolimnological reconstructions: A summary of examples from the Laurentian Great Lakes. Org. Geochem. 34, 261-289.

Midwood, A.J. and Boutton, T.W. (1998) Soil carbonate decomposition by acid has little effect on□^{13}C of soil organic matter. Soil Biol. Biochem. 30 (10/11), 1301-1307.

Mingram, J., Schettler, G., Nowaczyk, N., Luo, X., Lu, H., Liu, J. and Negendank, J.F.W. (2004) The Huguang maar lake - a high-resolution record of palaeoenvironmental and palaeoclimatic changes over the last 78,000 years from South China. Quat. Int. 122. 85 – 107.

Morely, J.J., Heusser, L.E. (1997) Role of orbital forcing in East Asian monsoon climates during the last 350 kyr: Evidence from terrestrial and marine climate proxies from core RC14-99. *Paleoceanography*. 12, 483 – 494.

Muccio, Z., Jackson, G.P. (2009) Isotope ratio mass spectrometry. Analyst. 134, 213 – 222.

Muller, P.J. (1977) C/N ratios in Pacific deep-sea sediments: Effect of inorganic ammonium and organic nitrogen compounds sorbed by clays. Geochim. Cosmochim. Ac. 41, 765-776.

Nakagawa, T., Okuda, M., Yonenobu, H., Miyoshi, N., Fujiki, T., Gotanda, K., Tarasov, P.E., Morita, Y., Takemura, K., Horie, S. (2008) Regulation of the monsoon climate by two different orbital rhythms and forcing mechanisms. Geology. 36(6), 491 – 494.

Newton, P.P., Lampitt, R.S., Jickells, T.D., King, P., Boutle, C., (1994) Temporal and spatial variability of biogenic particle fluxes during the JGOFS northeast Atlantic process studies at 47^{o}N, 20^{o}W. Deep-Sea Res.. 41, 1617-1642.

Nieuwenhuize, J., Erftmeijer, P.L.A., Mass, Y.E.M., Verwaal, M. and Nienhuis, P.H. (1994a) Pretreatment artefacts associated with the removal of calcareous epiphytes from seagrass leaves. Aquat. Bio. 48, 355-361.

Nieuwenhuize, J., Mass, Y.E.M. and Middleburg, J.J. (1994b) Rapid analysis of organic carbon and nitrogen in particulate materials. Mar. Chem. 45, 217-224.

Ng, J.S.S., Wai, T-C., Williams, G.A. (2007) The effects of acidification on the stable isotope signatures of marine algae and molluscs. Mar. Chem. 103, 97 – 102.

O’Leary, M.H. (1988) Carbon Isotopes in Photosynthesis. Biosci. 38(5), 328-336.

Olsen, J., Bjorck, S., Leng, M.J., Gudmundsdottir, E.R., Odgaard, B.V., Lutz, C.M., Kendrick, C.P., Andersen, T.J., Seidenkrantz, M.-S. (2010) Lacustrine evidence of Holocene environmental change from three Faroese Lakes: a multiproxy XRF and stable isotope study. Quat. Sci. Rev. 29, 2764 – 2780.

Ostle, N.J., Bol, R., Petzke, K.J., Jarvis, S.C. (1999) Compound specific δ^{15}N‰ values: amino acids in grasslands and arable soils. Soil Biol. Biochem. 31, 1751-1755.

Owens, N.J.P. (1987) Natural variations in ^{15}N in the marine environment. Adv. Mar. Bio. 24, 389.

Peng, G. (1989). ^{14}C dating of some Late Pleistocene stratigraphic profiles in South China coastal areas and sedimentary environments. Marine Geology and Quat. Geol. 9, 51–60 (in Chinese with English abstract).

Perdue, E.M., Koprivnjak, J.F. (2007) Using the C/N ratio to estimate terrigenous inputs of organic matter to aquatic environments. Estuar. Coast. Shelf S. 73, 65 – 72.

Pinnegar, J.K., Polunin, N.V.C., (1999) Differential fractionation of delta C-13 and delta N-15 among fish tissues: implications for the study of trophic interactions. *Func. Ecol.* **13**(2), 225-231.

Porter, S.C. and An, Z. (1995) Correlation between climate events in the north Atlantic and China during the last glaciation. Science. 375. 305 – 308.

Porter, S.C. (2000) Chinese loess record of monsoon climate during the last glacial-interglacial cycle. Earth Sci. Rev. 54, 115 – 128.

Prell, W.L. and Kutzbach, J.E. (1987) Monsoon Variability Over the Past 150,000 Years. J. Geophy. Res. 92 (D7). 8411 – 8425.

Prell, W.L. and Van Campo, E. (1986) Coherent response of Arabian Sea upwelling and pollen transport to late Quaternary monsoonal winds. Nature. 323. 526 – 528.

Ramage, C.S. (1971) Monsoon Meteorology. New York, Academic Press. 296

Reimer, P.J., Baille, M.G.L., Bard, E., et al. (2009) INTCAL09 and MARINE09 radiocarbon age calibration curves, 0 – 50,000 years Cal BP. Radiocarbon. 51(4), 1111 – 1150.

Ruddiman, W.F. (2006) What is the timing of orbital-scale monsoon changes? Quat. Sci. Rev. 25. 657 – 658.

Ryba, S.A. and Burgess, R.M. (2002) Effects of sample preparation on the measurement of organic carbon, hydrogen, nitrogen, sulfur, and oxygen concentrations in marine sediments. Chemosphere. 48, 139-147.

Sampei, Y.. Matsumoto, E. (2008) C/N ratios in a sediment core from Nakaumi Lagoon, southwest Japan. Usefulness as an organic source indicator. Geochem. J. 35(3), 189-201.

Sandgren, P., Snowball, I.F. (2001) Application of mineral magnetic techniques to palaeolimnology. In: Tracking environmental change using lake sediments: Physical and geochemical methods, Last, W.M., and Smol, J.P. (Eds.). Kluwer Academic Publishers. Amsterdam.

Schaller, T., Moor, H.C., Wehrli, B. (1997) Reconstructing the iron cycle from the horizontal distribution of metals in the sediment of Baldeggersee. Aqu. Sci. 59, 326 – 344.

Schidlowski, M. (1987) Application of stable carbon isotopes to early biochemical evolution of the Earth. Annual Review of Earth. Planet. Sci. 15, 47 – 72.

Schmidt, M.W.I., and Gleixner, G. (2005) Carbon and nitrogen isotope composition of bulk soils, particle-size fractions and organic material after treatment with hydrofluoric acid. Eur. J. Soil Sci. 56, 407-416.

Schubert, C.J., Calvert, S.E. (2001) Nitrogen and carbon isotopic composition of marine and terrestrial organic matter in Arctic Ocean sediments: implications for nutrient utilisation and organic matter composition. Deep-Sea research I. 48, 789-810.

Schubert, C.J. and Nielsen, B. (2000) Effects of decarbonation treatments on $\delta^{13}C$ values in marine sediments. Mar. Chem. 72, 55-59.

Scholz, C.A., Talbot, M.R., Brown, E.T., Lyons, R.P. (2010) Lithostratigraphy, physical properties and organic matter variability in Lake Malawi Drillcore sediments over the past 145,000 years. Palaeo. Palaeo. Palaeo. doi:10.1016/j.palaeo.2010.10.028

Serrano, O., Serrano, L., Mateo, M.A. ., Colombini, I., Chelazzi, L., Gagnarli, E., Fallaci. M. (2008) Acid washing effect on elemental and isotopic composition of whole beach anthropods: Implications for food web studies using stable isotopes. Acta Oecologia. 34, 89 – 97.

Sharpe, Z. (2007) Principles of Isotope Geochemistry Prentice Hall. USA.

Sigman, D.M., Altabet, M.A., Francois, R., McCorkle, D.C., Gaillard, J-F. (1999) The isotopic composition of diatom-bound nitrogen in Southern Ocean sediments. Paleoceanogr. 14(2), 119 – 134.

Smith, B.N., Epstein, S. (1971) Two categories of $^{13}C/^{12}C$ ratios for higher plants. Plant Phys. 47, 380 – 384.

Snowball, I.F. (1993) Mineral magnetic properties of Holocene lake sediments and soils from the Karsa Valley, Lappland, Sweden, and their relevance to palaeoenvironmental reconstruction. Terra Nova. 5, 258 – 270.

Snowball, I.F. (1994) Bacterial magnetite and the magnetic properties of sediments in a Swedish lake. Earth. Planet. Sci. Lett. 126, 129 – 142.

Spiker, E.C., Hatcher, P.G. (1987) The effects of early diagenesis on the chemical and stable carbon isotopic composition of wood. Org. Geochem. 5, 283 – 290.

Stevenson, F.J., Cheng, C.N. (1972) Organic geochemistry of the Argentine Basin sediments: carbon-nitrogen relationships and Quaternary correlations. Geochim. Cosmochim. Acta. 36, 653 – 660.

Street-Perrot, F.A., Ficken, K.J., Huang, Y., Eglinton, G. (2004) Late Quaternary changes in carbon cycling on Mt. Kenya, East Africa: an overview of the $\delta^{13}C$ record in lacustrine organic matter. Quat. Sci. Rev. 23, 861 – 879.

Street-Perrott, F.A., Huang, Y., Perrot, R.A., Eglinton, G., Barker, P., Ben Khelifa, L., Harkness, D.D., Olago, D.O. (1997) Impact of lower atmospheric carbon dioxide on tropical mountain ecosystems. Science. 278, 1422 – 1426.

Stuiver, M. (1975) Climate versus changes in 13C content of the organic component of lake sediments during the Late Quaternary. Quat. Res. 5, 251 – 262.

Stumm, W., Morgan, J.J. (1996) Aquatic chemistry. Chemical equilibria and rates in natural waters. John Wiley and Sons. New York. Pp. 1022.

Talbot, M.R., Johannessen, T. (1992) A high resolution palaeoclimate record for the last 27, 500 years in tropical West Africa from the carbon and nitrogen isotopic composition of lacustrine organic matter. Earth Planet. Sci. Lett. 110, 23 – 37.

Talbot, M. (2001) Nitrogen Isotopes in Palaeolimnology In: Last, W.M., and Smol, J.P., Tracking Environmental Change Unsing Lake Sediments, Volume 2, Physical and Geochemical Methods. Kluwer Academic Publishers. Dordrecht.

Teranes, J.L., Bernasconi, S.M. (2000) The record of nitrate utilisation and productivity limitation provided by $\delta^{15}N$ values in lake organic matter – A study of sediment trap and core sediments from Baldeggersee, Switzerland. Limnol. Oceanogr. 45(4), 801 – 813.

Terwilliger, V.J., Eshetu, Z., Colman, T., Bekele, A., Gezahgne, M.L., Fogel, P. (2008) Reconstructing palaeoenvironment from $\delta^{13}C$ and $\delta^{15}N$ values of soil organic matter: A calibration from arid and wetter elevation transects in Ethiopia. Geoderma. 147, 197 – 210.

Thompson, L.G., Yao, T., Davies, M.E., Henderson, K.A., Mosely-Thompson, E., Lin, P.-N., Beer, J., Synal, H.-A., Cole-Dai, J. and Bolzan, J.F. (1997) Tropical Climate Instability: The Last Glacial Cycle from a Qinghai-Tibetan Ice Core. Science. 276, 1821 – 1825.

Thornton , S.F. McManus, J. (1994) Applications of Organic Carbon and Nitrogen Stable Isotope and C/N Ratios as Source Indicators of Organic Matter Provenance in Estuarine Systems: Evidence from the Tay Estuary, Scotland. Estuar. Coast. Shelf S. 38, 219-233.

Turney, C.S.M. (1999) Lacustrine bulk organic $\delta^{13}C$ in the British Isles during the Last Glacial-Holocene Transition (14 – 9 ka ^{14}C BP) Arc. Antarc. Alp. Res. 13(1), 71 – 81.

Turney, C.S.M., Wheeler, D., Chivas, A.R. (2006) Carbon isotope fractionation in wood during decarbonisation. Geochim. Cosmochim. Ac. 70, 960-964.

Tyson, R.V. (1995) Sedimentary Organic Matter Organic facies and palynofacies. Chapman and Hall. London.

Tzedakis, P.C., Andrieu, V., de Beaulieu, J.-L., Crowhurst, S., Follieri, M., Hooghiemstra, H., Magri, D., Reille, M., Sadori, L., Shackleton, N.J., Wijmstra, T.A. (1997). Comparison of terrestrial and marine records of changing climate of the last 500,000 years. Earth Planet. Sci. Lett. 150, 171 – 176.

Tzedikas, P.C., McManus, J.F., Hooghiemstra, H., Oppo, D.W., Wijmstra, T.A. (2003) Comparison of changes in vegetation in northeast Greece with records of climate variability on orbital and suborbital frequencies over the last 450 000 years. Earth Planet. Sci. Lett. 212, 197 – 212.

Urey, H. (1947). The thermodynamic properties of isotopic substances, *J. Chem. Soc. (London)*,1947: 562-581.

Van Iperen, J. and Helder, W. (1985) A method for the determination of organic carbon in calcareous marine sediments. Mar. Geol. 64, 179-187.

Verardo, D.J., Froelich, P.N. and McIntyre, A. (1990) Determination of organic carbon and nitrogen in marine sediments using the Carlo Erba NA-1500 Analyzer. Deap-Sea Res. 37 (1), 157-165.

Verosub, K.L., Roberts, A.P. (1995) Environmental magnetism: Past, present and future. J. Geophys. Res. 100, 2175 – 2192.

Vob, M., Emeis, K.-C., Hille, S., Neumann, T., Dippner, J. (2005) The nitrogen cycle of the Baltic Sea from an isotopic perspective. Glob. Biogeochem. Cyc. 19, Doi: 10.1029/2004GB002338.

Voss, M., Emeis, K.-C., Hille, S., Neumann, T., Dippner, J. (2005) The nitrogen cycle of the Baltic Sea from an isotopic perspective. *Global Biogeochem. Cyc.* 19. DOI: 10.1029/2004GB002338.

Wang, Y.J., Cheng, H., Edwards, R.L., An, Z.S., Wu, J.Y., Chen, C.-C. and Dorale, J.A. (2001) A High-Resolution Absolute Dated Late Pleistocene Monsoon Record from Hulu Cave, China. *Science.* 294. 2345-2348.

Wang, P., Clemens, S., Beaufort, L., Braconnot, P., Ganssen, G., Jian, Z., Kershaw, P. and Sarnthein, M. (2005) Evolution and variability of the Asian monsoon system: state of the art and outstanding issues. Quat. Sci. Rev. 24. 595 – 629.

Wang, Y., Cheng, H., Lawrence-Edwards, R., Kong, X., Shao, X., Chen, S., Wu, J., Jiang, X., Wang, X., An, Z. (2008) Millennial- and orbita-scale changes in the East Asian monsoon over the last 224,000 years. Nature. 451, 1090 – 1093.

Waples, D.W., (1985) Organic and inorganic nitrogen in sediments from Leg 80, Deep Sea drilling Programme, In: Graciansky, P. C. de, Poag, C. W., et al., *Init. Repts. DSDP*, 80: Washington (US. Govt. Printing Office).

Webster, P.J. (1987) The Elementary Monsoon. In: Fein, J.S. and Stephens, P.L. (Ed.) Monsoons. New York, John Wiley and Sons Ltd.

Wei, Z., Jibin, X., Yanming, Z., Qiaohong, M., Jun, O., Ying, C., Zhiguo, Z., Wei, L. (2010) Bulk organic carbon isotopic record of lacustrine sediments in Dahu Swamp, eastern Nanling Mountains in South China: Implication for catchment environmental and climatic changes in the last 16, 000 years. J. Asian Earth Sci. 38, 162 – 169.

Wilson, G.P., Lamb, A.L., Leng, M.J., Gonzalez, S., Huddart D. (2005) δ^{13}C and C/N as potential coastal palaeoenvironmental indicators in the Mersey Estuary, UK. Quat. Sci. Rev. 24, 2015 – 2029.

Wolfe, B.B., Edwards, T.W.D., Aravena, R. (1999) Changes in carbon and nitrogen cycling during tree-line retreat recorded in the isotopic content of lacustrine organic matter, western Taimyr Peninsula, Russia. The Holocene. 9, 215 – 226.

Wunsch, C. (2010) Towards understanding the Paleocean. Quat. Sci. Rev. 29, 1960 – 1967.

Yancheva, G., Nowaczyk, N.R., Mingram, J., Dulski, P., Schettler, G., Negendank, J.F.W., Liu, J., Sigman, D.M., Peterson, L.C., haug, G.H (2007) Influence of the intertropical convergence zone on the East Asian monsoon. Nature. 445, 74 – 77.

Yamamuro, M. and Kayanne, H. (1995) Rapid direct determination of organic carbon and nitrogen in carbonate-bearing sediments with a Tanaco MT-5 CHN analyzer. Limnol. Oceanogr. 40 (5), 1001-1005.

Yarincik, K.M., Murray, R.W., Petersen, L.C. (2000) Climatically sensitive eolian and hemipelagic deposition in the Cariaco basin, Venezuela, over the past 578,000 years: Results from Al/Ti and K/Al. Paleoceanogr. 15(2), 210 – 228.

Yoshii, K., Wada, E., Takamatsu, N., Karabanov, E.B., Kwai, T. (1997) ^{13}C and ^{15}N abundances in the sediment core (VER 92/1-St-10-GC2) from northern Lake Baikal. Isotopes in Environ. Health Stud. 33, 277 – 290.

Yu, F., Zong, Y.Q., Lloyd, J.M., Huang, G., Leng, M.J., Kendrick, C., Lamb, A.L., Yim, W.W.-S. (2010) Bulk organic δ^{13}C and C/N as indicators for sediment sources in the Pearl River delta and estuary, southern China. Est. Coast. S. Sci. 87, 618.

Yuan, D., Cheng, H., Lawrence Edwards, R., Dykoski, C.A., Kelly, M.J., Zhang, M., Qing, J., Lin, Y., Wang, Y., Wu, J., Dorale, J.A., An, Z. and Cai, Y. (2004) Timing, Duration, and Transitions of the Last Interglacial Asian Monsoon. Science. 304. 575 – 578

Yui, T-F., Gong, S-Y. (2003) Stoichiometry effect on stable isotope analysis of dolomite. Chem. Geo. 201, 359 – 368.

Zhang, G.M. (1980). Characteristics of fissure water in volcanic area of Leizhou Peninsula. Hydro. Eng. Geol. 2, 26 – 41. (In Chinese).

Zheng, Z., and Lei, Z.-Q. (1999) A 400,000 year record of vegetational and climatic changes from a volcanic basin, Leizhou Peninsula, southern China. Palaeo. Palaeo. Palaeo. 145, 339 – 362.

Zheng, Z. (2008) Personal communication.

Zhou, H., Guan, H. and Chi, B. (2008) Record of winter monsoon strength. Nature. 450. E10.

Zong, Y.Q., Lloyd, J.M., Leng, M.J., Yim, W.W.-S., Huang, G. (2006) Reconstruction of Holocene monsoon history from the Pearl River Estuary, southern China, using diatoms and carbon isotope ratios. The Holocene. 16(2), 251-263.